IDENTIFICATION AND CHARACTERIZATION OF A PEPTIDE TOXIN INHIBITOR OF CLC-2 CHLORIDE CHANNELS

A Dissertation
Presented to
The Academic Faculty

By

Christopher Hal Thompson

In Partial Fulfillment
Of the Requirements for the Degree
Doctor of Philosophy in Biology

Georgia Institute of Technology

December 2008

IDENTIFICATION AND CHARACTERIZATION OF A PEPTIDE TOXIN INHIBITOR OF CLC-2 CHLORIDE CHANNELS

Nael A. McCarty, PhD
Division of Pediatrics
Emory University

H. Criss Hartzell, PhD
Department of Cell Biology
Emory University

Stephen C. Harvey, PhD
School of Biology
Georgia Institute of Technology

Robert H. Lee
Department of Biomedical Engineering
Georgia Institute of Technology

Julia Kubanek, PhD
School of Biology
Georgia Institute of Technology

Date Approved: October 22, 2008

For my family
Walter, Patricia, and Courtney

ACKNOWLEDGMENTS

The successful completion of this project has come with great effort and support from many people. First and foremost I would like to thank my parents, Walter and Patricia, as well as my sister Courtney for their unwavering support and encouragement. From a very young age they instilled in me a desire for knowledge, and gave me the confidence I needed to pursue my dreams. Without them none of this would have been possible and I am eternally grateful. I would like to thank my thesis advisor, Dr. Nael McCarty, who has been an excellent mentor. He took me into his lab despite the fact that I had no previous lab experience and taught me how to think like a scientist. Without his training, immense knowledge, willingness to teach and answer questions, and motivation this project would not have been possible. I would also like to thank all of the members of the McCarty Lab. I have forged some lifelong friendships in the McCarty Lab, and that is in no small part due to the open environment created by Dr. McCarty. Thanks to Matt Fuller, who was instrumental in the completion of this project, always having a great idea, and who is a great friend. The progress made on this project would have been greatly reduced without the conversations we had over lunch or playing catch in the hallways at Georgia Tech. Thanks to Zhi-Ren Zhang and Guiying Cui for teaching me how to patch, and always being patient when I would ask a million questions. I am grateful to David Fields, who provided critical help during the beginning phases of the project and taught me how to think outside of the box. Also, thanks to Pedro Olivetti, who provided much needed help during the isolation of this toxin. Thanks also to Gwyneth Halstead-Nussloch for providing an excellent starting point for the future of this

project, and generally for always having a great attitude. I would like to express my gratitude to Cody Freeman, who provided exceptional experimental help when I needed it, served as a sounding board, and is a wonderful friend. I would like to thank Karla Vincent for always being around for me to bounce ideas off of and always seem to be able to make me laugh, even when I'm in a bad mood. Her perspective, scientifically and otherwise, has been an invaluable asset, and her friendship has been essential for my success. A special thanks is required for Staci Cohen, who has been an excellent colleague and a great friend. She always challenged my way of thinking, and I have become a better scientist and person because of it. I would also like to thank Mary Beth Brown for being a fantastic colleague, and in general being good luck. I am grateful to all of my committee members, Dr. Stephen Harvey, Dr. Julia Kubanek, Dr. Robert Lee, and Dr. Criss Hartzell for their insights and suggestions. Thanks also the Dr. Jan Pohl, Dr. Robert French, and Dr. Denis McMaster for their wonderful collaborative efforts during this project. Finally, I would like to thank my friends Fred, Chris, Benson, Rich, Matt, Allison, Kymry, Frank, and Troy for providing much needed moral support and encouragement.

This work has been supported by the National Institutes of Health, the Cystic Fibrosis Foundation, the American Heart Association, and a GAANN fellowship.

TABLE OF CONTENTS

LIST OF TABLES

LIST OF FIGURES

LIST OF ABBREVIATIONS

9-AC	Anthracene-9-carboxylic acid
AChR	Acetylcholine receptor
ADP	Adenosine 5'-diphosphate
AgTx2	Agitoxin 2
AMP-PNP	Adenosine 5'-(β,γ-imido) triphosphate
ATP	Adenosine 5'-triphosphate
Bp	Base pairs
CaMKII	Ca2+/calmodulin-dependent protein kinase II
cAMP	Adenosine 3',5'-cyclic monophosphate
Ca_V	Voltage-gated calcium channel
CBS1	Cystathione beta synthase domain 1
CBS2	Cystathione beta synthase domain 2
cDNA	complementary Deoxyribonucleic acid
CF	Cystic Fibrosis
CFTR	Cystic Fibrosis Transmembrane Conductance Regulator
ChTx	Charybdotoxin
Cl_{Ca}	Calcium-dependent chloride channel
ClTx	Chlorotoxin
COS	CV-1 (simian) in Origin, and carrying the SV40 genetic material cell line
CPA	p- chlorophenoxyacetic acid

CPB	2-(p- chlorophenoxy)butyric acid
CPP	2-(p- chlorophenoxy)proprionic acid
cRNA	Complementary ribonucleic Acid
db-cAMP	N^6,2'-O- Dibutyryladenosine 3'5'-cyclic monophospate
DIDS	4'4'- Diisothiocyano-2,2'-Stilbene disulfonate
DMSO	Dimethyl sulfoxide;
DNA	Deoxyribonucleic acid
DNDS	4,4'- Nitrostilbene- 2,2' disulfonate
DPC	Diphenylamine 2-carboxylic Acid;
EGTA	Ethylene glycol-bis(β-aminoethyl ether)-N,N,N',N'-tetraacetic acid
FFA	Flufenamic acid
GABA	γ-aminobutyric acid
GaTx1	Georgia anion toxin 1
GaTx2	Georgia anion toxin 2
G_{Cl}	Chloride conductance
G_K	Potassium conductance
GTP	Guanine 5'-triphophate
HEK	Human embryonic kidney cell line
Hsp90	Heat shock protein 90
HTx	Hanatoxin
IBMX	3- isobutyl-1- methylxanthine
IGF-I	Insulin-like growth factor 1

K_{Ca}	Calcium-dependent potassium channel
KCC2	Potassium chloride cotransporter 2
kDa	Kilodalton
K_V	Voltage-gated potassium channel
LpII	Leiuropeptide II
LpIII	Leiuropeptide III
Lqh pf-venom	Leiurus quinquestriatus hebraeus partially fractionated venom
Lqh	Leiurus quinquestriatus hebraeus
MALDI-MS	Matrix-assisted laser desorption/ionization mass spectrometry
MALDI-TOF	Matrix-assisted laser desorption/ionization time-of-flight mass spectrometry
mRNA	Messenger ribonucleic acid
MTSET	(2-(trimethylammonium)ethyl)methanethiosulfonate
nAChR	Nicotinic acetylcholine receptor
Na_V	Voltage-gated sodium channel
NCL	neuronal ceroid lipofuscinosis
NDI	Nephrogenic diabetes indipidus
NFA	Niflumic acid
NHERF2	Sodium-hydrogen exchange regulatory cofactor 2
NIH/3T3	Fibroblast cell line
NPPB	5-nitro-2-(3-phenylpropylamino)benzoic acid
PDZ	Protein binding domain
PKA	Cyclic AMP-dependent protein kinase A

P_O	Open probability
Q_{10}	Temperature coefficient
RP-HPLC	Reversed phase high performance liquid chromatography
SHB-IR	Shaker B- inactivation removed
siRNA	small interfering ribonucleic acid
SITS	4-Acetamido-4'-isothiocyanato-2,2' stilbene disulfonic acid
TEVC	Two electrode voltage clamp
TMCA	Thermodynamic mutant cycle analysis
$V_{1/2}$	Half-maximal activation voltage
V_M	Membrane potential
VSTx1	Voltage sensing toxin 1
WT	Wild type

SUMMARY

ClC proteins encompass a large protein family consisting of both voltage-dependent chloride channels and chloride/proton exchangers that are found in both eukaryotes and prokaryotes. These proteins mediate Cl^- flux across the plasma membrane or intracellular membranes of many cell types including neurons, epithelial cells, and skeletal muscle in mammals. In prokaryotic systems they are thought to be critical for extreme acid resistance. Mutations in genes encoding these proteins underlie several human genetic diseases including myotonia, epilepsy, Bartter's syndrome, and Dent's disease. Much of the research devoted to ClC proteins has focused on understanding ion conduction and gating of only a few members of the family, with ClC-0 and ClC-1 being the most prominent. Unlike other ion transport proteins, ClC proteins are homodimeric, "two pore", proteins with each subunit containing 18 helical domains, as well as large intracellular domains in the eukaryotic members. For the ion channel members of the ClC family, chloride conduction through these channels is regulated by two separate gating mechanisms; a fast gating mechanism which independently controls conduction through each pore, and a slow gating mechanism which controls both pore simultaneously. While structure/function studies, coupled with a crystal structure of a bacterial ClC transporter, have led to improved understanding of some aspects of ClC fast gating and conduction, many issues remain unresolved including the nature of slow gating, and the differences that underlie ion transport through ClC channels versus ClC transporters. This has been hampered by the lack of selective, potent inhibitors of this family of proteins that could be used for structure/function studies.

In the cation channel field highly potent and selective inhibitors exist that have been very useful for structure/function studies. Some of the most useful of these compounds have been peptide toxins isolated from venomous animals such as scorpions, spiders, and cone snails. These proteins typically interact very high affinity, usually in the nM or pM range, and are very selective for their particular targets. Peptide toxins have been critical for elucidation of mechanisms underlying gating and ion conduction of various voltage-gated and ligand-gated cation channels. However, no peptide toxins have been discovered that interact with any member of the ClC family, and only one has been identified which inhibits a chloride channel of known molecular identity. Georgia anion toxin 1 (GaTx1), isolated from the venom of *Leiurus quinquestriatus hebraeus* (Lqh), inhibits the cystic fibrosis transmembrane conductance regulator (CFTR) chloride channel. Identification and characterization of a peptide toxin capable of selectively inhibiting a member of the ClC protein family would open a new avenue of structure/function studies of these proteins, as well as help answer critical questions regarding the physiological role that some of these proteins play. Preliminary experiments from Dr. McCarty's lab suggested that Lqh venom contained a component capable of inhibiting the ClC-2 chloride channel. Results shown in Chapters 2 - 9 describe the initial characterization of the activity of Lqh venom, and isolation and characterization of the active toxin.

The first goal of this project was to characterize the activity of Lqh venom against members of the ClC protein family, and to determine if the active component was a peptide. We found that venom contained a component that selectively inhibited the ClC-2 chloride channel when applied to the extracellular face of the channel. Further

characterization of the active component revealed that the inhibitory nature of the active component could be abolished by treatment with trypsin, suggesting that this component was indeed a peptide. Finally, investigation into the mechanism of inhibition suggested that the active component of Lqh-venom acted as a gating modifier, slowing channel opening, and shifting the voltage-dependence of inhibition to more hyperpolarizing membrane potentials.

Our second goal was to purify the active toxin from venom, determine the primary amino acid sequence, and perform a more detailed characterization of the inhibitory activity against ClC-2. From venom, we isolated a peptide with a molecular mass of 3.2 kDa using reversed-phase HPLC, which we named Georgia anion toxin 2 (GaTx2). Sequence analysis revealed that this toxin had been previously isolated in 1997, although no target was identified. Our worked showed that GaTx2 is the highest affinity inhibitor available for any chloride channel, inhibiting ClC-2 with a K_D in the low pM range. Like venom, GaTx2 also appeared to slow channel opening. Finally, our data suggest that GaTx2 is specific for ClC-2; it was unable to inhibit currents mediated by other members of the ClC family, CFTR, other major chloride channels, and voltage-dependent potassium channels.

Our results demonstrate the existence of a peptide toxin that is capable of inhibiting the ClC-2 voltage-gated chloride channel. This toxin is the first peptide toxin inhibitor of any ClC protein, and is the highest affinity inhibitor of any chloride channel identified to date. This toxin will provide a new tool for structure/function studies of ClC-2, and will hopefully serve as only the first toxin inhibitor available for this protein family.

CHAPTER 1

INTRODUCTION

ClC proteins form a family of chloride transport proteins that are expressed in nearly all phyla. These proteins may be separated into two functional groups: those which form voltage-gated chloride channels, and those which form Cl^-/H^+ exchangers (Fig. 1). While evolutionarily these proteins are very similar, the basic mechanisms by which they perform their functions are very different. The functional unit of the ClC protein family is generally homodimeric, although heterodimers can form, with the mammalian proteins bearing a large intracellular domain that is absent in bacterial homologs. ClC channels generally show a halide permselectivity and conductivity sequence of $Cl^- > Br^- > I^-$, and are impermeable to cations; ClC transporters exchange 2 Cl^- ions for 1 H^+ during their transport cycle. There are nine mammalian members of the ClC family, with representatives from both functional groups. In mammalian systems, ClC proteins mediate chloride transport across the plasma membrane and intracellular membranes in nearly all cell types. The functional effect of this chloride transport is the maintenance of resting membrane potential, cell volume regulation, and acidification of intracellular compartments such as endosomes. We will discuss, in detail, the properties of each of the mammalian ClC proteins, as well as ClC-0 from *Torpedo* electric organ, which was the first cloned ClC family member. We will also dissect the ClC protein structure, and the insights into channel gating that can be inferred from the available crystal structures, as well as the limitations of these structures. Finally, we will discuss the available

pharmacological tools for ClC proteins, as well as the lack of high affinity probes such as those available for cation channels.

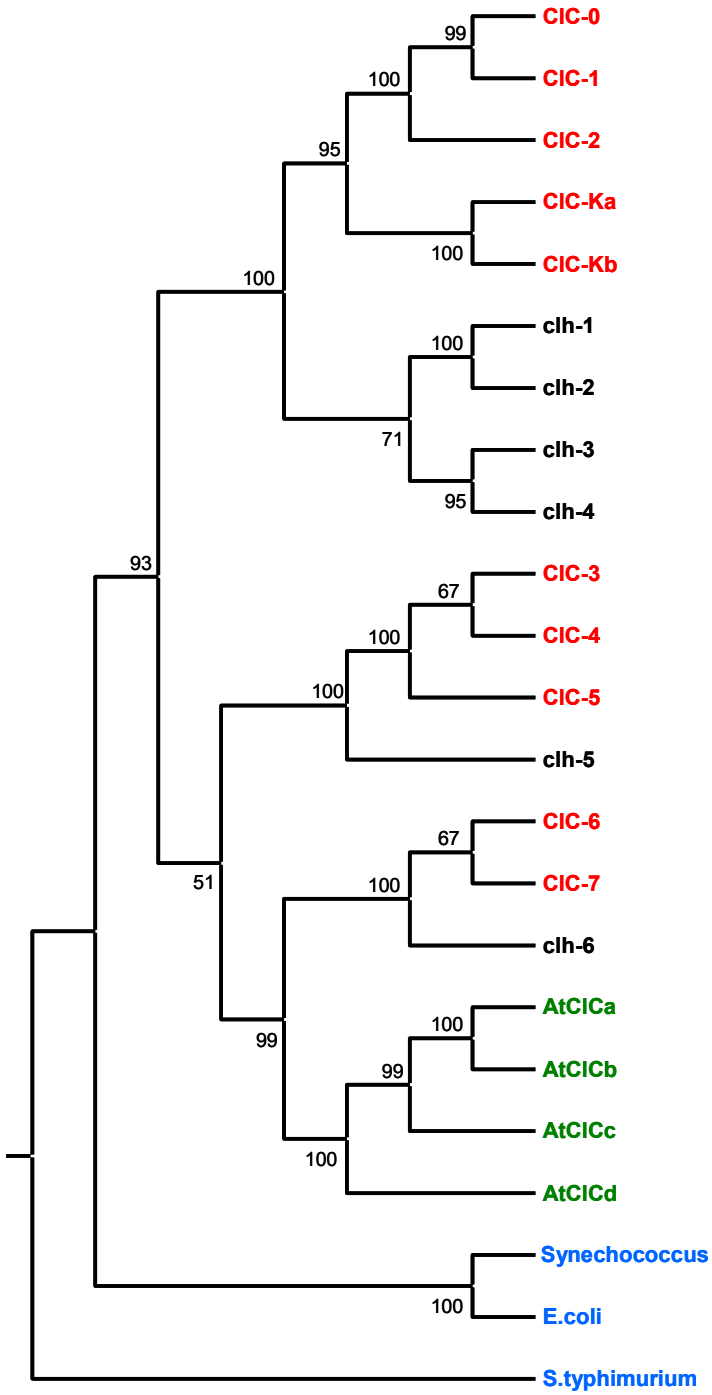

Figure 1: ClC protein phylogeny. This phylogenetic tree is constructed from protein sequences of ClC protein representatives from *Homo sapiens* (red), *C. elegans* (black), *Arabadopsis* (green), and bacteria (blue).

1.1 Properties and physiology of ClC channels

ClC channels are mainly voltage-gated chloride channels that mediate chloride transport across the plasma membrane of many cell types. In mammals, there are 4 channel subtypes of the ClC family: ClC-1, -2, -Ka, -Kb (Table 1). The canonical ClC channel to date, however, has been ClC-0, cloned from the electric organ of the *Torpedo* electric ray. As will be discussed below, many of the biophysical characteristics of these channels are quite similar, although they mediated vastly divergent physiological roles.

1.1.1 ClC-0

The first member of the ClC family to be identified was the ClC-0 voltage-gated chloride channel from the electroplax of the *Torpedo* electric ray. This conductance was identified functionally by White and Miller in 1979, during attempts to insert membrane vesicles containing the nicotinic acetylcholine receptor (nAChR) from electroplax into planar lipid bilayers [1]. The insertion of membrane vesicles into bilayers showed a very weakly voltage-dependent conductance that was nearly perfectly anion selective, and inhibited by the non-selective chloride channel blockers SITS and DIDS. Also derived from this study was the realization that the nAChR and this voltage-dependent chloride channel localize to different parts of the electroplax membrane. The nAChR in electroplax is found at high density in the innervated membrane, while ClC-0 is localized to the non-innervated membrane [2]. Thousands of electroplax cells are then arranged in stacks similar to batteries placed in series. This arrangement allows for the high voltage/large current discharges that these animal use to stun or kill prey.

Table 1: Properties of ClC Chloride Channels. Members of the ClC protein family that act as voltage-dependent chloride channels are listed with decriptions of basic biophysical properties, tissue expression, physiological role, and associated pathophysiology.

Table 1: Properties of ClC Chloride Channels

	Function	***Expression***		***Physiological Role***	***Pathophysiology and Knockout***
		Tissue	**Cellular Localization**		
ClC-0	Voltage-gated channel Slow gate: Hyperpol. Fast gates: Depol. $Cl^- > Br^- > I^-$	*Torpedo* electric organ	Non-innervated PM	Stabilization of membrane potential	
ClC-1	Voltage-gated channel Slow and Fast gates: Depol. $Cl^- > Br^- > I^-$	Skeletal muscle	Sarcolemmal PM	Stabilization of membrane potential, Primary Cl^- conductance of skeletal muscle	Generalized myotonia Myotonia congenita Myotonic dystrophy
ClC-2	Voltage-gated channel Slow and Fast gates: Hyperpol $Cl^- > Br^- > I^-$	Ubiquitous	Epithelial Apical or Basolateral PM, PM of VSMC, PM of Pyramidal Neurons	Transepithelial transport, Cell volume regulation, Stabilization of membrane potential	Epilepsy Degeneration of Testis and Retina (KO) Leukoencephaolopathy (KO)
ClC-Ka/b + Barttin	Voltage-independent channel $Cl^- > Br^- > I^-$	Kidney	Basolateral membrane	Transepithelial transport	Bartter's Syndrome Diabetes insipidus (KO)

Prior to the cloning of the ClC-0 gene, much work was performed on single voltage-dependent chloride channels isolated from *Torpedo* membranes. The first studies of single Torpedo voltage-dependent chloride channels showed very interesting behavior. When these channels were observed at the single channel level, two equidistant conductance levels were always present during the recording, suggesting that more than one channel had been inserted into the bilayer [3, 4]. However, Miller and White showed that these conductance levels were always observed together as discrete bursts that were separated by long quiescent periods [3], suggesting that the conductance levels arose from a single protein. Analysis of the burst behavior showed that the distribution of conductance levels between closed, open level 1, and open level 2 exhibited a binomial distribution, suggesting that each conductance level was independent of the other during an open burst. The separation of these bursts by long quiescent periods indicated that a separate process was capable of simultaneously regulating channel activity. Taken together, it was suggested that the oligomeric structure of the voltage-dependent chloride conductance from *Torpedo* was that of a two-pored ion channel, possessing at least two separate gating processes [3, 5]. This "double-barreled" open channel behavior and complex gating behavior appears to be conserved among ClC channels (Fig. 2).

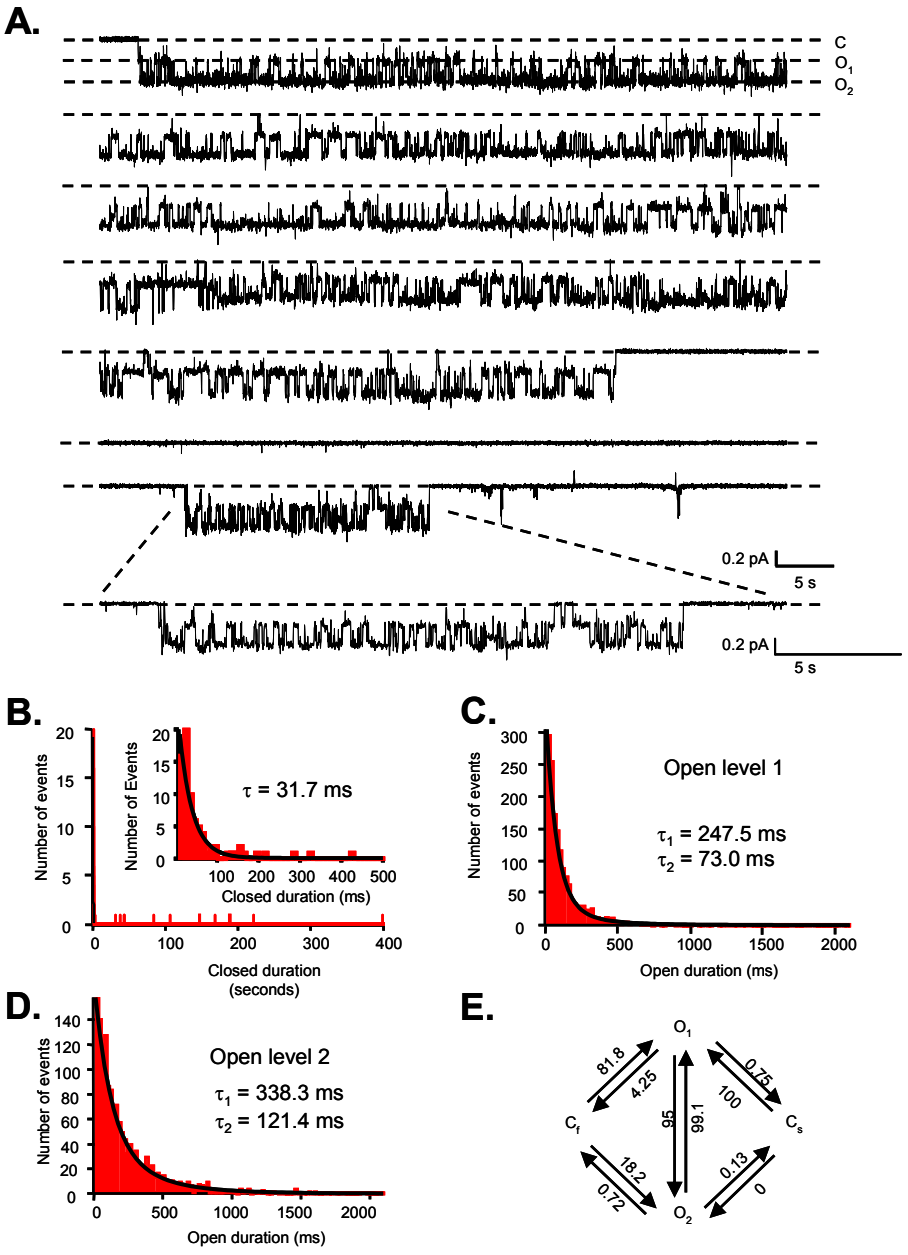

Figure 2: ClC single channel behavior. **(A)** Typical single channel recording of the ClC-2 channel. Like other ClC proteins, ClC-2 transitions rapidly from the closed state (c) to two conducting states (O1, O2). Rapid transistions between O1 and O2 are regulated by the fast gates, while the long closures (> 1 second) represent closures of the slow gate. **(B-D)**. Dwell time histograms of the closed state **(B)**, and the two open states **(B, D)**. The closed dwell time histograms shows two distinct closed states, brief closures consistent with closures of the fast gate, and long closures consistent with closures of the slow gate. Each open time histogram is best described by the sum of two exponential functions, as would be expected from the closure of two independent fast gates. **(E)**. Transition diagram showing the probability of the channel transitioning from one state to any other.

The ClC-0 channel is encoded by a mature transcript of 2673 bases that is translated into an 805 amino acid protein with a mass of 89 kDa [6]. When cRNA of the ClC-0 clone was injected into *Xenopus* oocytes, currents with macroscopic behavior similar to that of the voltage-dependent chloride conductance from *Torpedo* were observed. These currents showed similar sensitivity to the chloride channel inhibitors DIDS and DPC [1, 2, 7]. Also similar to the chloride channel from electric organ, the cloned voltage-gated chloride channel showed double-barreled behavior, with two equidistant conductance levels exhibiting the same single channel conductance as channels isolated directly from the electric organ, ~10 pS for open level 1 and 20 pS for open level 2, suggesting that the cloned channel provides the voltage-dependent chloride conductance observed for the electric organ [8-10].

Since its cloning in 1990, ClC-0 has served as the canonical member of this large family of voltage-dependent chloride channels. In fact, much of the knowledge of ClC channel biophysics has come from studies initially performed on ClC-0. Early studies of the voltage-dependent Cl^- conductance isolated from *Torpedo* and reconstituted into planar lipid bilayers suggested that the functional unit contained two independent chloride conduction pathways. The architecture of ClC-0 was further refined in 1996, when two independent studies suggested that ClC-0 was a homodimeric structure, with two separate pores [11, 12]. Middleton and coworkers tested the homodimeric model of the ClC-0 protein by introducing a point mutation into the protein that altered single channel conductance. The cRNA encoding the mutant channel was then co-injected with cRNA encoding wild-type ClC-0 into *Xenopus* oocytes. Single channel recording was

then performed and the transitions between conductance levels were observed. Three populations of openings were observed. Two populations showed 3 equidistant conductance levels consistent with WT-WT and mutant-mutant dimers. However, one population showed openings to 4 distinct conductance levels: closed, an opening to a single WT pore, an opening to a single mutant pore, and an open level with the summed conductance of the WT and mutant pore [12]. This model was separately tested by Pusch and coworkers in a separate study in which concatameric channels were created between WT and mutant subunits, which showed similar single channel behavior as described above for mixtures of WT and mutant cRNAs, with four conductance levels [11]. Both studies confirmed the homodimer nature of the ClC-0 protein.

Gating of ClC-0 channels is a very complicated process. Single ClC-0 channels show bursting behavior in which both pores independently conduct ions. During open bursts channels rapidly transition between the closed level and open levels 1 and 2 [9, 13]. These rapid transitions are controlled by a process known as fast gating, with each pore controlled by its own fast gate; the main contributor to fast gating appears to be a conserved glutamate residue that resides within the pore domain of each subunit [14]. These channel bursts are separated by long periods with no channel activity. The long closures are controlled by a separate gating process known as slow-gating; the molecular determinants of this process are only now beginning to come into focus. On the single channel level the fast and slow gating processes are easily distinguished based on the time scales on which they act; there is a large amount of data characterizing these processes at both the macroscopic and single channel levels, which will be discussed. Both fast and slow gating processes are temperature dependent; the Q_{10} of fast gating is

~1.4, while the Q_{10} of slow gating is ~40, suggesting a major conformational change is associated with slow gating, and only a modest change is associated with fast gating [15]. The structural determinants of these gating processes will be discussed in further detail in section 1.4.

For ClC-0, both the fast and slow gating processes are voltage-dependent, with the slow gate being opened slowly by membrane hyperpolarization, and the fast gates being opened rapidly by membrane depolarization [10, 11], which results in the macroscopic behavior as shown in Figure 3. Analysis of the primary structure of ClC-0, and in fact all ClC channels, reveals no region of localized charge that may act as a voltage sensor, similar to the S4 helix in voltage-gated cation channels (Fig. 4A) [7, 16]. The calculated gating charge for ClC-0 is ~1, whereas the gating charge for a voltage-gated K^+ channel is ~14 [16]. Pusch and colleagues determined that the gating of ClC-0 is very dependent on the permeant ion by investigating the effects of altering the external $[Cl^-]$. ClC-0 exhibited shifts in the $V_{1/2}$ that were dependent on the external $[Cl^-]$, as well as effects on the $V_{1/2}$ for fast-gating associated with anomalous mole fraction behavior with mixtures of Cl^- and NO_3^-, suggesting that the permeant ion itself acts as the gating charge [11]. Analysis of single ClC-0 channels showed that there is a high degree of asymmetry in the transitions to and from the slow-gate closed state from a conducting state. Open bursts tended to begin with a transition from the slow-gate closed state to open level 2, and to return to the slow-gated closed state from open level 1. The transition pattern observed by Richard and Miller implied that ClC-0 gating is cyclical, preferentially transitioning from C→2→1→C. A gating cycle that exists in thermodynamic equilibrium should be able to open to either 1 or 2 with equal probability,

likewise for channel closing. Therefore, the transition pattern observed by Richard and Miller suggests that ClC-0 gating is a non-equilibrium process. This asymmetry was also shown to be dependent on the electrochemical gradient for Cl^- [9]. It was further reported that the non-equilibrium gating of ClC-0 predicts that the closed state of the channel may differ structurally depending on whether Cl^- is bound to the channel. It was shown experimentally that the Cl^- bound closed state opens at a much higher rate than the unbound state [17]. The suggestion that Cl^- itself acts as the gating charge, and the recognition that the Cl^- bound state of the channel opens at a higher rate, implies a very strong link between permeation and gating in ClC-0: the voltage-dependence of gating is derived from the voltage-dependent movement of Cl^- within the pore [17]. Other work has suggested that this is also the case for other ClC channels as well [18]. Fast-gating of ClC-0 is only weakly controlled by internal Cl^-. Raising $[Cl^-]_{int}$ to non-physiological concentrations (i.e. > 150 mM) reduced the closing rate of the channel, having no effect on the opening rate [17, 19]. Given the very high concentrations required to modulate fast-gating, it is likely that this type of regulation is not physiologically relevant.

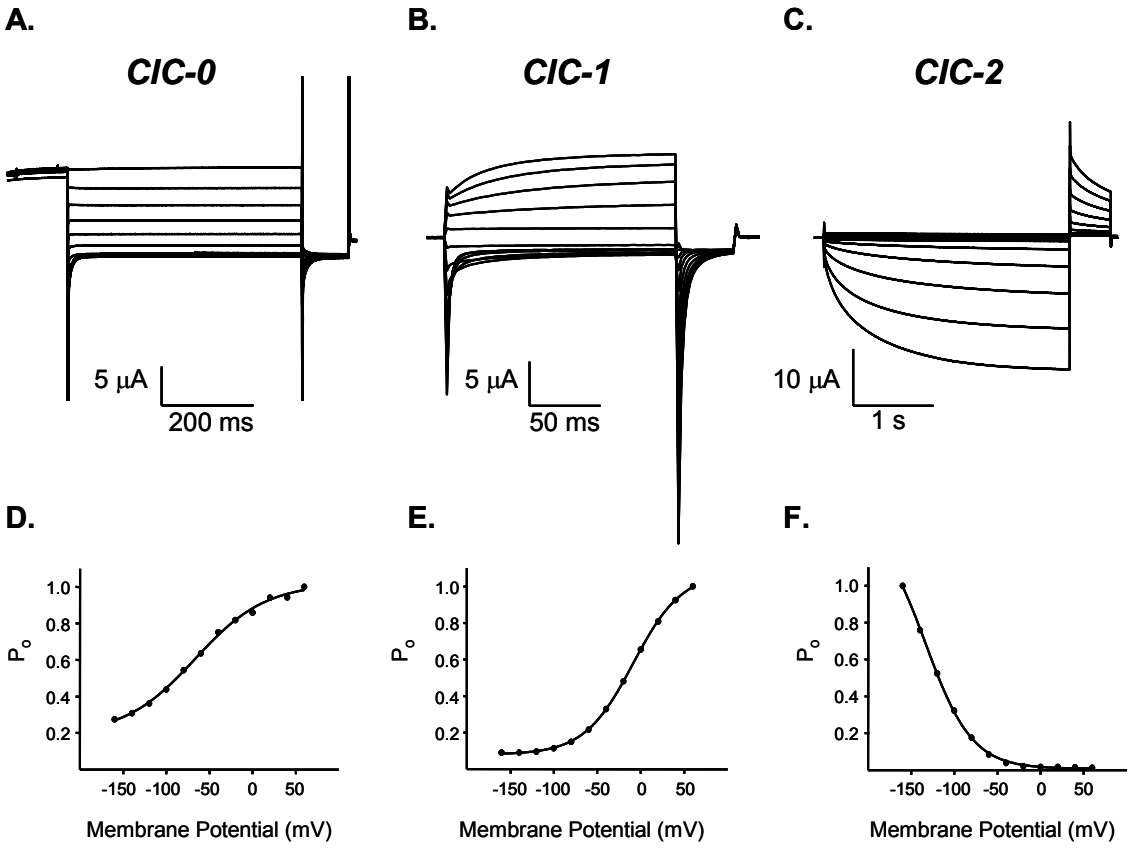

Figure 3: Typical macroscopic behavior of ClC channels. **(A-C)**. Typical macroscopic two-electrode voltage clamp recordings of ClC-0 **(A)**, ClC-1 **(B)**, and ClC-2 **(C)** in response to specific voltage protocols. **(D-F)** Open probability versus voltage curves for the corresponding trace for ClC-0 **(D)**, ClC-1 **(E)**, and ClC-2 **(F)**. Both ClC-0 and -1 are activated by membrane depolarization, as indicated by high open probability at positive membrane potentials. ClC-2 is activated by hyperpolarization. Note that the ClC-2 activation curve never truly saturates, so the true open probability can only be estimated.

In addition to regulation of channel activity by the membrane potential, ClC-0, as well as other ClC channels, is dependent on pH. Hanke and Miller showed before the cloning of the ClC-0 gene that channel activity was dependent on pH, with activity increasing as the external pH decreases [4]. At very negative potentials, protonation of the channel increases the opening rate of the fast-gate, yet has no effect on the closing rate [4, 20], and increases the minimum P_O of the fast-gate to ~0.6 [20]. The effect of protonation is independent of Cl^- concentration, suggesting that the Cl^- dependence and pH dependence of channel activation arise from different regions of the protein [20].

As discussed earlier, ClC channel activity is controlled by two gating mechanisms, a fast gate and a slow gate. Of the two, slow gating is less well understood. While the fast gate controls ion conduction through both channel pores individually, slow gating controls both pores simultaneously. During attempts to discover a peptide inhibitor of ClC-0, Chen found that Zn^{2+} inhibits ClC-0 current in a reversible manner by facilitating the closure of the slow gate [21]. Mutation of residue C212 to serine (C212S) rendered channels insensitive to inhibition by Zn^{2+}, and eliminated the long closed durations associated with closure of the slow gate [22]. Slow gating can also be abolished by the point mutations H736A and E763K, which reside in the intracellular C-terminal domain, specifically in the cystathione β-synthase 2 (CBS2) domain [23]. Investigation into the chloride dependence of slow gating revealed that upon reduction on intracellular $[Cl^-]$, slow-gate activation shifted to more hyperpolarizing potentials, reducing the maximal activation of ClC-0 channels [18].

Macroscopic ClC-0 currents are typified by rapid channel deactivation at very negative membrane potentials, with "crossover" current in this same voltage range (Fig. 3) [11]. However, in some cases atypical behavior is observed, which lacks crossover at hyperpolarizing membrane potentials, especially when ClC-0 channels are expressed in *Xenopus* oocytes and recorded using two-electrode voltage clamp (TEVC). Li and coworkers showed that these atypical currents are related to the oxidation state of the channel; pre-incubation of cells in a reducing agent such as DTT restores typical channel behavior, while incubation in an oxidizing agent can induce abnormal behavior [24]. The same study concluded that the effect of oxidation is on channel slow-gating; channels bearing the C212S mutation are insensitive to the effect of oxidation. It was postulated that channel oxidation reduces the ability of ClC-0 to recover from a state in which the slow gate is closed.

Over the years, ClC-0 has served as the prototype ClC channel, with much of the biophysical knowledge of all ClC channels being derived from these studies. However, there are important biophysical differences between the members of this family which will be discussed in further detail.

1.1.2 ClC-1

1.1.2.1 Biophysical Characteristics of ClC-1

The first mammalian ClC channel that will be discussed is ClC-1. ClC-1 is the main chloride channel present in skeletal muscle plasma membrane, providing greater than 80% of the normal resting membrane conductance [25]. Defects in this channel lead to generalized myotonia and myotonia congenita, which will be discussed further in

section 1.1.2.2 [26-28]. The cDNA encoding the rat skeletal muscle chloride channel, named ClC-1, was identified by homology screening to the *Torpedo* voltage-dependent chloride channel ClC-0. The cDNA encoding rat ClC-1 yields a 994 amino acid protein that is 54% identical to ClC-0 [25, 29]. The human ClC-1 clone was identified by a homology screen to the rat ClC-1, and was localized to chromosome 7 [26].

Macroscopic ClC-1 currents are very similar to those of ClC-0 (Fig. 3B), with a similar P_O/V curve (Fig. 3E), and as will be discussed below, are mediated by both fast and slow gating processes. Channels rapidly deactivate at strongly hyperpolarizing potentials, with P_O increasing as the membrane becomes more depolarized. Unlike ClC-0, it is very difficult to perform ClC-1 single channel recordings due to the very small single channel amplitude. When ClC-1 is transfected into HEK-293 cells, the macroscopic current is very similar to that shown in Figure 3B, albeit with faster gating kinetics. However, non-stationary noise analysis revealed that the single pore conductance of ClC-1 is only ~1pS, approximately 10 fold lower than the single pore conductance of ClC-0 [30]. Therefore, determination of the oligomeric structure of ClC-1 was not initially feasible by site directed mutagenesis in conjunction with single channel recording. Instead, the oligomeric structure of ClC-1 was determined by analysis of dominant negative ClC-1 mutations associated with myotonia congenita [31]. In principle, currents mediated by ClC-1 should be reduced by incorporation of mutant subunits with altered conductance properties into the functional unit of the channel, and the degree to which activity is reduced should depend on the number of mutant subunits incorporated into the channel. The functional unit of channels incorporating G230E subunits appears to be a dimer, reducing channel current to ~35% of WT channels, while P480L subunits tend to

incorporate into tetrameric channels , reducing current to <10% that of WT [31]. Other studies utilizing chemical modifying methanethiolsulfonate (MTS) reagents suggested that ClC-1 was composed of just a single pore [32]. Single channel experiments in *Xenopus* oocytes performed by Saviane and coworkers showed that ClC-1 displayed double-barreled activity similar to ClC-0 [33]. These experiments very beautifully illustrated the two-pore behavior of ClC-1 channels, despite the single pore conductance of just 1.2 pS, and this behavior was well described by a model incorporating a single protein with two independent conductance pathways [33].

Like ClC-0, ClC-1 channels are voltage-dependent channels with very shallow voltage-dependence, $z \sim 0.9$ [30]. Indeed, as previously stated, the macroscopic behavior of ClC-1 is very similar to ClC-0 currents isolating currents mediated by fast gating when the slow gate $P_O \sim 1$(Fig. 3). Also analogous to ClC-0, ClC-1 channels show complicated gating behavior, possessing both a fast and slow gate, although the two gating behaviors are not easily separable, as they are in ClC-0. Unlike ClC-0, CLC-1 channels lack a hyperpolarization-activated slow gate; instead, slow-gating is activated by membrane depolarization. Channel deactivation at very hyperpolarizing potentials is best described by bi-exponential fits, which presumably correspond to the fast and slow-gating processes. These gating processes were initially described by Fahlke and coworkers, who suggested that one gating process acted on the microsecond time-scale, with each pore possessing a single residue, titratable by protons, acting as a voltage sensor, and a separate process acting on the millisecond time-scale [34], both of which were activated by membrane depolarization. The time constants for these gating processes are separated by a factor of ~10, but according to Fahlke and coworkers there is no voltage-dependence

of these gating processes over a voltage range of -195 to -45 mV. Later studies by Rychkov , however, suggested that the fast component of channel deactivation was weakly voltage-dependent, while the slower component was strongly voltage-dependent [35]. Both of these studies were corroborated by Accardi and Pusch [36], showing that at very negative potentials the time constants for fast and slow gating were ~10 fold different, and not voltage dependent, but as membrane potential increased, the gating processes showed strong voltage-dependence with ~100-fold difference in time constants. Moreover, the voltage dependence of ClC-1 gating was qualitatively very similar to that of the fast gating process of ClC-0. Both fast and slow gating processes had Q_{10} values of ~4 – 5, which would suggest a modest structural rearrangement during both gating processes, while shared voltage-dependence would suggest that these gating processes may be coupled [37].

ClC-1 is also regulated by external $[Cl^-]$, and by changes in both external and internal pH. Lowering the extracellular $[Cl^-]$ substantially speeds channel deactivation at negative potentials, and reduces the overall steady-state current level at all voltages [35, 36]. This decrease in current is due to a drastic rightward shift in the P_O/V curve, making stronger depolarization necessary for channel opening [35, 36]. Under normal conditions, the minimum P_O of the slow gate is >0.6; however, upon lowering of $[Cl^-]_{ext}$, minimum P_O is reduced by ~50%, and is accompanied by a > 40 mV rightward shift in the P_O/V curve of the slow gate. This would suggest that current is reduced primarily by increasing the closed duration of the slow gate. Like ClC-0, the cytosolic CBS domains may also play a role in common gating [38], as does residue C277, which when mutated to serine shows complete loss of common gating, similar to the C212S mutation in ClC-0 [39, 40].

Regulation of ClC-1 channels by pH is complex, being affected by both internal and external pH. The effects of internal pH may be further complicated by the presence of ATP. When extracellular pH is decreased, the degree of channel deactivation at hyperpolarizing potentials is decreased, leading to larger steady-state currents according to Rychkov and colleagues. Similar to the effect of low bath pH on ClC-0 activation, low pH leads to an increase in the minimum P_O of ClC-1, raising it from near 0 to ~0.5 [35]. This suggests that ClC-0 and ClC-1 are regulated by pH via a similar mechanism, with the effect of protonation being independent of $[Cl^-]_{ext}$ for both channels [20, 35]. However, these results contradict studies from whole muscle fibers, which showed that G_{Cl} decreased upon extracellular acidification [41, 42]. These disparate results have not currently been reconciled, though the differences between the *in vitro* setting of cultured cells and the *in vivo* environment of intact muscle fibers is likely to play a significant role.

Likewise, regulation of ClC-1 current by intracellular changes in pH is currently a controversial topic. Intense muscle activity is generally associated with intracellular acidification of muscle fibers that stems from the build-up of lactic acid within the cell [41], leading to muscle fatigue and a reduced ability to conduct action potentials. However, it was recently found that this acidification-induced fatigue was counteracted by decreased chloride permeability, thereby making the muscle hyper-excitable [43]. This contradicts previous results by Accardi and Pusch, showing that when ClC-1 is expressed in a heterologous system, reduction of intracellular pH increased ClC-1 current by shifting the P_O/V curve of both the fast and slow gating processes to more hyperpolarizing potentials [36]. However, this was later challenged by Bennetts, who

showed that intracellular acidification shifted slow gating to more depolarized potentials, while fast gating was shifted to more hyperpolarized potentials [44, 45]. Both studies, however, show an increase in steady state current. It is possible that these slightly disparate results are byproducts of experimental systems, as Accardi and Pusch utilized the *Xenopus* expression system, while Bennetts *et al.* performed whole-cell recording of HEK-293 cells. This controversy is further complicated by the notion put forth that inhibition of ClC-1 by binding of ATP, presumably to the cytosolic CBS domains, is greatly enhanced by intracellular acidification [46]. Inhibition of ClC-1 currents by ATP + low pH has been shown in HEK-293 cells by Bennetts and coworkers, as well as *Xenopus* oocytes by Tseng and colleagues [44-46]. However, Zifarelli and Pusch were unable to recapitulate these results in *Xenopus* oocytes using the exact same voltage protocols, clone, and ATP from the same manufacturer [47], and further suggested that ATP has an indirect effect on ClC-1 behavior. Given this current controversy, it is unclear how intracellular acidification may regulate ClC-1 conductance, although it seems likely that the combination of intracellular acidification during exercise and the high [ATP] concentration in cells plays a significant physiological role.

1.1.2.2 Physiological role of ClC-1 and associated pathophysiology

As stated above, ClC-1 provides >80% of the membrane conductance of skeletal muscle tissue. Northern blot analysis revealed that ClC-1 was highly expressed in skeletal muscle, with virtually no expression in other tissues including brain, lung, kidney, and heart [25]. Early experiments, prior to the molecular identification of ClC-1, attempted to determine the localization of the major skeletal muscle Cl^- (G_{Cl}) and K^+ (G_K)

conductances by disruption of the transverse tubular network by equilibrating the fiber in hypertonic glycerol, then returning the preparation to isotonic Ringer's solution. This treatment induced a large reduction in G_{Cl}, while leaving G_K largely intact, suggesting that G_{Cl} is localized to the T-tubules, while G_K resides in the sarcolemma [42]. However, immunofluorescence experiments later showed that ClC-1, the major determinant of G_{Cl}, is distributed along the sarcolemmal surface, and could be immunoprecipitated from sarcolemmal preparations [48]. Furthermore, this expression was not uniform across the sarcolemma, and Papponen and coworkers suggested that expression of ClC-1 at the sarcolemmal surface may be dependent on phosphorylation/dephosphorylation signals, with surface expression of ClC-1 being increased by incubation of cells with the kinase inhibitor staurosporine [49].

Unlike neuronal tissues, which utilize K^+ current to repolarize the cell following an action potential, skeletal muscle fibers rely on Cl^- current mediated by ClC-1 to repolarize the membrane. This is an important physiological feature considering that repolarization of muscle via outward-directed K^+ conductance would lead to K^+ accumulation in the small spaces of muscle fiber and would induce membrane depolarization. This is not an issue if Cl^- currents are the major component of the repolarization phase. However, disruption of ClC-1 mediated Cl^- current is the basis for the genetic disease myotonia.

Myotonia is characterized by muscle "stiffness" which can stem from defects in genes encoding voltage-gated sodium channels and the voltage-gated chloride channel ClC-1 [50]. Mutations in genes encoding these channels are fundamentally different in that mutations in sodium channel genes associated with myotonia are generally gain-of-

function mutations, increasing sodium conductance, while mutations in ClC-1 are loss-of-function mutations, leading to decreased chloride conductance [50. These alterations in channel conductance lead to hyperexcitability of the muscle, which can lead to trains of action potentials stemming from a single nerve stimulation, known as “myotonic runs”, 51, 52]. Myotonia resulting from defects in the ClC-1 channel can be passed on through multiple modes of inheritance; it can be either dominant (myotonia congenita, Thomsen’s disease) [26, 50, 53], or recessive (generalized myotonia, Becker-type myotonia) [26, 50, 53], with specific genotypes varying the severity of the disorder. Clinically, recessive myotonia is more severe than dominant myotonia, as patients with recessive myotonia are homozygous for mutant ClC-2 alleles, which could almost completely knockout chloride conductance in skeletal muscle [53]. Myotonia is also one of the main symptoms of myotonic dystrophy, a multi-systemic disorder, which shows a drastic reduction in the amount of RNA encoding ClC-1 [54, 55].

Specific myotonia-causing mutations associated with ClC-1 were first identified in mice, where it was shown that the gene encoding ClC-1 had been incorrectly spliced to a member of the ETn family of mouse transposons [27, 29]. Subsequently, mutations in human ClC-1 were identified through screening of families showing symptoms of generalized myotonia [26]. Mutations have since been identified in goats [56] and dogs [57], as well. In total, more than 60 myotonia causing mutations in the ClC-1 gene have been identified, the vast majority of which show an autosomal recessive mode of inheritance [50]. These mutations may lead to decreased surface expression of the channel, but many show alterations in channel behavior. For example, Fahlke and coworkers showed that the mutation D136G caused recessive generalized myotonia, and

changed ClC-1 channel biophysics such that instead of fast deactivation at hyperpolarized potential, channels activated very slowly at these potentials, creating an inwardly rectifying current [58]. The mutations I290M, R317Q, P480L, and Q552R, associated with dominant myotonia, drastically shift channel gating to more positive potentials, generally reducing channel P_O within the physiological voltage range [58, 59]. Finally the mutation G230E shows altered permeability, with an increase in Na^+ conductance, and overall reduction in Cl^- conductance [31].

As has been illustrated above, ClC-1 plays a critical role in muscle physiology. This channel is essential to normal muscle function, plays a role in the onset and recovery from muscle fatigue, and is mutated in the genetic disease myotonia. As will be described in section 1.4, knowledge gained from studying both the physiological role of WT channels, and understanding the biophysical characteristics of both the WT and mutant channel have provided invaluable insights into ClC channel structure and dynamics.

1.1.3 ClC-2

1.1.3.1 Biophysical characteristics of ClC-2

The second mammalian member of the ClC family to be identified was ClC-2. Like ClC-1, mRNA encoding ClC-2 was identified by screening cDNA libraries using a cDNA encoding the rat skeletal muscle channel ClC-1 as a probe [60]. Initial screening identified an identical novel Cl^- channel encoding mRNA in both rat heart and brain. Sequencing revealed a 3217 bp transcript encoding a 907 amino acid protein with a predicted molecular mass of ~99 kDa [60]. Additionally, Northern blot analysis revealed that ClC-2 mRNA was found nearly ubiquitously, being present in skeletal muscle, heart,

lung, kidney, pancreas, stomach, intestine, and liver [60]. ClC-2 was also identified in multiple human cell lines that are regularly used as model experimental systems. Comparison of the amino acid sequence revealed that ClC-2 is 49% identical to ClC-0 and 55% identical to ClC-1 [60] (Fig. 1).

Initial biophysical characterization of ClC-2 currents was performed by expression of rat ClC-2 in *Xenopus* oocytes, with currents recorded via TEVC. Like other channel members of the ClC family, ClC-2 is a voltage-gated Cl^- channel. However, Thiemann and colleagues showed that, unlike both ClC-0 and ClC-1, ClC-2 currents were activated very slowly upon membrane hyperpolarization, but only when potentials were stronger than -50 mV (Fig 3C) [60]. Full activation of ClC-2 at very hyperpolarizing potentials took longer than 20 seconds. Almost no activation was observed at more physiological potentials, and channel deactivation was observed upon stepping to a non-activating potential (*e.g.* +40 mV) immediately following channel activation, as shown in Figure 3C. Analysis of the P_O/V curve obtained from TEVC experiments in *Xenopus* oocytes shows that ClC-2 never achieves maximal activation in this experimental system, even at very negative membrane potentials, and a $P_O \sim 1$ is never reached within the voltage range that can accurately be applied to an oocyte. Ion selectivity of ClC-2 is also similar to other ClC channels, maintaining both a permeability and conductance sequence of $Cl^- > Br^- > I^-$ [60, 61]. ClC-2 gating is very complex. In addition to being a voltage-gated Cl^- channel, gating is also modulated by other factors including external pH and cell swelling upon exposure to hypotonic conditions [62].

The basic architecture of the ClC-2 channel was initially suspected to be homodimeric, based on the high degree of homology to both ClC-0 and ClC-1, which had

been shown to be double barreled ion channels via single channel recordings [10, 33], and a shared predicted membrane topology [7, 25]. Early characterization of purified ClC-2 from Sf9 membranes reconstituted into lipid bilayers by Ramjeesingh *et al.*, suggested that ClC-2, like ClC-0, showed double-barreled open channel activity, with the minimum functional unit being ClC-2 dimers [63]. However, it was also suggested that activity of a ClC-2 dimer resembled a single pore, with double-barreled activity becoming apparent only when a ClC-2 tetramer was formed. Additionally, the unitary conductance was calculated to be 32 and 64 pS for each open level [63]. A number of investigators now have shown these conclusions to be incorrect, and may have been a byproduct of the expression system. Recording of ClC-2-like current in astrocytes [64], ClC-2/ClC-2 concatamers [65], and single channel recording of WT ClC-2 channels in *Xenopus* oocytes (Fig. 2A), have shown that ClC-2 channels do indeed show double-barreled activity as a dimer, with a unitary conductance of ~3 and 6 pS, 10-fold lower than the calculated values from Sf9 membranes fused to lipid bilayers [63]. Furthermore, inspection of ClC-2 single channel currents reveals that similar gating mechanisms exist for the ClC-2 channel, *i.e.* channels possess both a fast gate and a slow gate, as indicated by both long closured between bursts, and rapid transitions between conductance levels within a burst (Fig. 2A) [64, 65]. However, like ClC-1, the low conductance of ClC-2 channels has thus far precluded highly analytical single channel analysis. Thus analysis of ClC-2 gating has relied on other techniques.

The detailed gating mechanisms of ClC-2 have only recently been elucidated. It has long been known that the time course of activation of ClC-2 is best described by the sum of two exponentials [60, 61]. The proposal that ClC-2 possesses both fast and slow

gating processes is supported by mutational studies performed initially in the lab of F. Sepulveda. In ClC-0, two specific point mutations have been identified that independently affect either fast or slow gating; E166A, which eliminates fast-gating [14], and C212S, which eliminates slow gating [22]. Equivalent mutations were made in ClC-2 channels, E217A and C256S, and analysis of macroscopic current revealed constitutively active channels with altered channel kinetics, altered dependence on external pH, and reduced the inhibitory effect of Zn^{2+}, suggesting the presence of two gating mechanisms in ClC-2 channels [66, 67]. De Santiago and coworkers examined fast and slow gating using voltage protocols specifically designed to separate these two gating processes [68]. These experiments revealed that fast and slow gating share the same voltage-dependence, with about a 10-fold separation of the time constants for these processes [68]. Interestingly, the amplitudes of these gating steps show opposite voltage-dependence, with fast gating showing diminished contribution at more depolarizing potentials, while fractional contribution of slow gating increased. Open probability of the fast-gate reaches a P_O of 0 at depolarizing membrane potentials, while the minimum P_O of slow gating is ~0.6 . De Santiago further analyzed the specific effects of the gating mutations described above. While those equivalent mutations only affect either fast or slow gating in ClC-0, in ClC-2 they affect both gating processes simultaneously [68], suggesting that not only are fast and slow-gating linked in terms of voltage-dependence, but they may also share a physical link. Like ClC-1, the Q_{10} values for both fast and slow gating for ClC-2 are ~4 – 5, consistent with a similar degree of structural change. Additionally, the mutation H811A located in the CBS2 domain, the equivalent of which was shown to remove slow gating in ClC-0, alters both fast and slow gating in ClC-2 channels [69]. The theory of a

physical coupling between fast and slow gating has not been rigorously tested, but also seems likely given lack of a mutation in ClC-2 that singularly effects either fast or slow-gating.

As stated above, ClC-2 currents are activated by membrane hyperpolarization, and can be further activated by hypotonicity, which shifts the voltage-dependence of activation to more depolarizing potentials and increases the activation rate of the channel. Through the use of channel chimeras constructed from ClC-2 and either ClC-0, or -1, Grunder and coworkers determined that the N-terminal domain, localized to a region between residues 16-61, is responsible for swelling-induced currents, as well as voltage-dependence of channel activation [70]. However, the effect of this N-terminal deletion on voltage-dependence of activation is still unclear; when currents from this construct are recorded using inside-out macropatches, they appear to still be both voltage- and time-dependent [67]. Further evaluation of the contribution of the N-terminal domain to channel gating is needed in order to clarify this apparent contradiction.

Similar to other ClC channels, ClC-2 currents can also be potentiated by extracellular acidification. Acidification of the bath solution to just pH 6.5 led to a large population of channels that were constitutively active at -38 mV, which was not observed at pH 7.5 [62, 71]. This is of particular importance because this shifts the voltage-dependence of activation to well within the physiological voltage range. Also, raising the pH to 8.0 inhibited ClC-2 currents by shifting the voltage-dependence of activation to more hyperpolarizing potentials [62]. Further analysis of the effect of protonation state on ClC-2 currents revealed a bimodal dependence on proton concentration. A very high proton concentration associated with a pH of 5.5 inhibited channel currents, rather than

potentiated them [72]. Early quantitation of this phenomenon suggested that ClC-2 contains multiple protonation sites, one which activates the channel with a pK of 7.3, and a second one with a pK of 6.0, where protons inhibit channel activity . Furthermore, the effect of channel protonation is dependent on the state of channel activity; if the pH is decreased to 5.5 when the channels are in the closed state, current is reduced upon channel reactivation. However, if pH is decreased to 5.5 while the channels are in the open conformation, current is transiently increased, then slowly returns to the basal current level obtained at pH 7.4 [72]. This type of state-dependence is not observed if the pH is raised above 7.4, suggesting the protonation of the second site is dependent on channel conformation. Interestingly, according to Grunder, deletion of the N-terminal region between residues 16 – 61 also removes the pH dependence of ClC-2 channel activation, although experiments performed by Varela and coworkers using whole-cell recording of HEK-293 cells expressing ClC-2 suggests that this may not be the case [70]. The differences in experimental system between oocytes and HEK cells may be an important factor, as HEK cells more likely represent a more physiologically relevant environment, although the recording technique is usually associated with complete dialysis of cell contents, possibly removing vital cellular factors. Regulation of ClC-2 by pH appears more complicated than for other members of the ClC family, with multiple proton binding sites, which may reflect the wide array of tissues in which ClC-2 is expressed.

A well-characterized trait of ClC gating is its regulation by the permeant ion. For ClC-0 and -1, gating is regulated by changes in the extracellular chloride concentration [11, 20, 35]. ClC-2 activity, however, is only modestly controlled by the extracellular

anion concentration. Reduction of $[Cl^-]_{ext}$ to 1 mM increased ClC-2-mediated inward currents in *Xenopus* oocytes by increasing the number of active channels at the holding potential, presumably by shifting channel activation to more depolarized potentials [18]. This is in contrast to both ClC-0 and ClC-1, which exhibited reduced macroscopic currents upon reduction of the extracellular Cl^- concentration [20, 35]. Changing in the intracellular chloride concentration, which had no significant effect on currents mediated by either ClC-0 or -1, can drastically alter ClC-2 channel gating. Pusch and coworkers showed that increases in $[Cl^-]_{int}$ dramatically shifted the channel activation to more depolarizing potentials [18]. However, it is unknown which gating process is affected by changes in chloride concentration, because fast and slow gating only recently have been separately biophysically characterized. This opposite dependence of channel gating on $[Cl^-]$ may be related to the fact that ClC-0 and ClC-1 mediate mainly chloride influx, while ClC-2 serves as a chloride efflux pathway.

It is now coming into focus that ClC-2 channels are dependent on the nature of the lipid environment in which they are expressed. Vastly different activation kinetics may be observed if you express ClC-2 in oocytes, which displayed very slow activation kinetics, versus mammalian cell systems, where ClC-2 is activated much more rapidly [60, 61, 67, 68]. Hinzpeter and colleagues showed that channel kinetics may be significantly slowed in HEK-293 cells upon enrichment of the cell membrane with cholesterol [73]. Likewise, channel activation kinetics may be enhanced upon depletion of cholesterol. Regulation of ion channel activity by membrane composition is now becoming a common theme among many types of ion channel families; it is therefore no surprise to find that members of the ClC family are likewise regulated [74].

1.1.3.2 Physiological role of ClC-2 and associated pathophysiology

The precise physiological role of ClC-2 is largely still unknown. As stated above, this channel is expressed nearly ubiquitously [60, 75]; however, the subcellular localization is a matter of contention in the field. ClC-2 has been identified on the apical membrane in intestinal tissue of mice and humans [76, 77], as well as lung epithelia [78, 79], where it may participate in Cl^- secretion. Expression of ClC-2 at the apical membrane of the lung epithelia, where it may participate in Cl^- efflux, where it may exist along side the cystic fibrosis transmembrane conductance regulator (CFTR) is an attractive hypothesis [79], because defects in CFTR alter Cl- conductance in lung epithelia, leading to the devastating disorder cystic fibrosis. However, other studies have proposed a basolateral localization of ClC-2 in rat small intestine and guinea pig colon [6, 80, 81], where it would play a substantial role in NaCl absorption by mediating Cl^- exit across the basolateral membrane. Convincing data have been provided by Pena-Munzenmayer and colleagues, showing that native ClC-2 was exclusively localized to the basolateral membrane of surface colonic cells, as well as in MDCK and Caco-2 cell lines when transfected with a construct encoding human ClC-2-GFP [81]. Furthermore, localization to the basolateral membrane was mediated by a dileucine motif (L812/L813); mutation of these residues to alanine altered ClC-2 localization such that it was expressed on the apical membrane [81]. Indeed, localization of ClC-2 in epithelial cell has become a hotly debated topic. The possibility has not been addressed that ClC-2 may have altered membrane localization which is dependent on the specific cell type in which it is expressed. It has been shown that ClC-2 interacts with the heat shock proteins Hsp70 and

Hsp90 *in vitro*, and with Hsp90 in mouse brain, and that this interaction may play a role in ClC-2 trafficking [82]. Interaction with specific chaperones in certain cell types would suggest that cell type specific trafficking may be likely.

In addition to being expressed in cell types of epithelial origin, ClC-2 is also expressed in cardiac tissues. RT-PCR analysis has shown that ClC-2 mRNA is present in atrial and ventricular cardiac tissue, while immunohistochemistry confirms protein expression in these tissues with a distribution in the sarcolemmal membranes [75, 83]. One proposed role of ClC-2 in cardiac cells is cell volume regulation [83]. Proliferation of vascular smooth muscle cells requires high rates of both mitosis and migration, which require changes in cell volume. Consistent with this, Cheng and coworkers showed that IGF-I induced proliferation of these cells is suppressed by the Cl^- channel inhibitor NPPB, but not DIDS, consistent with ClC-2 mediated Cl^- currents. Proliferation of vascular smooth muscle cells was also inhibited by siRNA treatment directed against ClC-2 [84]. Indeed, novel cardiac ClC-2 splice variants have been identified in both rat and guinea pig [75]. Britton and coworkers showed that these alternately spliced ClC-2 variants encode proteins with deletions of either 15 amino acids (Δ509-523) in rats, or 35 amino acids (Δ509-543) in guinea pigs. These channels activated with properties similar to full length channels, and are inhibited by anti-ClC-2 antibodies, which was critical for the identification of these currents as *bona fide* ClC-2 mediated currents [75].

It has been postulated that ClC-2 channels may be involved in signal transduction cascades. Tewari and colleagues suggested that ClC-2 channels are activated by cAMP-dependent protein kinase A (PKA), and arachadonic acid when expressed in HEK-293 cells, as well as in cell lines in which ClC-2 is endogenously expressed [85]. In addition

to activation by PKA, Cuppoletti has proposed that ClC-2 is activated by the bicyclic fatty acid lubiprostone when expressed in T84 cells, an intestinal cell line, which the authors propose would increase Cl^- secretion, and reduce constipation [86]. These results are highly questionable considering that the currents obtained by whole-cell recording in these cell types show no resemblance to typical ClC-2 mediated currents; they show no inward rectification, lack time-dependent activation at hyperpolarizing potentials, and have an incorrect permeability sequence ($I^- > Cl^-$). The lubiprostone data are additionally suspect considering the fact that ClC-2 showed basolateral localization in the intestine. Activation of ClC-2, if localized to the basolateral membrane, would lead to increased Cl^- uptake, exacerbating constipation. It is also unlikely that lubiprostone directly acts on its target, as its effects take >20 minutes to be observed.

Northern blot analysis also has shown ClC-2 mRNA to be present in brain tissue [60]. A hyperpolarization-activated current with properties similar to ClC-2 was identified in hippocampal pyramidal neurons. *In situ* hybridiztion confirmed that ClC-2 is expressed in these neurons, as well as in Purkinje neurons and in the epithelium of the choroid plexus [87]. In these neurons, ClC-2 functions as a chloride efflux pathway in order to stabilize E_{Cl} below the resting membrane potential [87]. The physiological role for this channel was confirmed in dorsal root ganglion (DRG) neurons by *de novo* expression of ClC-2. Over expression of ClC-2 in these neurons had no significant effect on the resting membrane potential, but reduced the amplitude of the GABA mediated response, and completely eliminated action potential firing, which is consistent with the notion that ClC-2 stabilizes E_{Cl} such that GABA receptor activation produced an inhibitory post-synaptic response in pyramidal neurons [88]. Furthermore, ClC-2 is only

expressed in a subset of neurons, suggesting a highly regulated role in neuronal physiology.

In large part, the physiological role of ClC-2 is still largely undefined due to the fact that the phenotype of ClC-2 knockout animals does not echo the diverse expression pattern of ClC-2. Complete knockout of ClC-2 leads to severe retinal and testicular degeneration [89], as well as leukoencephalopathy [90]. Knockout of ClC-2 led to altered morphology of Sertoli cells and disruption of the retinal pigment epithelium [6]. Homozygous knock-out of ClC-2 also led to the formation of fluid filled vacuoles between myelin sheets of central neurons [90]. In all cases, elimination of ClC-2 led to the disruption of the blood-testes barrier, blood-retina barrier, and the blood-brain barrier. It was proposed that ClC-2 regulated ion homeostasis in narrow extracellular spaces [89-91]. However, it should be pointed out that complete knockout of a nearly ubiquitously expressed protein may lead to unexpected consequences.

A number of mutations in the gene encoding ClC-2 have been identified which are associated with idiopathic generalized epilepsy, although the role of ClC-2 mutations as causative to an epileptic phenotype is controversial. Originally, three epilepsy-associated mutations were identified in the ClC-2 gene [92]. Two mutations were truncation mutations; one introduced a stop codon in transmembrane helix F (M200fsX231) (Fig. 4), while another was a deletion of most of helix B (Δ74-117). Neither ClC-2 mutation produced functional channels, although both were localized to the plasma membrane of tSA-201 cells. Non-functional ClC-2 channels would thus lead to intracellular chloride accumulation, and push E_{Cl} toward threshold potential, and could result in excitatory, rather than inhibitory GABA responses . However, expression of

these truncation mutations at a 1:1 ratio with WT ClC-2 subunits in HEK cells did not reduce current density compared to expression of just WT subunits. Additionally, confocal microscopy of HEK-293 cells expressing just the truncation mutants showed that they do not reach the plasma membrane [93]. The difference between the tsA-210 cell data and HEK cell data have not currently been addressed. Niemeyer and coworkers suggest that haploinsufficiency may one mechanism by which these mutations are associated with epilepsy. The third mutation identified was a point mutation, G715E, which led to a depolarizing shift in the channel P_O/V curve, such that more channels would be open at less hyperpolarizing potentials [92]. This mutation would result in errant chloride efflux during membrane repolarization, and thus hyperexcitability that could result in increased seizure frequency. In HEK cells, however, the effects of this mutation on channel gating could not be recapitulated [93]. Additionally, ClC-2 knock-out animals do not show increased seizure susceptibility, as would be expected from the loss-of-function mutations described above, suggesting that mutations in the ClC-2 gene may not be causative to epilepsy, but may possibly be part of a polygenic mutational epileptic disorder [90]. Mutations in the ClC-2 gene associated with epilepsy are extremely rare, but may act as a susceptibility locus [94, 95].

Finally, data suggesting that ClC-2 is expressed at the apical membrane of lung epithelial cells has generated much interest in the possibility that ClC-2 may act as an alternate Cl^- efflux pathway for patients afflicted with the genetic disorder cystic fibrosis (CF) [79], which results from mutations in the CFTR chloride channel. CF is a disease characterized by severe lung, pancreas and intestinal symptoms, including chronic lung inflammation and infection, as well as intestinal blockage [96]. This disease is the most

common lethal autosomal recessive disorder among Caucasians [96], with the most common mutation being a deletion of F508 (ΔF508), which leads to misfolded CFTR that does not reach the plasma membrane in humans [97]. Advances in therapeutics have reduced the severity of the intestinal symptoms, and as a result, mortality results from complications from the lung disorder. CF leads to reduced volume of the airway surface liquid (ASL) stemming from reduced chloride secretion through CFTR [96, 98]. The reduction in volume of the ASL leads to the formation of thick mucus at the lung epithelium, and reduced mucociliary clearance, which results in chronic infection from colonization by *Pseudomonas aeruginosa* . It was proposed that ClC-2 may act as an alternate Cl^- efflux pathway, leading to increased ASL volume, and relieve the CF phenotype. Zdebik and coworkers postulated that knockout of ClC-2 in a ΔF508 homozygous background should increase the death rate in mice if ClC-2 acted as an alternate Cl^- transport pathway in the lung. These mice did not show a higher death rate than CFTR ΔF508 mice alone; in fact, survival was marginally better in the double mutant, leading to the speculation that ClC-2 is localized to the basolateral membrane, and would not serve as an alternate Cl^- efflux pathway [99]. However, it should be pointed out that mice bearing the ΔF508 mutation do not suffer from a lung disorder, and that functional ΔF508 is able to reach the plasma membrane in murine cells [97]. Therefore, the possibility remains that activation of ClC-2 in a human CF patient may provide some benefit.

Given the nearly ubiquitous expression of ClC-2, it is likely that this channel plays a vital role in many cellular processes. It has been shown to play a critical role in neuronal physiology, and is suspected to play a major role in epithelial cells and cell

volume regulation. However, many basic aspects of ClC-2 physiology are still undefined, as are many of the biophysical characteristics of the channel.

1.1.4 ClC-K

1.1.4.1 Biophysical characteristics of ClC-K channels

Two research groups nearly simultaneously cloned the two members of the ClC-K subfamily. Uchida and coworkers cloned the first isoform from rat kidney, ClC-K1, via an RT-PCR cloning strategy using primers designed against regions of cDNAs encoding ClC-0, -1 and -2 that are completely conserved [100]. Kierferle and colleagues, utilizing a similar cloning strategy, likewise identified ClC-K1, but also cloned another isoform named ClC-K2 from rat; highly related human homologues were also identified in this same study, named ClC-Ka and ClC-Kb [101]. Evolutionarily, the ClC-K channels represent a ClC subfamily, having diverged from ClC-0 prior to the divergence of ClC-1 and -2 from ClC-0 (Fig. 1). Rat ClC-K1 and -K2 are 80% identical to each other, while the human isoforms bear 90% identity to each other [100, 101]. Sequence analysis has revealed that ClC-K1 corresponds to the human ClC-Ka, while ClC-K2 is equivalent to ClC-Kb. Northern blot and RT-PCR analysis showed that both ClC-K isoforms are predominantly expressed in the kidney [100-102], although some expression was later identified in the ear.

Quantitative biophysical characterization of ClC-K channel isoforms has lagged far behind that of other ClC channels. Initial characterization of these channels was very limited shortly after the channels were cloned, as only ClC-K1 produced currents that were distinguishable from endogenous channels when injected into *Xenopus* oocytes

[100, 101]. Unlike any other ClC channel characterized, ClC-K1 showed only slight outward rectification, and almost no time-dependent component to channel activation [100]. Because of the lack of time-dependent activation, and the near linearity of channel currents, the ClC-K subfamily is largely considered voltage-independent, although some studies suggest the voltage-dependence of activation may be shifted out of the physiological voltage range [53, 103]. In fact, of all the ClC proteins, the ClC-K isoforms are the only members of the ClC family that lack the glutamate residue which is thought to the major determinant of fast gating; this residue is substituted by valine in the ClC-K subfamily [103]. Waldegger and Jentsch showed that introduction of this fast-gate glutamate residue, by making the V166E mutation in ClC-K1, drastically altered channel gating. V166E-ClC-K1 channels were time-dependent, showing very slow activation upon membrane hyperpolarization [103]. Thus, introduction of this conserved glutamate residue into the ClC-K1 channel at a site homologous to that of the conserved glutamate in ClC-0 was enough to introduce voltage-dependent gating.

The regulation of other ClC channel family members by the extracellular *milieu* has been well described, especially regulation by extracellular pH and chloride concentration, as described in the previous sections. Uchida and coworkers showed that ClC-K1, like other members of the ClC channel family, is regulated by extracellular pH. However, unlike other CLC channels, which are inhibited by extracellular alkalinization and potentiated by extracellular acidification, ClC-K1 was inhibited by acidification and potentiated by alkalinization [104]. The molecular determinants by which ClC-K1 is regulated by extracellular pH current are not known; the V166E mutation had no significant effect on pH-dependent regulation of these channels [18]. Surprisingly,

Uchida and coworkers showed that ClC-K1 is potentiated by the presence of extracellular Ca^{2+}; complete removal of Ca^{2+} from the bath solution reduced current density in *Xenopus* oocytes expressing ClC-K1. Injection of EGTA into the oocyte, effectively reducing $[Ca^{2+}]_{int}$ to 0, had no effect on ClC-K1 mediated currents, indicating that the effect of Ca^{2+} is restricted to the extracellular face of the channel [104]. Further investigation into this matter by Waldegger and Jentsch showed that increasing $[Ca^{2+}]$ up to 5 mM increased ClC-K1 mediated currents [103]; this effect was not a non-specific effect of divalent cations, as addition of 5 mM Mg^{2+} or Ba^{2+} had no effect. The V166E mutation likewise has no effect on Ca^{2+} regulation of ClC-K1 mediated currents. No other member of the ClC family has been shown to be directly regulated by extracellular Ca^{2+}.

Interestingly, injection of cRNA encoding ClC-K1 into oocytes yielded no current unless a 5'-untranslated sequence from ClC-0 replaced the first ATG in the ClC-K1 sequence [100]. Injection of cRNA encoding other ClC-K isoforms yielded currents that were indistinguishable from currents endogenously found in oocytes [101]. Keiferle and coworkers found, via immunoprecipitation, that all ClC-K proteins were made by the oocyte, but were not conductive, suggesting that an auxiliary subunit may be required for proper channel function [101]. This β-subunit was identified by Estevez and colleagues by positional cloning, and named barttin [105]. Barttin is a 320 amino acid integral membrane protein with two transmembrane helices, a relatively short cytosolic N-terminus, and a large C-terminal domain that contains a PY motif [105]. Co-expression of ClC-Ka or –Kb with barttin induced large currents with conductance sequences of $Cl^- > Br^- > I^-$ for both channels [105]; expression of just barttin alone did not induce currents

larger than endogenous background current, nor did barttin have any effect on ClC-1 or ClC-2 mediated currents [105]. ClC-K1 currents also were enhanced by co-expression of barttin [105, 106]. As for ClC-K1, ClC-Ka and -Kb currents were potentiated as extracellular pH is increased when these channels were co-expressed with barttin. Currents mediated by these channels also were increased by elevated $[Ca^{2+}]_{ext}$. Interestingly, deletion of the PY motif by truncation of the C-terminus destroys barttin function [105]. Scholl and coworkers have found that barttin serves to control both trafficking and conduction properties of ClC-K channels. The transmembrane region of barttin promotes surface expression of ClC-K, while the large C-terminus is important for controlling unitary conductance and open probability [107]. Interestingly, a common polymorphism in the ClC-Kb channel, T481S, shows large currents in the absence of barttin; mutation of the equivalent residue in both ClC-Ka and ClC-K1 also led to large, barttin independent currents [108]. The authors suggested that increased current mediated by this channel may be a result of increased open probability, due to the fact that the change in surface expression is not enough mediate such a large change in current density [108].

Unlike other ClC channels, there is thus far no consensus regarding the unitary conductance of any of the ClC-K channels. This is largely due to the lack of convincing single channel data of any ClC-K channel, either in the absence or presence of barttin. ClC-K1 currents have been purportedly obtained from reconstitution of vesicles from rabbit distal tubules into lipid bilayers; a 14 pS conductance was observed that was inhibited by extracellular acidification [109]. This channel also was potentiated by increases in $[Ca^{2+}]_{ext}$, although regulation of this current by Ca^{2+} did not occur within the

same concentration range as observed for ClC-K1 expressed in heterologous systems, as no effect was observed until the Ca^{2+} concentration was raised above 20 mM in the bilayer system [109]. Lourdel and coworkers examined a chloride conductance isolated from mouse distal convoluted tubule. This current showed a single channel conductance of 9 pS, and also was inhibited by extracellular acidification and potentiated by extracellular alkalinization [110]. The molecular identity of this channel was unknown, with no accompanying biochemical data, although both ClC-K1 and -K2 are expressed the distal convoluted tubule [110]. Scholl and colleagues performed non-stationary noise analysis on V166E-ClC-K1, and calculated a unitary conductance of 6.5 pS in the absence of barttin, and 19.4 pS in the presence of barttin [107]. It is possible that these data all represent single channel currents from ClC-K channels under various conditions; it is likely that recording obtained from kidney tissue represents both the channel and barttin. None of these studies showed the presence of clear double-barreled activity associated with other ClC channels, however. Clear characterization of this channel at the single channel level, from heterologous systems, is needed in order to clarify the properties of the channel, including conductance properties, gating behavior, and oligomeric structure.

1.1.4.2 Physiological role of ClC-K and associated pathophysiology

The ClC-K channels have a well defined role in renal physiology. Both the rat and human homologues were cloned from kidney, and have been localized in rodents to both the thin ascending limb of Henle's loop (ClC-K1, -Ka), and the medullary thick ascending limb of Henle's loop and distal collecting duct (ClC-K2, -Kb) [100-102, 104].

Uchida and colleagues showed that ClC-K1 is expressed on both the apical and basolateral membrane, where it provides transepithelial chloride conductance across the kidney epithelium in the thin ascending limb, which bears the highest chloride permeability of any of the nephron segments [104]. Kobayashi and coworkers showed that expression of ClC-K1 is very highly developmentally regulated. In the early prenatal stage, ClC-K1 not was present in the thin ascending limb of Henle's loop, but it started to appear five days after birth, which coincided with increased urine concentrating ability [111]. Increased expression of ClC-K1 was associated with decreased NKCC2 expression [111]. In the medullary thick ascending limb, the nephron segment that is specialized in NaCl reabsorption, ClC-K2 (-Kb) is expressed on the basolateral membrane where it mediates chloride efflux [112, 113]. These channels have been identified in the inner ear as well, where they localize to the basolateral membrane of marginal cells of the cochlea [114]. ClC-Ka/Kb channels mediated chloride recycling across the basolateral membrane of strial cells to provide a counterion pathway for the Na,K-ATPase [114].

There is one report identifying both ClC-Ka and Kb in human lung. Mummery and workers identified, in Calu-3 cells, a chloride conductance that is regulated by both pH and extracellular Ca^{2+} as has been previously described for ClC-K channels in heterologous systems [115]. RT-PCR and western blotting confirmed the presence of mRNA encoding ClC-K channels and the β-subunit barttin, as well as protein for both human ClC-K isoforms and barttin. It is important to note that barttin has been shown to colocalize with ClC-K channels in all native tissues in which it is found [105, 106], further supporting the notion that this subunit is absolutely essential for normal endogenous ClC-K channel function.

Mutations in the genes encoding ClC-K channels, as well as the barttin subunit, are associated with the genetic disorder Bartter's syndrome. Bartter's syndrome is characterized by either a severe reduction or complete loss of salt absorption in the thick ascending limb of Henle's loop [116, 117]. This results in salt wasting, hypokalemic metabolic alkalosis, and possibly low blood pressure [116, 118]. There are five types of Bartter's syndrome, all of which are autosomal recessive disorders [116]. Of the five types of Bartter's syndrome, two are associated with mutations encoding either ClC-Kb (type III Bartter's syndrome) [119, 120], or barttin (type IV Bartter's syndrome) [121, 122]. The mutations associated with type III Bartter's syndrome are associated with large deletions, as well as nonsense and missense mutations of the ClC-Kb gene [116, 119, 120]. Mutations in ClC-Kb drastically reduced salt absorption in the thick ascending limb of Henle's loop, although there have been no biophysical studies of known ClC-Kb polymorphisms to show whether there are severe alterations in chloride conduction properties, or altered interactions with barttin [120]. Interestingly, there are no mutations in ClC-Ka associated with Bartter's syndrome.

Bartter's syndrome type IV, stemming from mutations in the gene encoding barttin, *BSND*, is a more severe clinical disorder than Bartter's type III. This disease manifests in renal failure and sensorineural deafness [121, 122]. It has been well established that barttin is essential for the correct function of ClC-K channels in all ClC-K expressing cell types in which they have been studied [105]. Mutations in barttin, therefore, would affect channel function in all cell types. Hayama and coworkers showed that mutations in barttin drastically reduced surface expression of ClC-K2 [122], while Waldegger and colleagues showed decreased current density from ClC-K1 when co-

expressed with a barttin subunit bearing single point mutations that are sufficient to induce Bartter's syndrome type IV [106]. The lack of ClC-K1 surface expression resulting form mutant barttin results in impaired Cl^- transport throughout the thin and thick ascending limbs of Henle's loop, which leads to complete renal failure. In the inner ear, these channels act to mediate Cl^- exit through the basolateral membrane of strial cells, to reduce Cl^- accumulation in the cytoplasm as a result of import through NKCC1 [114, 123]. Under normal conditions this Cl- recycling allows transport of K^+ into the cytoplasm, which is then exported out of the apical membrane via KCNQ1/KCNE1 K^+ channels, leading to a high $[K^+]_{ext}$, which is necessary for the depolarization of sensory hair cells. Reduction of ClC-K channel surface expression via barttin mutations indirectly reduces the $[K^+]_{ext}$, and prevents depolarization of hair cells, causing deafness [53, 114].

As discussed earlier, the T481S mutation in ClC-Kb yields channels that both express at the cell surface and function in the absence of the accessory protein barttin [108]. Jeck and coworkers identified this mutation in ~20% of patients in a study incorporating 200 people [108]. This gain-of-function mutation would theoretically lead to alterations in salt-handling in the nephron, and has been shown to contribute to elevated blood pressure in Dahl rats, which serve as a model system for salt-sensitive hypertension. In addition to possible effects on blood pressure, Frey and colleagues showed that this mutation also lowered hearing threshold, and may serve a protective role against hearing loss [123].

Interestingly, there are few physiological consequences manifesting only from mutations of the gene encoding ClC-K1 (-Ka). The only real effects of lack of ClC-K1 are revealed in data from knockout animals. As expected from the localization of this

channel in the thin ascending limb of Henle's loop, knockout of ClC-K1 led to nephrogenic diabetes insipidus (NDI), a disorder characterized by the production of a large amount of dilute urine [124]. Loss of ClC-K1 led to a 50% reduction of the sodium and chloride content of the inner medulla, as well as a reduction in urea accumulation. This finding suggests a novel mechanism for NDI, as most cases result from loss-of-function mutations either in the vasopressin V2 receptor, or the aquaporin AQP-2 channel [124].

Like other ClC channels, the importance of ClC-K channels is demonstrated from pathophysiology associated with these channels. Correctly assembled ClC-K/barttin complexes are necessary for proper kidney function and hearing. Despite a large amount of data describing the physiological role of these channels, many of their biophysical characteristics need more study. The lack of a consensus regarding the single channel behavior of ClC-K channels needs to be addressed, as does the oligomeric structure of these channels.

1.2 Properties and physiology of ClC exchangers

As discussed above, several members of the ClC protein family function as voltage-dependent chloride channels. However, it has recently come to light that many of these proteins mediate Cl-/H+ exchange rather than voltage-dependent anion channel activity. Unlike their channel counterparts, the exchanger subtypes are generally found on intracellular membranes. In mammals it is generally accepted that ClC-3,-4, -5, -6, and -7 are exchangers. Like ClC channels, however, the canonical exchanger is not mammalian, but instead is a bacterial ClC protein, ClC-ec1. In this section, the biophysics of these

proteins will be discussed, as will the physiological contributions of each protein (Table 2)

Table 2: Properties of ClC Cl^-/H^+ exchangers. Members of the ClC protein family that act as chloride/proton exchangers are listed with basic biophysical propterites, expression patterns, physiological roles, and accociated pathophysiology.

Table 2: Properties of ClC Cl^-/H^+ exchangers

	Function	***Expression***		***Physiological Role***	***Pathophysiology and Knockout***
		Tissue	**Cellular Localization**		
ClC-3	Cl^-/H^+ Exchanger	Ubiquitous High expression in brain	Synaptic Vesicles	Endosomal acidification	Hippocampal degeneragtion (KO)
ClC-4	Cl^-/H^+ Exchanger	Brain, Skeletal Muscle, Liver, Kidney	Endosomal membrane	Endosomal Acidification	
ClC-5	Cl^-/H^+ Exchanger	Kidney, Brain, Liver, Lung, Intestine	Endosomes of epithelial cells Plasma membrane	Endosomal Acidification Endocytosis	Dent's Disease
ClC-6	Cl^-/H^+ Exchanger	Lung, Instestine, Pancreas, Brain, Skeletal muscle	Lysomsomal Membrane	Lysosomal acidification	
ClC-7	Cl^-/H^+ Exchanger	Ubiquitous	Lysosomal membrane	Lysosomal Acidification Bone resorption	Neuronal Ceroid lipofuscinosis (KO), Osteopetrosis
ClC-ec1	Cl^-/H^+ Exchanger	Bacterial	Bacterial inner membrane	Acid resistance	

1.2.1 Prokaryotic ClC proteins

BLAST homology searches have identified many prokaryotic ClC proteins; some species contain as many as two ClC genes, while others have none. Maduke and coworkers purified and reconstituted a ClC protein, called EriC or ClC-ec1, from *E. coli* [125]. This protein was classified as a ClC family member based on primary sequence homology with other ClC members; therefore Maduke and colleagues postulated that this protein should function as a chloride channel. Indeed, $^{36}Cl^-$ flux assays demonstrated that vesicles containing ClC-ec1 were capable of conducting chloride against an electrochemical gradient, and that these proteins maintain the selectivity sequence observed for other ClC proteins: $Cl^- > Br^- > I^-$ [125]. Technical difficulties in obtaining very pure samples prevented reconstitution of ClC-ec1 into lipid bilayers; thus electrophysiological recording was not possible. Gluteraldehyde crosslinking experiments showed that ClC-ec1 exists as a homodimer, which was further confirmed by showing that no crosslinking occurred under reducing conditions [125]. Thus, it appeared that the ClC protein purified from *E. coli* was a chloride channel with similar selectivity and oligomeric structure as it mammalian counterparts.

In 2004, Accardi and Miller came to the dramatic conclusion that the bacterial ClC protein ClC-ec1 was, in fact, not a chloride channel as originally thought, but a Cl^-/H^+ exchanger. The studies by Miller and coworkers, taking advantage of crystallization-quality ClC-ec1, were the first to demonstrate ClC-ec1 currents from ClC-ec1 reconstituted into planar lipid bilayers [126, 127]. Accardi and colleagues showed that ClC-ec1 currents were Cl^- selective, as had been suggested by uptake assays, and that the unitary conductance was just 0.2 pS [127]. These currents were also linear, and showed

no voltage-dependent gating. The seminal finding, however, was that upon imposition of a Cl^- gradient, the shift in reversal potential was sub-nernstein, suggesting that ClC-ec1 is not perfectly selective for chloride [126]. Removal of all possible conductive cations had no effect on the shift of the reversal potential, suggesting that ClC-ec1 was permeable to protons [126]. Indeed, under symmetrical ionic conditions, imposition of a pH gradient shifted the reversal potential in a manner consistent with a Cl^-/H^+ exchanger, not an ion channel [126]. Calculation of the exchange stoichiometry showed that ClC-ec1 mediates transport of 2 Cl^- ions for every H^+. This stoichiometry is less strict when substitute anions were introduced; H^+ cotransport was reduced when Cl^- was substituted by polyatomic anions such as NO_3^- and SCN^- [128]. Interestingly, mutation of the conserved glutamate residue that is thought to be the major determinant for fast gating of voltage-dependent ClC channels, yielded ClC-ec1 proteins that are nearly perfectly Cl^- selective, and insensitive to changes in pH [126, 127]. Other work has shown that mutations near the central binding site may also uncouple Cl- transport from H+ transport [129-131].

Upon the revelation that bacterial ClC proteins mediated Cl^-/H^+ exchange, researchers began to ask if the transport of these ions utilized the same permeation pathway, or if they were separate. Accardi and colleagues undertook a mutational study to identify the molecular determinants of transport. Sequence alignments have shown that the equivalent of the ClC-ec1 residue E148 is conserved in nearly all ClC proteins, the exception being ClC-K channels [14]. Mutation of this residue, which acts as an extracellular proton transfer group and is important to Cl^- transport, leads to constitutively active proteins [14, 92]. Accardi and coworkers also identified another glutamate residue on the intracellular side of the channel, E203, that is conserved in all

ClC proteins believed to act as transporters, but is mutated to valine in all ClC channels. Mutation of this residue in ClC-ec1 to E203Q gave channels that conduct Cl^-, but in a manner that is not coupled to H^+ movement [132]. Additionally, this glutamate residue is not located near the predicted chloride permeation pathway. These data suggest that there are separate ion permeation pathways toward the intracellular side of the protein, one for Cl^- and one for H^+, which merge near E148 [132]. It is important to note that bacterial ClC proteins do not seem to have the slow gating processes associated with ClC channels. Instead, crosslinking experiments performed by Nguitragool and Miller suggested conformational changes during transport that are similar those thought to occur during fast gating of ClC channels [133].

The functional role that bacterial ClC proteins play is not very well understood. Prokaryotes possess a number of ion channels that bear significant homology to human ion channels, but it is likely that the physiological roles of these proteins are very different in these systems. Iyer and coworkers suggested that *E. coli* ClC proteins are involved in extreme acid resistance [134]. Knockout of the genes encoding the two *E. coli* ClC proteins severely reduced bacterial survival when challenged with extremely low pH [134]. The extreme acid resistance mechanism involves electrogenic transport of glutamate into the bacterial cell. ClC-ec1 acts as an electrical shunt to facilitate Cl^- efflux to prevent inner membrane hyperpolarization. The ClC proteins may be ideally suited to this play this role. Cl^- uptake experiments show that ClC-ec1 becomes maximally activated at extremely low pH [126, 134].

1.2.2 ClC-3

1.2.2.1 Biophysical characteristics of ClC-3

ClC-3 was first identified from rat brain in 1994 by Sasaki and colleagues [135], while the gene encoding human ClC-3 was identified in 1995 by Borsani and coworkers via a homology screening approach using the cDNA for ClC-4 (*CLCN4*) as a template [136]. This approach identified a gene with 73% similarity with *CLCN4*, suggesting that this gene encodes a similar, yet distinct protein [136]. This gene, *CLCN3*, encodes a 760 amino acid protein, sharing only 20-30% identity to ClC proteins in the channel branch; however, it is nearly 80% identical to ClC-4. As shown in Figure 1, the split between ClC-0 and ClC-3 was an ancient one, and as we will discuss, this is reflected in vast functional differences between the ClC-0 subgroup, and the ClC-3 subgroup. Murine ClC-3, also identified using the same approach, only differs from human ClC-3 by two amino acids [136]. RT-PCR was performed on samples from many different tissues, and ClC-3 was identified nearly ubiquitously, but was highly expressed in the brain [136], suggestive of an important role in neurophysiology. A splice variant of ClC-3, ClC-3B, was identified by Ogura and colleagues. The C-terminus of this variant contains an extra 48 amino acids which contains a PDZ domain that likely participates in protein/protein interactions [137].

The biophysical properties of ClC-3 have been very difficult to characterize. Expression of this protein in heterologous systems often leads to currents that are indistinguishable from background currents; thus, much of the characterization of this channel is not clear. ClC-3 is likely a Cl^-/H^+ exchanger, much like bacterial ClC proteins, and other ClC proteins belonging to this branch (Fig. 1). However, massive

overexpression has allowed some characterization of currents mediated by ClC-3 [138-141]. In virtually all cell systems, ClC-3 is reported to mediate depolarization-induced, very strongly outwardly rectifying currents [140, 141]. There is some disagreement regarding the ion selectivity of ClC-3, however. All ClC channels, as well as the bacterial ClC protein ClC-ec1, show the conductivity sequence of $Cl^- > Br^- > I^-$. Studies from the Weinman lab show a canonical halide selectivity sequence when ClC-3 is expressed in CHO-K1 cells [140, 141]. Duan and coworkers, on the other hand, reported a selectivity sequence of $I^- > Cl^-$ that is switched to $Cl^- > I^-$ when asparagine 579 was mutated to lysine. Duan and colleagues also suggested that ClC-3 encodes the protein responsible for swelling-induced currents observed in cardiac cells. Work from the Weinman lab suggested that the endogenous swelling activated currents in CHO cells show a selectivity sequence of $I^- > Cl^-$. Interestingly, mutation of the conserved gating glutamate, E224, resulted in a constitutively active protein [141]. Due to the fact that work from the Weinman lab characterizing ion selectivity is more consistent with data from other ClC channels and exchangers, it is generally regarded as more reliable, although it is possible that differences in the expression system, and possible differences in ClC-3 isoforms, may explain the differences observed for halide selectivity.

Interestingly, Huang and coworkers reported that ClC-3 is activated by calcium/calmodulin-dependent protein kinase II (CaMKII). Transfection of human ClC-3 cDNA into tsA-201 cells induced a current that was not active under basal conditions, but was greatly stimulated by CaMKII. Characterization of this CaMKII induced current showed a strongly outwardly rectifying, depolarization-dependent current with an ion selectivity sequence of $I^- > Cl^-$ [142]. The selectivity of CaMKII-dependent ClC-3

currents could be switched to $Cl^- > I^-$ by mutation of glycine 280 to glutamate, suggesting that ClC-3, not an unidentified endogenous channel, was indeed activated by CaMKII, and that ion selectivity of wild-type ClC-3 was $I^- > Cl^-$, at least under some conditions [142, 143].

Due to the difficulties associated with heterologous expression of this protein, characterization of Cl^- and pH dependence has not yet been performed to any large degree. Matsuda and coworkers have shown that currents mediated by the ClC-3 short isoform were reduced upon lowering $[Cl^-]_{ext}$, and acidification of extracellular pH [144]. As observed for ClC-ec1, the shift in reversal potential upon changes in $[Cl^-]$ were sub-nernstein, suggesting that ClC-3 mediated Cl^-/H^+ exchange [144]. The E224A mutation abolished pH-dependent regulation of these currents, inducing a nearly perfectly anion selective current [144, 145].

Additionally, like ClC-K channels, description of single channel currents mediated by the ClC-3 is not well established, with no consensus regarding gating behavior or single channel conductance. Kawasaki and coworkers reported that ClC-3 single channel currents showed two open conductance levels, like previously characterized ClC channels, but that the conductance levels were not equidistant and the unitary conductance was very large [138]. Duan and colleagues reported that ClC-3 single channel currents exhibited only one open conductance level with a unitary conductance of ~ 40 pS [139]. The most reliable single channel data for ClC-3 were obtained by Wang and coworkers, who showed that CaMKII activated ClC-3 currents displayed two equidistant open conductance levels, with a unitary conductance of just 3 pS, which is more consistent with the turnover rate of a very fast transporter [146].

Characterization of any gating transitions for ClC-3 has not been performed to date, so it is currently unknown whether ClC-3 contains both fast and slow gating processes. However, inspection of the single channel currents obtained by Wang and colleagues, leads to the suggestion that both gating processes may be present, as both fast transitions between conductance levels and long closed durations between bursts are present, although these transitions were not quantitatively analyzed [146]. This would suggest that gating mechanisms associated with mammalian ClC transporters are more complicated than their prokaryotic counterparts.

1.2.2.2 Physiological role of ClC-3 and associated pathophysiology

As stated above, ClC-3 is nearly ubiquitously expressed, and the primary functional role of this protein is to mediate Cl^-/H^+ exchange. While all ClC channel subtypes are localized to the plasma membrane, ClC-3 seems to be primarily localized to intracellular membranes, but may also rarely reach the plasma membrane [75, 141, 145, 147-149]. A dileucine motif in the N-terminus is involved in cellular localization; mutation of this motif to alanine leads to plasma membrane expression [150]. Much of the characterization of ClC-3 has come from knockout animals; there is no known human disorder associated with mutations in the gene encoding ClC-3, although very interesting phenotypes occur as a result of complete knockout of this protein, including the complete loss of the hippocampus [147].

The role of ClC-3 in neuronal tissue is the most well understood, and well accepted. Kawasaki and coworkers found that ClC-3 is abundant in the hippocampus, the olfactory bulb, and in the Purkinje cells of the cerebellum, where it initially was proposed

to act as a Ca^{2+}-dependent Cl^- channel [138]. Stobrawa and colleagues confirmed ClC-3 protein expression in the brain, and found that ClC-3 localized to synaptic vesicles, as well as other intracellular membranes; ClC-3 colocalized with a number of intracellular markers in both neuronal and non-neuronal tissue [147]. In ClC-3 knockout animals, acidification of synaptic vesicles via a V-type H^+-ATPase proceeded more slowly, suggesting that ClC-3 may provide the parallel Cl^- conductance needed for the H^+-ATPase to efficiently acidify synaptic vesicles. Additionally, localization of ClC-3 to small synaptic vesicles, as well as overall expression level, was impaired in mice lacking the adaptor protein AP-3 [151]. The interaction between AP-3 and ClC-3 could also be disrupted pharmacologically using drugs targeting AP-3, suggesting lack of ClC-3 in synaptic vesicles was due to disruption of a necessary ClC-3 trafficking complex [151]. Interestingly, knockout of ClC-3 led to severe hippocampal and retinal degeneration, although the mechanism underlying this degeneration is still not known [147].

In addition to altered ClC-3 localization and hippocampal degeneration in knockout animals, Dickerson and colleagues showed that ClC-3 KO animals displayed altered GABAergic signaling during hippocampal degeneration. They showed that during degeneration, there was a progressive loss of GABA producing cells in the dentate gyrus [152]. However, this was accompanied by an increase in $GABA_A$ receptor density, causing altered inhibitory neurotransmission [152]. Dickerson and coworkers suggested that this may be a compensatory mechanism in response to chronic excitatory stimulation, or reduced inhibitory input, but these possibilities have not been investigated further. The role of ClC-3 in modulating synaptic transmission was further invested by Wang and coworkers in a study showing that ClC-3 modulated excitatory

neurotransmission in immature neurons. Knockout of ClC-3 reduced NMDA-induced excitability by reducing mEPSP decay time. Quantal size is also reduced in knockout animals, confirming the presence of ClC-3 on synaptic vesicles [146]. Wang and colleagues suggested that Ca^{2+} influx through NMDA receptors leads to the activation of ClC-3 via CaMKII; ClC-3 activation subsequently leads to membrane depolarization and increased excitability [146]. Enhanced excitability upon ClC-3 activation is abolished once expression of the KCC2 K^+/Cl^- co-transporter is upregulated during neuronal development, which reduces $[Cl^-]_{int}$ from 40 to 5 mM as neurons mature [146]. The mechanism by which ClC-3 activation induces membrane depolarization is not known, and may involve indirect effects on other channels in the membrane, as ClC-3 activation would lead to Cl^- influx, and thus hyperpolarization. Yoshikawa and coworkers suggested that the elevated pH of endosomes associated with ClC-3 deficiency may result in the neurological disorder neuronal ceroid lipofuscinosis (NCL), a disorder causing numerous neurological symptoms including seizures and impaired learning, and resulting in a vegetative state and death [153]. However, analysis of naturally-occurring animal models for late-onset NCL showed no mutations of *CLCN3*, even though several polymorphisms in ClC-3 were identified [154].

ClC-3 has been proposed to be one of the main chloride channels involved in cell-volume regulation in cardiac tissue. Britton and colleagues showed that ClC-3 is widely expressed in cardiac tissue, with both sarcolemmal and intracellular localization [75]. This work showed that expression of ClC-3 in NIH/3T3 cells resulted in novel swelling-activated currents [75]. Native swelling activated currents in cardiac tissue could be inhibited by ClC-3 specific antibodies [155]. Therefore, work from the Hume lab has

suggested that ClC-3 provides the native volume-activated chloride currents in cardiac cells, and may by involved in regulatory volume decrease [156, 157]. However, work by Stobrawa and coworkers, and well as by Wang and coworkers, showed that swelling activated currents in neuronal tissue and cardiomyocytes were not altered in ClC-3 knockout mice [146, 147]. Work by Arreola and colleagues also suggests that the swelling activated current observed in salivary acinar cells were not mediated by ClC-3, as they also are unchanged in knockout animals [148]. Thus, it is likely that ClC-3 is not involved in cell volume regulation, and those cell-volume regulated currents observed in the studies by Hume and coworkers were those of native currents upregulated upon expression of non-native proteins and were inhibited by non-specific effects of the ClC-3 antibody.

Work from a number of labs has suggested that the primary role of ClC-3 may be acidification of intracellular compartments including synaptic vesicles [147], endosomes [145, 149, 158], and lysosomes [141]. All evidence suggests that ClC-3 provides a charge shunt to offset the positive membrane potential created by H^+ pump activity. ClC-3 has also been implicated in host defense. Mice lacking ClC-3 showed reduced NADPH oxidase activity, imparied phagocytosis, and a decrease in reactive oxygen species (ROS) production [159]. Also Miller and coworkers showed that ClC-3 is necessary for activation of NF-κB [160]. The role that ClC-3 plays in cardiac tissue requires further characterization. Despite this gap in knowledge, it is quite clear that ClC-3 plays a critical role in cellular physiology.

1.2.3 ClC-4

1.2.3.1 Biophysical characteristics of ClC-4

ClC-4 was identified in 1995 by van Slegtenhorst and coworkers [161]. Human ClC-4 is a 760 amino acid protein that is found predominantly in brain, skeletal muscle, liver, and kidney, and belongs to the same branch of ClC proteins as ClC-3 and ClC-5 (Fig. 1). Like most members of this particular branch of ClC proteins, biophysical characterization has lagged far behind that of the ClC channel subtypes. Unlike ClC-3, however, expression of ClC-4 in heterologous systems yields reliable surface expression, although this protein most likely localizes to intracellular membranes *in vivo* [162]. Expression of ClC-4 in *Xenopus* oocytes gave rise to strongly outwardly-rectifying voltage-dependent currents [162]. Upon membrane depolarization, channels activated very rapidly, with virtually no current induced by membrane hyperpolarization [162]. Characterization of ion selectivity showed that ClC-4 was similar to other ClC proteins, with a conductance sequence of $NO_3^- > Cl^- > Br^- > I^-$ [162]. When expressed in *Xenopus* oocytes, changes in extracellular pH had no major effect on ClC-4 mediated currents until pH was lowered to 5.5, which reduced macroscopic currents. Mutation of the conserved gating glutamate residue in ClC-4 to alanine, E224A, drastically altered macroscopic currents. Consistent with the consequences of mutation of this residue in other ClC channels or transporters, E224A-ClC-4 currents were voltage-independent, with no time-dependence for activation at any potential, consistent with a constitutively active protein [162].

Characterization of ClC-4 at the single channel level has been very elusive, despite plasma membrane expression of this protein in heterologous systems. Vanoye and George showed that ClC-4 mediated a strongly outwardly rectifying channel at the single

channel level with a slope conductance of ~3 pS [163]. Interestingly, this study also showed that ClC-4 currents were sustained by ATP, with rundown of channel activity being accelerated by the non-hydrolyzable ATP analogue AMP-PNP, as well as GTP, although this was not shown on the single channel level [163]. Hebeisen and colleagues, on the other hand, suggested that the single channel amplitude of ClC-4 was just 0.1 pA at +140 mV, as measured by noise analysis, much smaller than the 3 pS conductance suggested by Vanoye and George [164]. The discrepancy between these measurements is unclear, although Hebeisen and colleagues suggested that the difference may lie in the recording method; noise analysis was performed on currents from whole-cell recording, while the Vanoye study utilized excised inside out patches.

It is now clear that ClC-4, like other members of this branch of ClC proteins, mediates Cl^-/H^+ exchange, as has been convincingly shown by two separate studies. Picollo and Pusch showed that ClC-4 mediated significant proton transport by measuring changes in extracellular pH very close the plasma membrane of *Xenopus* oocytes. This proton transport could be abolished by removing chloride from the bath solution, suggesting that chloride transport was required for proton transport [165]. Additionally, *bona fide* ClC channels such as ClC-0 and ClC-2 showed no changes in extracellular pH upon channel activation [165]. Scheel and coworkers corroborated this conclusion by showing that intracellular pH alkalinizes upon ClC-4 activation [166]. This study additionally showed that H^+ transport depended on membrane voltage, as no proton transport was present upon membrane hyperpolarization. As state above, mutation of the gating glutamate, E224, produces constitutively active proteins. Zdebik and coworkers showed that the E224A mutation also abolished H^+ transport. Mutation of the equivalent

of the internal H^+ binding site identified for ClC-ec1, E281, abolished both Cl^- and H^+ transport; Cl^- transport could be restored with the additional E224A mutation [167]. This is consistent with the idea that Cl^- binding is dependent upon H^+ binding when the gating glutamate is still in place.

1.2.3.2 Physiological role of ClC-4 and associated pathophysiology

As stated above, ClC-4 is expressed in the brain, skeletal muscle, liver, and kidney. The role that this protein plays in these tissues in not well understood, however. No disease phenotype is associated with mutations in the gene encoding ClC-4. Suzuki and coworkers showed, by immunofluorescence, that ClC-4 strongly colocalized with both ClC-3 and ClC-5 on intracellular membranes of HEK-293 cells [168]. Homo-oligomers of ClC-4 were abundantly detected by co-immunoprecipitation, but Suzuki and coworkers also showed that hetero-oligomers between ClC-3, -4, or -5 subunits could also be formed [168]. The functional consequences of ClC hetero-oligomerization are not understood, but may include important effects on pH dependence of activity, voltage-dependence of activation, or possibly localization to the plasma membrane versus intracellular membranes.

Confocal microscopy showed that ClC-4 is expressed endogenously on endosomal membranes of cultured epithelial cells [169]. Mohammad-Panah and coworkers showed that disruption of endogenous ClC-4 by transfection of antisense ClC-4 cDNA impaired endosomal acidification, suggesting that this protein is necessary for correct endosomal acidification, similar to the role ClC-3 plays in synaptic vesicles [169]. Interestingly, confocal microscopy showed that ClC-4 colocalized with CFTR in the

brush border of the epithelial cells lining intestinal crypts [170]. This finding led Mohammad-Parah and colleagues to postulate the ClC-4 may cycle between the plasma membrane, where it aids in Cl^- secretion, and intracellular membranes, where it is involved in endosomal acidification [53, 169, 170].

As stated above, there are no diseases associated with known mutations of ClC-4. This has severely hampered defining the role that this protein may play in physiological processes. Indeed, many of the properties of this protein need to be confirmed *in vivo*, such as the potential hetero-oligomerization, as well as the role it may play in chloride secretion at the plasma membrane. ClC-4 is very likely to be involved in endosomal acidification, but it is not known if ClC-4 plays this role in all cell types in which it is expressed. Also, while the basic biophysical properties of transport may be known for ClC-4, the stoichiometry of Cl^-/H^+ exchange still needs to be rigorously established. Additionally, the effects of potential hetero-oligomerization on the transport properties need to be addressed.

1.2.4 ClC-5

1.2.4.1 Biophysical characteristics of ClC-5

The final member of this branch of ClC proteins, ClC-5, is the most extensively studied of the ClC transporters. ClC-5 was cloned from human kidney in 1994 by Fisher and colleagues [171, 172]. This 746 amino acid protein is encoded by a 2,238 bp transcript, and is >70% identical to both ClC-3 and ClC-4 (Fig. 1) [172]. While ClC-5 is clearly expressed in the kidney, transcripts encoding this protein also have been identified in brain, liver, and lung, although abundance in lung is very low [173]. Like both ClC-3

and ClC-4, it is likely that ClC-5 acts as a Cl^-/H^+ exchanger; the evidence for this will be discussed below [166]. Despite this, ClC-5, much like ClC-4, is readily expressed on the plasma membrane in heterologous systems [162, 173, 174]. Currents mediated by ClC-5 were strongly outwardly rectifying, eliciting current only when membrane potentials were more depolarizing than +20 mV [173]. Steinmeyer and colleagues showed that ClC-5, like other ClC proteins, had a conductance sequence of $Cl^- > Br^- > I^-$ [173]. Two groups have shown that ClC-5 is modestly controlled by changes in extracellular pH; currents are reduced as extracellular pH becomes more acidic [162, 165].

Like other ClC proteins, mutation of the ClC-5 gating glutamate to alanine, in this case E211A, drastically altered macroscopic behavior. E211A-ClC-5 proteins were constitutively active, with no outward rectification; in fact, currents were slightly inwardly rectifying [162]. Activation of WT ClC-5 shows very little time-dependence. Freidrich and coworkers identified several mutations which slow channel activation, which initially led to the hypothesis that ClC-5 was an ion channel [162]. However, it is now generally accepted that ClC-5 works as a Cl^-/H^+ exchanger. Picollo and Pusch showed that activation of ClC-5, like ClC-4, acidified the extracellular pH very close to the plasma membrane, consistent with H^+ efflux driven by Cl^- influx. The decrease of extracellular pH was accompanied by alkalinization of intracellular pH [165]. As stated above, macroscopic ClC-5 currents are inhibited by acidification of extracellular pH. The pH dependence of ClC-5 current was eliminated by the E211A mutation. This mutation also eliminated Cl^-/H^+ coupling, as activation of E211A-ClC-5 by membrane depolarization was no longer accompanied by changes in intracellular pH [167]. Like ClC-4, mutation of the inner glutamate residue, E268, abolished both Cl^- and H^+ transport

[167]. Cl^- transport could be restored by additional mutation of the gating glutamate (E211). This suggests that in the WT protein, Cl^- transport is only possible when H^+ are bound near the intracellular glutamate. Like ClC-4 however, the stoichiometry of transport still needs to be determined.

Two groups have shown that the cytoplasmic domains of ClC-5 are capable of binding adenosine nucleotides [175, 176]. The structural basis of this binding will be discussed in section 1.4, although significant functional consequences of ATP binding to the cytosolic domains also have been shown for ClC-1 [44]. Interestingly, the cytosolic domains are nonselective for adenosine nucleotide, with ATP, ADP, and AMP all binding with a K_d ~90 μM. While no functional effect on Cl^-/H^+ counter-transport have been shown for binding of ATP, mutation of residues critical for binding nucleotide, specifically Y617A, did not alter pH dependence or voltage dependence of activation [175]. Thus, the functional role of nucleotide binding still needs to be determined.

To date, no single channel data for ClC-5 have been obtained. However, noise analysis of ClC-5 currents suggested that the unitary conductance was just 0.5 pS, consistent with a transport mechanism, rather than uncoupled diffusion of ions through a pore [167]. Interestingly, Zdebik and colleagues proposed that ClC-5 exhibited both silent and transporting states similar to the gating processes observed for ClC channels [167].

1.2.4.2 Physiological role of ClC-5 and associated pathophysiology

Of the ClC proteins belonging to this branch, ClC-5 is the only protein linked to a human disease. Mutations in ClC-5 are linked to the rare hereditary kidney disorder

Dent's disease, corresponding to the high expression of ClC-5 in the kidney [177-179]. Dent's disease is a devastating disorder associated with low-molecular weight proteinuria, hypercalciuria, nephrocalcinosis, kidney stones, and renal failure, and can often be fatal [173, 180, 181]. Due to the fact that mutations in ClC-5 are a primary cause of this disease, much effort has been devoted to the characterization of this protein. In addition to high expression of ClC-5 in the kidney, it is also expressed in brain, liver, and lung [173]. As stated above, ClC-5 acts as Cl^-/H^+ exchanger [165, 167]. Gunther and coworkers showed that ClC-5 was expressed primarily on endosomes, and colocalized with the H^+-ATPase, suggesting that ClC-5 may provide an electrical shunt to allow proton accumulation associated with endosomal acidification [182]. Vandewalle and colleagues also identified ClC-5 in the small intestine, and found that it colocalizes with endosomal markers, which is suggestive of ClC-5 playing a similar role in acidification of endosomes in the small intestine [183]. When studied in a heterologous expression system, ClC-3, -4, and -5 colocalize in endosomes, suggesting that these three proteins may play similar roles [168]. In fact, it has been proposed that they may form hetero-oligomers, although the functional consequences of this type of interaction have not been determined [168]. It is possible that this is an artifact of overexpression, and that native cells they are present at different stages of the endocytic pathway.

One of the main symptoms of Dent's disease is low molecular weight proteinuria, stemming from defective reabsorption of low molecular weight proteins in proximal tubular cells, where ClC-5 is normally very highly expressed [184, 185]. Altered endosomal acidification by mutations in the gene encoding ClC-5 could lead to impaired endocytosis of low molecular weight proteins by preventing proper endosome

maturation. Piwon and colleagues showed that knockout of ClC-5 led to strongly reduced endocytosis at the proximal tubular apical membrane [180]. Disruption of the gene encoding ClC-5 led to severely impaired receptor-mediated endocytosis, fluid-phase endocytosis, and endosome recycling [180, 181]. This study also showed that endosomes acidified at a slower rate, suggesting that endocytosis is reduced due to impaired endosomal acidification [181]. This may be, in part, due to decreased trafficking of ClC-5 to endocytic vesicles, as observed from ClC-5 knockout mice, as well as mutations in the CBS2 domain[186, 187]

Endosomal acidification may not be the primary role of ClC-5, however. It has been suggested that primary endocytic vesicles are not acidified [188]. In support of this, endosomal acidification also was observed to proceed in ClC-5 knockout mice, consistent with the presence of alternate conductances in the endosome that may participate in acidification. Additionally, Hara-Chikuma and coworkers showed that acidification is only modestly impaired in early endosomes from proximal tubular cells [189]. Both acidification and chloride accumulation could be completely eliminated by non-specific chloride channel inhibitors in both wild-type and ClC-5 knockout cells [189]. In normal kidney, low molecular weight proteins (< 70 kDa) are reabsorbed by endocytosis via the multiligand tandem receptors megalin and cubilin at the brush border of proximal tubular cells. The megalin/cubilin complex is the main albumin receptor in the proximal tubule, making it essential for albumin endocytosis [184]. Christensen and coworkers showed that in ClC-5 knockout mice, expression of the megalin/cubilin complex at the plasma membrane was drastically reduced, greatly reducing albumin uptake [184]. Also, data from knockout mice showed that the V-type H^+-ATPase in proximal tubular cells is

mislocalized to the basolateral membrane [190]. This suggests that ClC-5 may participate in the trafficking of cell surface receptors that are intimately involved in endocytosis of low molecular weight proteins [184, 190].

The reorganization of proteins receptors involved in uptake of low molecular weight proteins provided indirect evidence that ClC-5 may be directly involved in the endocytic process [191]. This is further supported by immunofluorescence data showing that a small amount of ClC-5 localized not only to apical vesicles just below the brush border membrane, but also at the brush border membrane itself [182, 184]. Hryciw and colleagues showed, both by yeast two-hybrid screening and GST-pulldown assays, that the C-terminus of ClC-5 interacted with the actin depolymerizing protein cofilin [192]. Phosphorylation of cofilin, which abolishes the interaction of cofilin with actin, greatly reduced albumin endocytosis [192]. Thus, ClC-5 directly interacts with the endocytic machinery for albumin uptake, and is directly involved in the localization of the albumin receptor megalin/cubilin complex. Interestingly, a recent study from the Poronnik lab showed that the PDZ domain in the C-terminus of ClC-5 interacted with the PDZ scaffolding protein NHERF2 in opossum kidney cells. siRNA directed against NHERF2 greatly reduced albumin endocytosis [193]. Taken together, these data suggest ClC-5 is necessary for the formation of macromolecular complexes involved in endocytosis of low molecular weight proteins such as albumin, and that disruption of this complex by removal of ClC-5 leads to the low-molecular weight proteinuria associated with Dent's Disease.

ClC-5 also has been implicated in calcium transport. Other well known symptoms of Dent's Disease are hypercalciuria, nephrocalcinosis, and kidney stones, all of which

stem from altered calcium transport in the kidney [172, 179, 194, 195]. Knockout mice developed by the Guggino lab showed the typical hypercalciuria associated with Dent's Disease, as well as kidney stone formation, and in some cases spinal deformity [196]. The mechanism of altered calcium transport in knock-out mice is currently unclear. It has been suggested that ClC-5 may be directly involved in endocytosis of calcium microcrystals [195]. If these microcrystals are not endocytosed, they provide a nucleation point for the formation of larger crystals, and eventually kidney stones [195]. To support this hypothesis, Carr and colleagues have shown that disruption of ClC-5 by transfection of collecting duct cells with antisense ClC-5 cDNA dramatically altered localization of annexin A2 [197]. Annexin A2 is a crystal binding molecule in renal epithelial cells, which colocalized with caveolin-1, and is directly involved in both binding and endocytosis of calcium microcrystals [197]. Disruption of ClC-5 greatly increased the surface expression of annexin A2. Given that ClC-5 is clearly involved with endocytosis, increased surface expression of annexin A2 likely stems from decreased endocytosis. Thus, disruption of annexin A2 endocytosis would severely reduce calcium microcrystal endocytosis, providing nucleation points for the formation of larger crystals, resulting in kidney stones.

ClC-5 has been extensively studied, with the physiological role in the kidney being very well defined. It has become clear that ClC-5 plays a complicated role in endocytosis, being involved not only in endosomal acidification, but also serves as an essential member of macromolecular complexes involved in endocytosis. However, there is still work to be done in order to define the role that ClC-5 may play in other tissues. It has been shown recently that ClC-5 is expressed in retinal pigment epithelial cells [198,

199]. Additionally, Edmonds and colleagues have identified ClC-5 in the apical membrane of airway epithelial cells [200]. It is not currently known if ClC-5 plays a similar role in these tissues as it does in the kidney. While it now is accepted that ClC-5 acts as a Cl^-/H^+ exchanger, it would be interesting to know more detailed biophysical characteristics of ClC-5 activity. The implication that ClC-5 transitions between silent periods and active periods may be very important in understanding the evolution of ClC channel behavior, which display similar quiescent and active periods.

1.2.5 ClC-6

1.2.5.1 Biophysical and physiological properties of ClC-6

The final branch of mammalian ClC proteins is composed of ClC-6 and ClC-7, which were cloned simultaneously (Fig. 1). ClC-6 was first identified from expressed sequence tags (ESTs) in 1997 by Brandt and Jentsch using the TBlastN algorithm, and was directly isolated from a human brain cDNA library using specific oligonucleotides [201]. The ClC-6 protein is comprised of 869 amino acids, with a molecular mass of 97 kDa. While this protein showed significant homology to ClC-7 (~45%), ClC-6 showed only distant homology to the ClC-3 branch (~29%), and even less to the channel branch (~23%) [201]. Northern blot analysis showed that ClC-6 mRNA was present in a broad range of tissues, including brain, heart, skeletal muscle, lung, liver, pancreas, and kidney [202]. Interestingly, Nilius and coworkers identified three alternatively spliced ClC-6 isoforms, which are named ClC-6b, -6c, -6d [203]. All of these isoforms form truncated proteins, with none of them being longer than 353 amino acids (ClC-6c). Even though RT-PCR analysis revealed that mRNA encoding ClC-6c is present solely in the kidney,

the functional role of this truncated protein is not known, and the presence of ClC-6c protein has yet to be verified in any tissue. Despite broad expression of full-length ClC-6 mRNA, Jentsch and coworkers were only able to identify ClC-6 protein in the nervous system, suggesting a role in neurobiology [201].

Biophysical characterization of ClC-6 has so far eluded researchers. Injection of cRNA encoding ClC-6 into *Xenopus* oocytes failed to elicit currents that were discernable from endogenous channels. ClC-6 currents also have not been detected in mammalian cells transfected with ClC-6 DNA [204]. In fact, confocal imaging of COS and CHO cells expressing ClC-6 showed that ClC-6 resided on intracellular membranes [205]. ClC-6 colocalized with the SERCA2b Ca^{2+} pump in the endoplasmic reticulum [205]. Evolutionarily, ClC-6 is more closely related to ClC transporters than to ClC channels (Fig. 1). ClC-6 contains a cytoplasmic glutamate residue that is conserved among ClC exchangers; thus, it is likely that ClC-6 acts as a Cl^-/H^+ exchanger on intracellular membranes, however, this has not been conclusively proven.

The physiological role of ClC-6 has not been well defined as yet. As stated above, ClC-6 mRNA is very broadly expressed; however, the protein is only found in nervous system [201, 202], with abundant expression in dorsal root ganglia. Overexpression of ClC-6 leads to both ER and early/recycling endosome localization [206]. In these heterologous systems, ClC-6 copurified in detergent resistant membrane fractions, *i.e.* lipid rafts. However, in a cell line that endogenously expresses ClC-6, the human neuroblastoma cell line SH-SY5Y, ClC-6 colocalized with LAMP-1, a late endosome/lysosomal marker [206]. ClC-6 knockout mice developed by Jentsch and coworkers showed signs of the lysosomal storage disease NCL, similar to knockout of

ClC-3. Disruption of ClC-6 led to enlargement of proximal axons as a result of accumulation of material in the lysosome [207]. These mice displayed neurological symptoms similar to NCL, including reduced sensitivity to pain and modest behavioral changes that included an increase in the acoustic startle response and a decrease in exploratory activity [207]. Interestingly, lysosomal pH is not altered in ClC-6 knockout mice, suggesting that ClC-6 may not be directly involved in lysosomal acidification [207]. Sontheimer and colleagues proposed that ClC-6 may participate in regulatory volume decrease of glioma cells, although they also named ClC-2, -3, -5, and -7 as candidate proteins [208].

ClC-6 is the least understood of all the ClC proteins. Both the biophysical characteristics and the physiological role of this protein still need to be further elucidated. Mutations in the gene encoding ClC-6 have been associated with human NCL, although these mutations are rare [207]. Uchida and coworkers suggested that ClC-6 forms homo-oligomers, but this has not been rigorously tested [168]. ClC-6 is classified as a Cl^-/H^+ exchanger largely based on data from multiple sequence alignments. The lack of surface expression of ClC-6 has been a major hurtle for the biophysical characterization of this protein. It is possible that ClC-6 associates an accessory protein similar to the association of barttin and Ostm1 with ClC-K and ClC-7 respectively. In short, there is still much work to be done in order to understand even the most basic characteristics of ClC-6.

1.2.6 ClC-7

1.2.6.1 Biophysical properties of ClC-7

Cloned at the same time as ClC-6, ClC-7 is the final mammalian member of the ClC protein family. The gene encoding this protein was identified by homology screening using primers based on the DNA sequence of ClC-6. ClC-7 is an 803 amino acid, 89 kDa protein [201, 209]. Like ClC-6, ClC-7 showed very little homology to other ClC exchangers, or the ClC channels. ClC-7 is also very broadly expressed, with mRNA being found in pancreas, kidney, skeletal muscle, brain, liver, and lung [201]. As will be discussed further below, ClC-7 is also associated with an accessory protein, Ostm1, and plays a critical function in bone-resorbing osteoclasts.

Biophysical characterization of ClC-7 proteins has been very difficult until just recently. Brant and Jentsch found that injection of ClC-7 cRNA into *Xenopus* oocytes yielded no functional channel [201]. However, Nawrath and colleagues suggested that ClC-7 mediated acid-activated Cl^- current in oocytes. Acidification of bath pH to 5.0 induced large outwardly rectifying Cl^- currents that were not present in mock-injected cells [210]. Furthermore, western blot analysis of ClC-7 injected oocytes showed that ClC-7 protein was present, although there was no attempt made to separate plasma membrane fractions from intracellular membranes [210]. Multiple sequence alignments created by Miller and coworkers showed that ClC-7 contains the interior glutamate residue common to all ClC exchangers [132], leading to the conclusion that ClC-7 is most likely also an exchanger. Concentrative uptake experiments performed by Mindell and coworkers showed that ClC-7 did indeed mediate Cl^-/H^+ exchange. Chloride transport could be altered by changing both the $[Cl^-]$, as well as the pH gradient. Similar to other ClC proteins, ClC-7 had a selectivity sequence of $Cl^- > Br^- > I^-$ [211]. This is the

first experimental evidence that ClC proteins of this branch of ClCs act as Cl^-/H^+ exchangers.

1.2.6.2 Physiological role of ClC-7 and associated pathophysiology

Like ClC-6, mRNA encoding ClC-7 was present in a very wide variety of tissues, as noted above. However, it has been shown by several groups that ClC-7 plays a vital role in osteoclasts [212-216]. Most ClC exchangers are expressed primarily on intracellular membranes, where they participate in acidification of endosomal compartments. Consistent with this, Jentsch and colleagues have shown that ClC-7 was primarily expressed in late endosomes and lysosomes; immunofluorescence studies showed that ClC-7 nearly completely overlapped with the lysosomal marker LAMP-1 [212]. There was modest expression in both the trans-Golgi network and the endoplasmic reticulum [212]. ClC-7 knockout mice develop severe osteopetrosis, a disorder that is associated with increased bone density. In wild type mice, ClC-7 was highly expressed in embryonic osteoclasts at the ruffled membrane [212]. Under normal conditions, the ruffled border functions much like late endosomes, with late endosomal markers such as the V-type H^+-ATPase and LAMP-2 also being present at the ruffled membrane. Osteoclasts attach to bone, form the ruffled membrane, then secrete acid to degrade the bone [53, 212]. In ClC-7 knockout mice, osteoclast development is not impaired; however, they fail to properly secrete acid, and thus do not degrade bone [212]. In addition to the development of an osteopetrosis phenotype in knockout mice, several polymorphisms have been identified in patients with autosomal dominant osteopetrosis type II [213, 214, 217].

In addition to osteopetrosis, ClC-7 knockout mice develop a severe lysosomal storage disorder with massive accumulation of materials in lysosomes of neurons [218]. Jentsch and coworkers showed that after correction of ClC-7 expression in osteoclasts to prevent osteopetrosis, the lysosomal disorder led to severe neurological defects including hypomotility and loss of motor control [214]. Mindell and coworkers recently have shown that ClC-7 provides the main chloride permeation pathway in the lysosome, mediating Cl^-/H^+ exchange [211]. In contrast to the study by Jentsch and coworkers, Mindell and colleagues found that knockdown of ClC-7 expression by siRNA treatment severely reduced the ability of lysosomes to acidify *in vivo* [211]. This suggests that ClC-7 does indeed play a critical role in lysosomal acidification, as well as acid secretion at the ruffled membrane.

Interestingly, Fuhrmann and coworkers showed that ClC-7 associated with Ostm1 [219], a 172 amino acid intregral membrane protein that contains a single transmembrane domain. Vacher and colleagues identified Ostm1 as the gene defective in *grey lethal* mice, which show severe osteopetrosis [220-222]. ClC-7 could be pulled down with Ostm1, and *vice versa* [219], suggesting that Ostm1 acts as a true β-subunit for ClC-7. In fact, it has been shown that ClC-7 is required for Ostm1 localization to the lysosome, while Ostm1 is not required for ClC-7 to reach that compartment. In ClC-7 knockout mice, Ostm1 expression is greatly reduced, while in *grey lethal* mice ClC-7 protein expression was severely reduced [219]. This suggests that the ClC-7/Ostm1 complex is necessary for normal lysosomal function. The mechanism by which ClC-7 protein expression becomes unstable in the absence of Ostm1 is not known, and is an interesting dilemma considering that Ostm1 is not required for ClC-7 trafficking. Fuhrmann and

colleagues suggested that Ostm1 may play a protect ClC-7 from degradation. ClC-7 is the only ClC protein that is not glycosylated, which is a novel feature for a lysosomal protein, most of which are normally highly glycosylated to protect against lysosomal enzymes. Ostm1 is a highly glycosylated protein that may therefore shield ClC-7 from degradation when the proteins properly interact [219]. In *grey lethal* mice that lack Ostm1, ClC-7 protein may be abnormally degraded in the lysosome, leading to decreased lysosomal acidification, as well as reduced osteoclast function, leading to lysosomal storage disease and osteopetrosis.

ClC-7 has a very well defined role in lysosomal function, where it participates in acidification of the lysosome, and is also critically involved in proper osteoclast function. Interestingly, ClC-7 knockout mice are also blind, due to rapid degeneration of the retina. Further investigation is required to define the role that ClC-7 plays in physiology of the eye. The nearly ubiquitous expression of ClC-7 suggests that this protein may play a similar role in all tissues in which it is expressed, although this may not be the case. Further investigation is warranted to determine if ClC-7 plays a common role in all cell types, or may have divergent roles in other cells.

1.3 Other ClC proteins

As outlined above, there are 9 mammalian ClC proteins, but quite a lot of research has been devoted to non-mammalian members of the ClC family. Both the canonical channel (ClC-0) and exchanger (ClC-ec1) are non-mammalian members of this family. Indeed, members of this large family of proteins are present in all phylogenetic domains and have provided insights into ClC protein function. ClC proteins from *C. elegans*, for

example, have been very useful for analyzing structural elements of the ClC protein family [223-228]. As can be seen from Figure 1, ClC family members from this organism include voltage-dependent channels, while at least two of the six *C. elegans* isoforms are predicted to function as exchangers, although transporter function has not been tested for these proteins. Interestingly, no plant ClC protein has been shown to be a true voltage-dependent channel. All *Arabadopsis* ClC proteins exist within a branch that only contains exchangers [229, 230]. In fact, at least one of these proteins, AtClCA, has been recently shown to be a NO_3^-/H^+ exchanger, not a Cl^-/H^+ exchanger [231]. While we will not go into detail about the functional properties of ClC proteins in non-mammalian systems, it is clear that this diverse group of proteins plays a vital role in many biological systems ranging from prokaryotes and plants to higher animals.

1.4 ClC Protein Structure

Among ion channels and exchangers, the structure of ClC family proteins is unique. Prior to the cloning of ClC-0, studies performed on the voltage-dependent chloride conductance from *Torpedo* electroplax suggested that the functional unit of this protein contained two chloride conductance pathways [3, 12, 232]. After the cloning of ClC-0, the functional oligomeric structure of this protein was indeed shown to be homodimeric, with each protopore possessing a chloride conduction pathway [232]. Single channel analysis, as well as hydropathy analysis, of other ClC channels, including ClC-1, -2, and -3 showed that this structure is most likely conserved between all family members [7, 25, 60, 136]. This quaternary structure is rare among transport proteins. In addition, the membrane topology of a ClC protein is a very complicated one. Hydropathy

analysis predicted that each mammalian ClC protein adopted a relatively conserved topology containing 13 helices [7, 25, 60]. Experiments from the Jentsch lab, utilizing a combination of *in vitro* glycosylation scanning and protease protection, predicted that at least 10 of these helices traverse the membrane, and that both the N- and C-termini are cytoplasmic [233]. Low resolution electron microscopy by Grigorieff and colleagues showed a dimeric structure for ClC-ec1, revealing a two-fold axis of symmetry from a top-down view of the protein and two water filled cavities off the axis of symmetry [234]. From this top down view the shape of the protein was roughly diamond shaped, with dimensions measuring approximately 100 Å in length, and 50 Å wide [234]. This structure, however, was not of sufficient resolution to accurately determine the number of transmembrane helices, or other structural features.

The questions remaining from these low resolution structure predictions were put to rest when, in 2002, the lab of Roderick MacKinnon successfully determined the high resolution crystal structures of two bacterial ClC proteins, from *S. typhimurium* and *E. coli* [14]. The high resolution structures showed that both of the bacterial ClC proteins formed homodimeric functional units, with both the N- and C-termini of each monomer being cytosolic (Fig. 4C). However, these structures also revealed that the membrane topology was much more complicated than originally proposed; each subunit was composed of 18 helices, 17 of which lay within the membrane (Fig. 4B) [14]. This basic structure of the membrane domain is thought to be conserved throughout the ClC protein family. Engh and Maduke tested the accuracy of a ClC-0 homology model, based on the bacterial crstyal structures, using cysteine accessibility studies, and found that the predictions of residue accessibility based on the model were relatively correct [235].

Additionally, MS/MS analysis of the ClC-2 membrane spanning domains revealed that the membrane boundaries predicted by the bacterial structures were correct [236]. Thus, for the membrane spanning domains, the bacterial crystal structures provide an excellent template for studies of other ClC proteins.

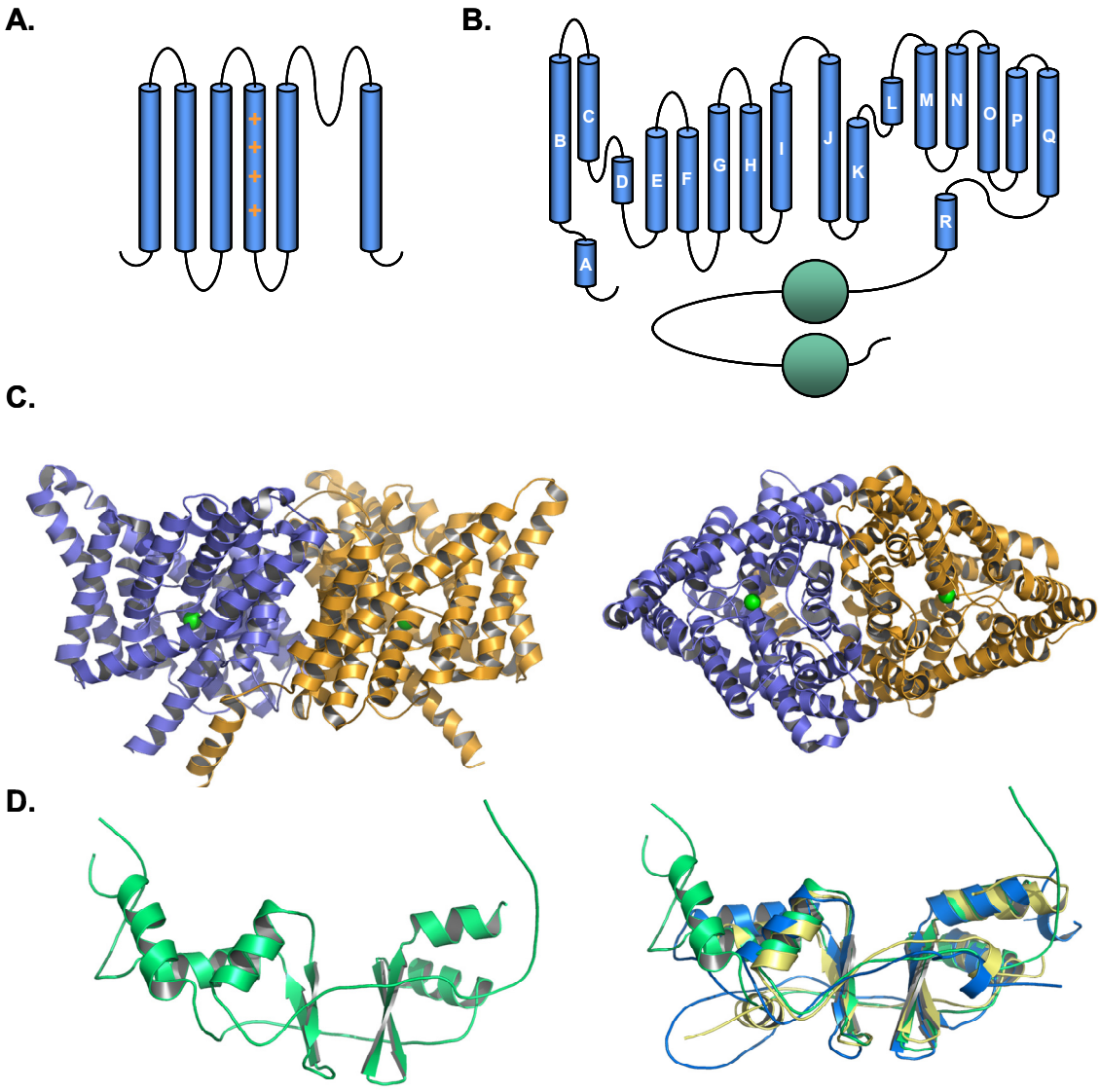

Figure 4: ClC protein structure. (A) Membrane topology of a voltage-dependent K^+ channel. These channels are composed of four identical subunits, with each subunit containing six transmembrane helices. The voltage sensor is mainly contributed by a high density of positive charges in the 4th transmembrane domain, while the pore resides between the 5th and 6th transmembrane helices. (B). Membrane topology of a ClC protein. Each ClC protein is composed of two identical subunits, each composed of 18 helical domains. Unlike voltage-dependent K^+ channels, no region of localized charge governs the voltage-dependent gating observed for ClC channels. (C) Crystal structure of the S. Typhimurium ClC protein shown from the side (left) and top down (right). Note that there is no clear ion permeation pathway as would be expected for an ion channel, consistent with data showing that this protein is a transporter (D). Crystal structure of the C-terminal domain of ClC-0 (left). The right panel shows an overlay of the C-terminal domains of ClC-0, -K, and -5. All these domains adopt a similar fold, and may be important in ClC channel slow gating.

Chloride ions bound within the structure confirmed the presence of two separate chloride permeation pathways, one completely contained within each subunit [14], quite unlike that of well characterized cation channels whose single, central permeation pathways are composed of contributions from each subunit (in the case of K^+ channels) or domain (for Ca^{2+} and Na^+ channels) [16]. Also, it has been well established by the MacKinnon lab that for at least K^+ channels, cations are coordinated by partial negative charges contributed by backbone atoms of the residues forming the selectivity filter [237, 238]. For ClC proteins however, this does not seem to be the case. Like cation channels, ClC proteins contain multiple ion binding sites, as revealed by the high resolution structures; however, for ClC channels, Cl^- ions, at least at the central binding site, are coordinated by the side chains of residues from multiple membrane helices: S107 (helix D), Y445 (helix R), and main chain amide nitrogen atoms at the end of helix N [14, 239]. However, long range interactions may also play an important role in ion coordination; Faraldo-Gomez and Roux showed via free energy calculations that K149, which is completely buried within the protein, acted to stabilize chloride binding, presumably by local hydrogen bonding as well as long range interactions [240].

Despite the fact that it has recently come to light that the bacterial proteins are not voltage-dependent channels, but Cl^-/H^+ antiporters, the structures have revealed some important features of gating of ClC channel proteins [126, 127]. As stated previously, there is no localized region of charged residues similar to the S4 helix of K_V channels that might provide a molecular basis for voltage-dependent gating (Fig. 4); instead, Cl^- itself provides the charge underlying the voltage-dependence of channel fast-gating, thereby coupling permeation and fast-gating [11]. This feature is very nicely explained by the

crystal structure, which revealed three chloride binding sites. The most external binding site, S_{ext}, may be occupied either by chloride, or the side chain of the conserved glutamate residue E148, which may be the primary molecular determinant for fast gating [239]. When E148 occupies S_{ext}, the permeation pathway is blocked, and Cl^-, therefore, cannot conduct. MacKinnon and colleagues suggested that Cl^- ions compete with E148 for the occupation of this site, imparting the $[Cl^-]_{ext}$ dependence of gating observed for many of these channels [239, 241]. Voltage-dependence of gating is imparted by a voltage-dependent Cl^- binding step, at least for ClC-0 [9, 11, 17]. Mutation of this glutamate residue in every ClC thus far tested has led to channels that completely lack a fast-gating processes; single channel records of E166A-ClC-0, for example, only rarely show transitions between two distinct open states, residing mainly in a conductance level in open level two, i.e. both pore are conducting [239]. In fact, analysis of a structure of *E. coli* ClC bearing the E148Q mutation showed that all three ion binding sites were simultaneously occupied by Cl^-, consistent with the notion that removal of this glutamate abolishes fast gating [239]. Further evidence for the importance of this glutamate residues comes from the fact that this residue is conserved in all but two ClC subtypes, the ClC-K channels [53, 103]. As stated above, introduction of a glutamate residue at the correct position in ClC-K channels gave channels that showed both voltage- and time-dependent activation [103]. Q_{10} calculations of fast gating suggested that the conformational changes associated with fast gating were likely very small; the Q_{10} for fast gating of ClC-0 was ~1.4, and ~4 for ClC-1 and -2 [15, 37, 67]. Local structural rearrangement of E148, or the equivalent residue, would be consistent with the prediction that fast gating only involves small conformational changes [239]. Inhibitor studies which will be described in

section 1.5, suggest that the conformational change associated with fast gating may involve more than just the rearrangement of the single glutamate residue, but are likely still only local rearrangements [242].

The crystal structures have been less helpful in identifying features of these proteins that may contribute to slow gating. This is likely due, in part, to the fact that the bacterial proteins are not ion channels. For ClC-0, the Q_{10} for slow-gating was ~40, suggesting a very large conformational change [15]. From the crystal structure it is impossible to determine which regions of the protein may move during the slow gating process. One critical difference between bacterial and mammalian ClC proteins is the presence of large intracellular domains in the mammalian ClCs. As outlined above, mutations in these cytosolic domains, in particular the CBS domains, may have drastic effects on slow-gating, suggesting that these regions may be directly involved in the gating process [23, 69]. Zheng and coworkers confirmed a large rearrangement of the cytosolic domains of ClC-0 during gating using spectroscopic microscopy. Using FRET, they observed an ~23 Å movement of the C-terminus; this movement was abolished in the presence of Zn^{2+}, which promotes closure of the slow gate, as well as by the C212S mutation [243]. Mutagenesis studies of ClC-1, performed by Roberts and coworkers, showed that several residues at the dimer interface may be involved in slow gating, including C277, which is conserved across all ClCs and may participate in inhibition by Zn^{2+} [39]. Since slow gating is proposed to regulate both pores simultaneously, involvement of the dimer interface is likely crucial, although structural rearrangements of the dimer interface have not been shown.

As stated above, the intracellular C-terminal domains of mammalian ClC proteins may be critically involved in channel gating or regulation. Each C-terminal domain contains two CBS domains, which have been shown to interact with each other within a subunit, but also with the C-terminal domain of the other subunit present in the functional ClC protein [175, 244]. The crystal structures of the C-terminal domains of three ClC proteins have now been solved: ClC-0, ClC-Ka, and ClC-5 (Fig 4E, F). The C-terminal domains of these proteins all adopt similar folds, which can be seen in the structural alignment shown in Figure 4F. While the crystal structure of the ClC-0 C-terminal domain did not show intersubunit dimerization of the C-terminal domains, Markovic and Dutzler did observe dimerization of the ClC-Ka C-terminal domains [244]. Ultracentrifugation studies of the soluble C-terminal domains suggested that intersubunit dimerization also occured for ClC-0, even though this was not captured in the crystal structure [245, 246]. Thus, intersubunit dimerization may be a common feature for mammalian ClC proteins, although the functional role is not yet known.

The crystal structure of the ClC-5 CBS domains showed that ATP was coordinated at the CBS1/CBS2 interface [175]. However, this does not seem to be a common feature of ClC proteins, as neither ClC-0 nor ClC-K have been shown to bind nucleotides. ClC-1 and ClC-2 have shown changes in activity based on ATP concentration, but it has not been conclusively proven that ATP binds directly to the CBS domains of these channels [44, 46, 47]. The interaction interface of the CBS domains is smaller than that of other CBS domain containing proteins, being only ~1500 $Å^2$, and Dutzler and colleagues suggest that this may be due, in part, to conformational changes that occur within the protein during gating, although this has not been conclusively

shown [175, 244]. Interestingly, mutations in the CBS domains of the *C. elegans* ClC protein equivalent to ClC-2 altered accessibility of extracellular residues to MTSET, suggesting that the C-terminal domains may interact directly with the intracellular face of the channel, and induce allosteric changes in protein structure that may significantly influence ion conduction and gating [224].

Over the past few years, structure/function studies of ClC proteins have been greatly aided by the availability of the bacterial crystal structures. The structural basis for fast-gating is now well understood, and the bacterial structures provide an excellent template for the eukaryotic ClC protein membrane regions. Molecular dynamics simulations aimed at dissecting ion conduction through ClC proteins suggests that that the permeation pathway may be similar for ClC channels, although these simulations have all been based on the structure of the bacterial ClC transporters [247, 248]. However, the structural basis of slow gating is still lagging far behind that of fast gating. Although it is known that a large structural rearrangement must occur during this process, the conservation of those rearrangements between ClC proteins needs to be determined. It is likely that the conformational changes during slow gating of ClC-1 and ClC-2 are much smaller than that for ClC-0, given that the Q_{10} value for this process is much smaller for these channels. Additionally, the interaction between the cytosolic domains and the membrane domains needs to be further characterized. Detailed analysis of this region may not be possible until the crystal structure of a full eukarotic ClC protein is obtained. However, pharmacological characterization of ClC proteins using common Cl^- channel inhibitors has provided some insights into ion conduction and gating, as will be

discussed below. This process, however, will be greatly aided by the discovery of high affinity inhibitors.

1.5 ClC Protein Pharmacology

Pharmacological characterization of ClC proteins has been performed generally using only a few types of molecules: heavy metal ions such Zn^{2+} or Cd^{2+}, clofibric acid derivatives, disulfonic stilbenes, and arylaminobenzoates. This limited number of inhibitors has been used to characterize only a small percentage of ClC family proteins; the majority of pharmacological characterization has been performed on ClC-0, -1, and -K. We will discuss the insights into ClC channel structure and function that have been gained through the use of these inhibitors, as well as the advantages and disadvantages of these molecules.

1.5.1 Divalent Heavy Metals

Some of the most useful inhibitors of voltage-gated cation channels have been peptide toxins isolated from animal venoms such as spiders, scorpion, and cone snails [249]. There are hundreds of these toxins that are known to inhibit cation channels. During the search for a peptide inhibitor of ClC-0 voltage-gated chloride channels, Chen discovered that spider venom contained a component capable of inhibiting ClC-0; however, this inhibitory activity was retained when channels were exposed to venom that had been previously burned, thereby destroying all peptide components [21]. Activity of the venom was subsequently attributed to the presence of divalent heavy metal cations that are present in venoms of many poisonous animals. Screening individual ions showed

that Zn^{2+}, Cd^{2+}, and Ni^{2+} could inhibit ClC-0 mediated currents, while Co^{2+} and Mn^{2+} could not [21]. Investigation into the mechanism of inhibition by these metals showed that they had no appreciable effect on the fast-gating process, but significantly increased the forward rate of channel inactivation due to closure of the slow gate, likely stabilizing a channel conformation in which the slow gate is closed [21]. The affinity of ClC-0 for Zn^{2+} is ~1 - 3 μM, which is among the highest affinity interactions for an inhibitor of ClC channels [21]. These transition metals are also known to inhibit other members of the ClC family, including ClC-1 and ClC-2 [250, 251], albeit with greatly reduced affinity (> 50 μM).

Investigation of the inhibitory mechanism of transition metals led to characterization of one of the molecular determinants of slow gating. Zn^{2+} and Cd^{2+} can be coordinated by both histidine and cysteine residues [22]. Chen reasoned that because Zn^{2+} acted to facilitate the closure of the slow gate, the binding site of this metal should be in a region that strongly contributes to the slow gating process. Site-directed mutagenesis of many cysteine residues showed that C212 of ClC-0 provided the binding site for these transition metals. Mutation of this residue not only severly impaired the ability of Zn^{2+} to inhibit ClC-0 channels, but also completely removed the slow gating process, yielding channels that were nearly constitutively open [22]. Sequence analysis revealed that this residue is conserved in both ClC-1 and ClC-2. Indeed, mutation of this equivalent residue in ClC-1 and ClC-2 significantly reduced the inhibitory effect of Zn^{2+} on these channels [67, 68, 251]. Additionally, mutation of this cysteine residue in both ClC-1 and ClC-2 reduced the contribution of slow gating to channel activation and deactivation, consistent with the notion that this particular residue is important for slow

gating of ClC channel-type proteins. Inhibition of ClC-1 by these transition metals, however, was irreversible, and Duffield and colleagues suggested that they may interact with a very low probability state of the slow-gate. They showed that the V321A mutation, which reduced open probablilty of the slow gate, greatly increased inhibition by zinc [252]. So while the overall effect of zinc on gating of ClC-1 may be qualitatively similar its effect on ClC-0, the exact mechanism may not be the same, and needs to be further investigated. Interesting, Osteen and Mindell recently found that the Cl^-/H^+ exchanger ClC-4 is also inhibited by zinc. This is particululary interesting due to the fact that this transporter does not have the equivalent of a slow-gate, and in this case, zinc is coordinated by a group of histadine residues that are absent in the ClC channels [253]. This suggests fundamentally different gating mechanisms regulate the ClC channels and transporters.

1.5.2 Clofibric acid derivatives

Of all available ClC channel inhibitors, the inhibitory effects of clofibric acid derived class of ClC inhibitors against their respective targets are the most well characterized. The basic structure of one such molecule is shown in Figure 5. Much of the work using these molecules has been devoted to characterizing ClC-0, ClC-1, and ClC-K. The main clofibric acid derivatives used to inhibit ClC channels are 2-(4-chlorophenoxy) propionic acid (CPP), 2-(p-chlorophenoxy) butyric acid (CPB), and p-chlorophenoxy acetic acid (CPA), which display complicated mechanisms of action, although they all act exclusively from the intracellular side of ClC-0 and -1 [242, 254, 255]. The effect of clofibric acid derivatives was first identified by Conte-Camerino and

coworkers, who found that clofibrate drastically reduced G_{Cl} in skeletal muscle by directly inhibiting the channel later identified as ClC-1 [256]. Further investigation showed that inhibition of ClC-1 mediated currents by these molecules greatly depended on the specific enantiomer used, as most of these molecules are chiral. Specifically, S-CPP and S-CPB were able to reduce G_{Cl} in intact muscle with K_Ds of 14 and 16 μM respectively, while the R-enantiomers had almost no effect [256]. Testing CPP directly on ClC-1 mediated currents in *Xenopus* oocytes showed that inhibition was very complicated, depending not only on the CPP enantiomer as previously described, but was also strongly voltage-dependent [257]. By studying the inhibition of steady-state ClC-1 currents by S-CPP, Conte-Camerino and colleagues measured a K_D of 40 μM at -80 mV, while K_D increased as membrane potentials became more positive. In contrast to the effect of S-CPP, R-CPP had no effect on ClC-1 currents at concentrations up to 1 mM [257]. Interestingly, while the binding site of CPP is likely in the ClC-1 pore, Roberts and colleagues showed that CPP actually inhibits channel gating; channels deactivate more rapidly at hyperpolarizing potentials, and CPP induces a shift in the $V_{1/2}$ of activation to more depolarizing potentials [258]. It is likely that CPP alters the fast gating process; the mutation C277S, which strongly reduces slow gate closures, does not alter the inhibitory effect of CPB, suggesting that clofibric acid derivatives have no effect on the slow gating process [40]. Also, other mutations that alter slow gating in ClC-1, F307S and A313T, also do not alter the inhibitory effect of CPP [259]. A mutational study undertaken by Pusch and colleagues probed the binding site of the clofibric acid derivative CPA, and the structurally unrelated molecule 9-anthracene carboxylic acid (9-AC) [260]. This worked suggested that these drugs share a binding site near the central Cl^- binding site, although

the orientation of these drugs in the pore is not known. Interestingly, while CPP is capable of inhibiting ClC-1 at low μM concentrations, this molecule inhibits ClC-0 and ClC-2 with K_Ds > 1mM, suggesting that the binding sites within the pores of ClC-0 and -2 are different from that of ClC-1 [257]. Although this molecule is classified as a gating modifier, it is possible that the operation of the fast gate is only indirectly affected, as occlusion of the ClC pore would likely also alter channel opening and closing due to the strong link between permeation and gating of these channels.

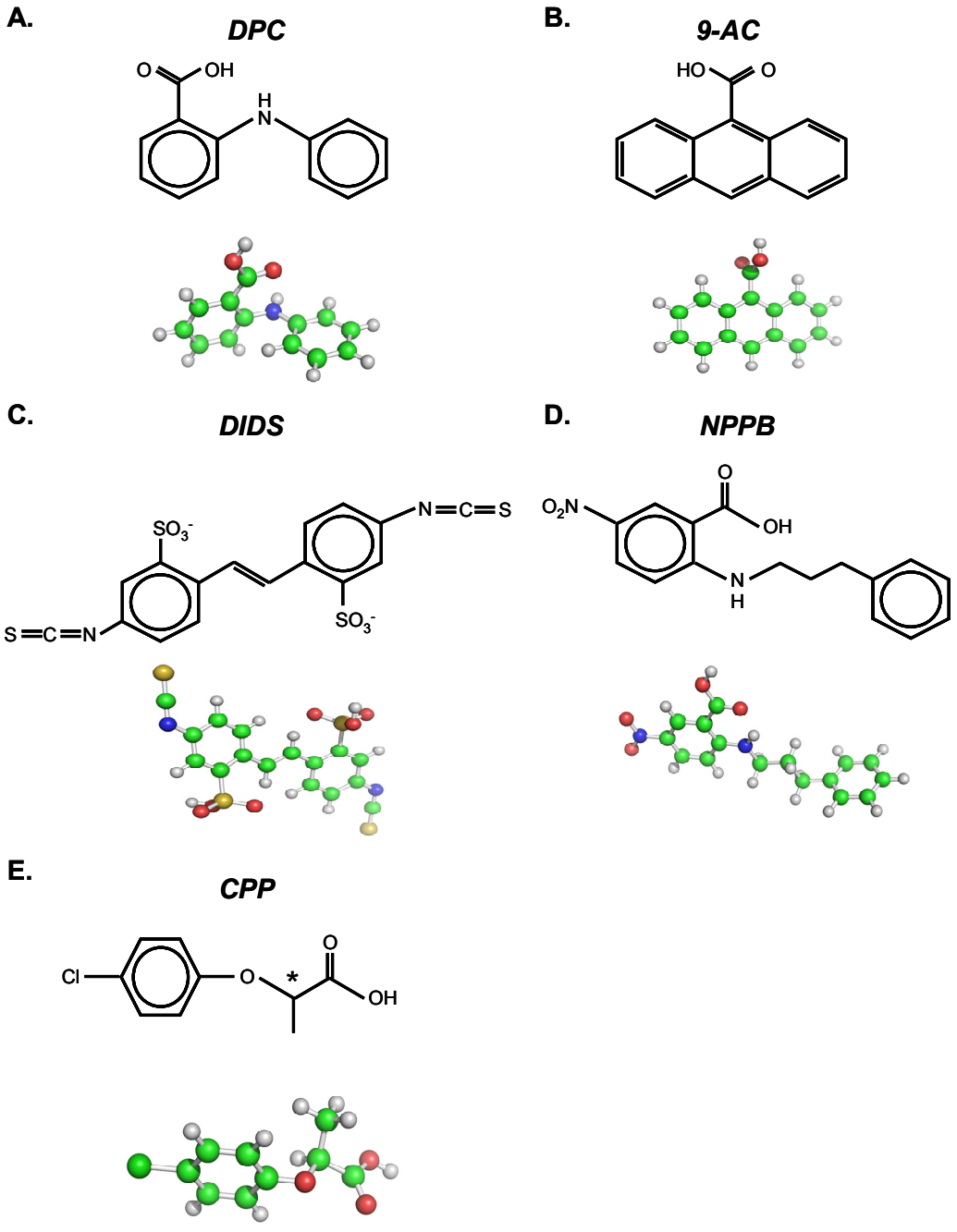

Figure 5: Organic molecule ClC inhibitors. These molecules have been shown to inhibit ClC proteins. The two-dimensional (top) and three dimensional (bottom) stuctures of DPC (A), 9-AC (B), DIDS (C), NPPB (D), and CPP (E) are shown. The * represents the carbon about which chain substitutions are made to create other members of the clofirbic acid family.

A number of CPP derivatives have been shown to inhibit ClC-K channels. While CPP itself does not inhibit ClC-K well (K_D > 1mM), addition of a benzene ring to the methyl group (3-phenyl-CPP) increased affinity to the 150 μM range [261]. Like the activity of CPP on ClC-1, CPP derivatives inhibited ClC-K1, and –Ka, in a voltage-dependent manner, being more potent at depolarizing membrane potentials. The potencies of these drugs were altered by changes in Cl^- concentration, with increased inhibitory activity at lower external chloride concentrations. Consistent with this, mutation of the extracellular residue N68 to aspartic acid reduced the affinity of 3-phenyl-CPP for ClC-Ka by more than 5-fold [262]. Additionally, introduction of this asparagine residue into the correct position in ClC-Kb resulted in sensitivity to 3-phenyl-CPP [262]. Thus, CPP analogues may prove useful in probing the pore structure of ClC-K channels, which are ion channels, but do not display voltage-dependent gating.

Recently, clofibric acid derivatives have been very useful in examining the conformational changes associated with fast gating. Similar to the effects of clofibric acid derivatives on ClC-1, these compounds inhibit ClC-0 strictly from the intracellular side. Interestingly, these molecules bind to the pore of ClC-0 in a strongly state dependent manner, preferentially binding to the closed state with ~20 fold higher affinity over the open state [242]. Consistent with a binding site within the pore, the C212S mutation, which eliminates slow gating, does not affect binding of CPB. Lowering internal chloride concentration increased the on-rate of the drug, suggesting that CPP derivatives may compete with Cl^- for occupation of the binding site [254]. However, this may be too simplistic, as removal of the gating glutamate by introducing point mutations at E166 increased the potency of CPA by > 200 fold, but did not eliminate the state-dependence

observed in WT channels [255]. Interestingly, lowering the intracellular chloride concentration had only modest effects on CPA binding to E166A-ClC-0 channels; affinity was increased by only ~3 fold at very depolarizing potentials. While the E166A mutation seemed to affect both open and closed channel inhibition, mutation of other residues near the intracellular mouth of the pore affected either only closed channel inhibition (T481S), or open channel inhibition (S123T, Y512A, K519Q) [242]. Based on the crystal structure, it was originally suggested by MacKinnon and colleagues that fast gating relied solely on the rearrangement of the E166 residue of ClC-0. While state dependent binding of CPP analogues may be explained by competition between the inhibitor and Cl^- ions within the pore, crystal structures have shown that all chloride binding sites are maximally occupied in both the open and closed states [239, 263]. Additionally, the ability of mutations to affect either closed channel inhibition or open channel inhibition suggests a more significant conformational change within the pore than just the rearrangement of a singular glutamate residue during opening and closing of the fast-gate. The possibility of larger conformational changes during fast gating needs to be further addressed, as this is likely to impact not only the current views on channel gating, but on the transport cycle of ClC exchangers as well.

1.5.3 Disulfonic stilbenes

Unlike heavy metal inhibitors such as zinc, and the clofibric acid derivatives, there has not been a great deal of characterization into the mechanism of inhibition of ClC proteins by disulfonic stilbenes. One such molecule, DIDS, has been shown to inhibit ClC-0 with affinity in the μM range, and was key in characterization of ClC-0, as

susceptibility of the cloned ClC-0 channel was the same as the endogenous voltage-dependent chloride conductance found in *Torpedo* electroplax [1, 3, 7]. DIDS is also capable of inhibiting ClC-Ka with an affinity in the 100 μM range [262]. Interesting, Maduke and coworkers showed that a pentameric hydrolysis product of DIDS could inhibit ClC-Ka with a $K_{1/2}$ of just 0.5 μM [264]. These molecules are presumed to inhibit channel activity by an open channel pore block mechanism; however, this has not been rigorously tested. Similar to CPP, DIDS is thought to occupy an extracellular binding pocket near the pore based on site-directed mutagenesis within the extracellular vestibule [262]. Interestingly, Hiraoka and colleagues showed that ClC-2 is completely insensitive to this class of molecule, showing no change in activity to DIDS, DNDS, and SITS at concentrations up to 10 mM [71]. Matulef and Maduke showed that the prokaryotic ClC transporter, ClC-ec1, can be inhibited by DIDS only when it is is applied to the intracellular face of the transporter. The Y445C mutation could potentiate transport when modified by MTSET only when MTSET was added to the intracellular face of the channel. This potentiation could be inhibited by preincubation with DIDS [265]. While there is not a great deal of mechanistic information associated with disulfonic stilbenes, these molecules have been useful for the basic characterization of some ClC proteins. However, the use of these molecules is quite limited; not only do they inhibit ClC proteins with very low affinity, they are incredibly non-specific, not only inhibiting some ClC proteins, but also CFTR and Cl_{Ca}, two structurally unrelated chloride channels [266, 267].

1.5.4 Arylaminobenzoates

Much like the disulfonic stilbenes, arylaminobenzoates are Cl^- channel inhibitors characterized by both very low affinity, and lack of specificity. Molecules such as DPC and NPPB are capable of inhibiting currents elicited from ClC-0 and ClC-2 from the extracellular face, with affinity for ClC-2 being ~ 1 mM [53, 71]. These molecules also inhibit CFTR channels with low affinity. The most interesting effects of arylaminobenzoates are the differential effects of niflumic acid (NFA) and flufenamic acid (FFA) on ClC-K channels. Pusch and colleagues showed that while FFA mediated only an inhibitory effect on ClC-Ka, NFA showed biphasic behavior, able to potentiate ClC-Ka currents at low concentrations, and inhibit current at high concentrations [268, 269]. Interestingly, Pusch and colleagues also showed that NFA only inhibited the ClC-Ka rat homolog, ClC-K1 [269]. The authors suggested the presence of multiple NFA binding sites which related to the differential effects of the drug. Furthermore, changes in extracellular chloride concentration did not alter the effects of NFA, suggesting that these binding sites are not located deep within the pore. Conte-Camerino and colleagues suggested that the differential effects of FFA and NFA are due the different conformational states that these molecules can adopt; NFA exists in a planar state, while FFA does not [268, 270]. Consistent with this idea, Conte-Camerino and colleagues showed that synthetic organic molecules that adopt a planar conformation similar to that of NFA were also capable of potentiating ClC-Ka currents [270], while non-planar molecules could only inhibit ClC-Ka channels. While the exact mechanism by which NFA or other planar molecules can potentiate ClC-Ka currents, they can potentially be used as lead compounds to treat Bartter's syndrome resulting from decreased ClC-K

conductance [270]. NFA is also capable of inhibiting ClC-1 by interacting with the cytoplasmic side of the channel with an affinity of ~42 nM, although the exact binding site has not been identified [271]. The effect of these molecules on other ClC proteins has not been thoroughly addressed.

With the exception of heavy metal inhibitors and the clofibric acid derivatives, ClC protein pharmacology is a largely undeveloped field with very few specific compounds, and no high affinity molecules. Additionally, very little single channel work has been done to further elucidate the mechanisms of inhibition by disulfonic stilbenes and arylaminobenzoates. Finally, while these molecules have been used with limited success to address both pore structure and conformational changes associated with channel gating, the pharmacological characterization of large scale rearrangements of ClC proteins and analysis of the structural differences between ClC family member subtypes requires new tools. These types of questions have been investigated for cation channels using peptide toxins isolated from animal venom. To date, however, no peptide toxin has been isolated that is capable of inhibiting a ClC protein.

1.6 Peptide toxins from venomous animals

The venoms from various poisonous animals have provided some of the most useful pharmacological tools in the form of small peptide toxins that bind to ion channels, altering their activity [249]. Thousands of these types of molecules have been isolated from the venoms of scorpions, spiders, cone snails, and snakes, some of which are shown in Figure 6. Peptide toxins have been especially useful for the study of cation channels including K_V, Ca_V, Na_V, and TRP channels, as well as K_{Ca} and pentameric AChRs [272-

276]. While these toxins primarily inhibit channel activity, there are some instances where channel activity is potentiated by toxin binding. Interestingly, while there are hundreds of these inhibitors that are known to affect cation channel activity, there is only one that exerts an effect on a chloride channel of known molecular identity. We will briefly discuss the benefits that these toxins have provided for detailed structure/function analysis of their targets, as well as the lack of these important tools for anion channel research.

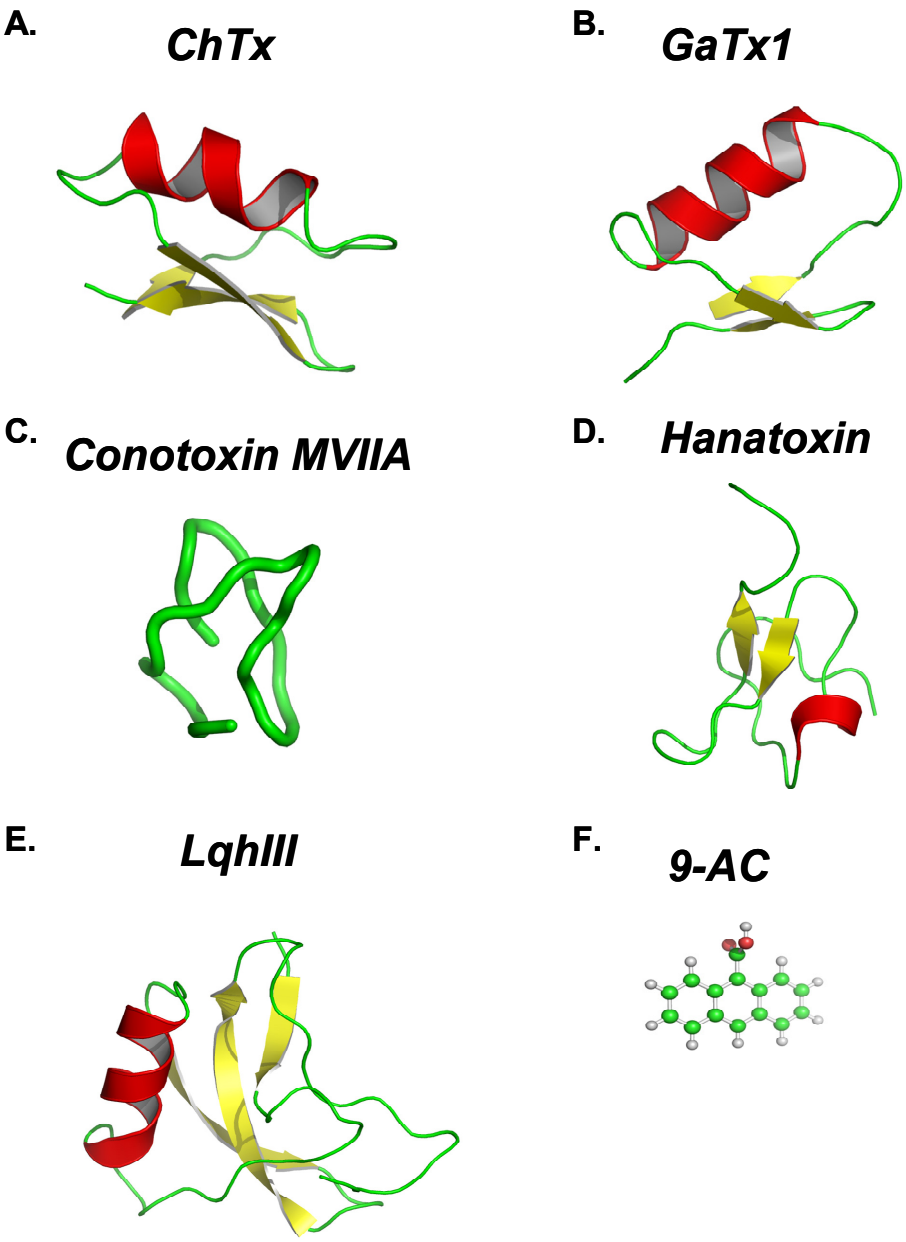

Figure 6: Ion channel peptide toxin inhibitors. Classic peptide toxins isolated from scorpion venom, snake venom, and cone snail venom. Three dimensional structures for Charybdotoxin (A), Georgia anion toxin 1 (B), Conotoxin MVIIA (C), Hanatoxin (D), and LqhIII (E) are shown in cartoon representation. These molecules represent classes of molecules which inhibit K^+, Na^+, or Ca^{2+} channels. GaTx1 is the only toxin which inhibits a Cl^- channels. 9-AC (E) is shown on the same scale for size comparison.

1.6.1 Peptide toxins active against cation channels

Peptide toxins exert their effects primarily by one of two distinct mechanisms; they may either occlude the permeation pathway, or alter channel gating by changing the energy barrier required for channel activation or deactivation. Most peptide toxins bind to their targets with both high affinity, and high specificity. For example, the cone snail toxin ω-conotoxin MVIIA, which inhibits neuronal $Ca_V2.2$ channels by blocking the channel pore, binds with an affinity of ~10 pM when measured in rat brain synaptosomal preparations [277], but has little effect on any other Ca^{2+} channel. Indeed, most peptide inhibitors show a binding affinity in the nanomolar range [249]. A few examples of both toxin specificity and affinity are shown in Table 3. Another important feature of these toxins is their relatively large interaction surface area, as compared to small organic molecules which inhibit channels (Table 3). The larger overall surface area generally leads to a very large interaction interface, the advantages of which we will discuss below.

Table 3: Selected inhibitors of ion channels. Listed are several peptide toxin inhibitors active at various cation and anion channels. Also shown are several organic inhibitors of chloride channels, many of which are not selective.

Table 3: Selected inhibitors of ion channel activity

	Molecular Weight	*Surface Area ($Å^2$)*	*Target*	*Affinity*
Toxins:				
Charybdotoxin	4.3 kDa	4212.2	KCa Kv1.3	2.1 nM 227 nM
Hanatoxin	4.1 kDa	3942.6	Kv1.2	42 nM
ω–Conotoxin-MVIIA	3.3 kDa	2589.6	Cav2.2	0.7 nM
LqhIII	7.0 kDa	7123.9	Nav1.2 Nav1.7	342 nM 13.6 nM
GaTx1	3.7 kDa	3728.4	CFTR	25 nM
Organic Compounds:				
CPP	200.6 Da	212.1	ClC-1 ClC-K	14 μM 150 μM
DPC	213.2 Da	231.6	CFTR ClC-0 ClC-2	237 μM ~ 50 μM > 1 mM
DIDS	454.5 Da	377.8	CFTR ClC-0	240 μM ~ 20 μM
NPPB	300.3 Da	330.9	CFTR ClC-2	35 μM 500 μM
9-AC	222.2 Da	223.3	ClC-1 ClC-2	13 μM > 1 mM

As stated above, many peptide toxins inhibit channel activity by physically occluding the channel pore with a 1:1 stoichiometry. Two of the most important pore blocking toxins are charybdotoxin (ChTx), which inhibits some K_V and K_{Ca} channels with nanomolar affinity [278, 279], and agitoxin2 (AgTx2) [280], which also binds to K_V channels. Prior to the crystallization of the KcsA bacterial K^+ channel, both ChTx and AgTx2 were used to probe the spatial localization of many residues that contribute to the outer pore vestibule of K^+ channels [278, 280, 281]. Using a process known a thermodynamic mutant cycle analysis (TMCA), MacKinnon and coworkers were able to probe the toxin binding interface between AgTx2 and K_V channels [280]. TMCA takes advantage of the high affinity, large surface area interaction between the toxin and the channel, and may be used to locate residues on the toxin and channel that interact with each other. Mutations are introduced individually into the toxin or the channel; if the residue that is mutated is important for binding, a change in affinity is observed. Next, the mutant toxin is tested for activity against the mutant channel. If the mutated residues are interacting, then the effect on binding affinity measured by testing the mutant toxin against the mutant channel will be greater than the effect of either mutation alone . Using this technique MacKinnon and coworkers were able to identify the residues on both AgTx2 and the *Shaker* K^+ channel that likely form the interaction interface between the two proteins, identifying several residues in the outer vestibule and selectivity filter that were involved in toxin binding [282, 283]. The results were confirmed with the elucidation of the KcsA structure, which showed that the residues predicted to interact with these toxins were major contributors to the outer mouth of the K^+ channel pore [237]. This pore architecture has since been shown to be conserved in other K^+ channels,

including both bacterial and mammalian voltage-gated K^+ channels, and is likely conserved in voltage-gated Na^+ and Ca^{2+} channels [284, 285].

Other peptide toxins inhibit channel activity by altering channel gating by changing the energy required for channel activation or deactivation. Toxins that modify channel gating do not bind near the channel pore, but near the channel gating domain, specifically the voltage sensors for voltage-gated cation channels [249, 274]. For voltage-gated cation channels, the voltage sensor is primarily composed of S3 and S4 helices, as shown in Figure 4A. For voltage-gated K^+ channels, four identical subunits comprise the functional channel; therefore, up to four toxins may be bound to the channel, as demonstrated for the spider toxin hanatoxin (Htx) [286]. Other voltage-gated cation channels are not composed of identical subunits, but are one protein composed of four similar, yet not identical domains. Thus, toxins which modify gating of these channels may only have one binding site, such as the toxin LqhIII, which binds to a short region between the S3 and S4 helix in domain IV of the human $Na_V1.2$ channel, and drastically slows channel inactivation [287]. The binding site at the linker between the S3 and S4 helix seems to be a conserved feature, as other gating modifier toxins such as ω-grammatoxin-SIA, hanatoxin, and VsTx1 all seem to bind at homologous locations [249, 273, 274, 288]. Despite the fact that the binding sites of these toxins are small compared to that of pore blocking toxins, their usefulness is not diminished. Gating modifier toxins have provided critical insights into the structure of the voltage sensor of voltage-gated K^+ channels [274]. The structure of the bacterial voltage-gated K^+ channel KvAP showed a very peculiar and controversial arrangement of the voltage sensor; the S3 and S4 helices were arranged in a manner that suggested that they moved together during gating, and

was deemed the paddle model [284]. This contradicted much experimental data suggesting that only the S4 helix moved during channel gating. Swartz and colleagues have used hanatoxin to show that the S3-S4 voltage sensor is a portable motif by creating chimeric proteins bearing the S3-S4 helix of Kv2.1 that are both voltage-gated, and sensitive to hanatoxin [289, 290]. In fact, hanatoxin sensitivity may be transferred to the newly identified family of proton channels, and voltage-dependent phosphatases, which contain a voltage-sensing domain similar to K_V channels, but lack a pore domain [290]. Thus, the S3-S4 structural domain seems to be an important feature for channel activity, although conformational changes associated with voltage-dependent gating have not been addressed using hanatoxin. Interestingly, MacKinnon and coworkers have shown that peptide toxins from spider venoms, such as hanatoxin and VsTx1, actually partition into the lipid, and reach their binding site by lateral diffusion across the membrane [291]. Other structure/function studies using the scorpion toxin Ts1, which modifies gating of $Na_V1.4$, showed that locking the S4 voltage sensor of one domain influences the position of the S4 helices in the other domains of the voltage sensor [292]. Ts1 binds $Na_V1.4$ with a 1:1 stoichiometry, which suggests that gating of the $Na_V1.4$ channel is a cooperative process [292]. Finally, peptide toxin activators of TRPV channels have been recently identified [293]. Although they have not yet been used to rigorously characterize TRP channel activity, these toxins appear to lower the barrier for activation.

Peptide toxins active against cation channels have been extremely useful molecules. It is likely that subtle differences in primary sequence of both toxins and channels underlie both the affinity and specificity that these toxins display. It is likely that these toxins will continue to play a very important role in structure/function studies,

although they also provide very important physiological tools; they can be used to silence background channels in native cells, and are becoming sources of peptidomimetic drugs used to treat chronic pain.

1.6.2 Peptide toxins active against anion channels

While there are hundreds of peptide toxins available for cation channel research, there is almost a complete lack of these tools available for the study of anion channels. Debin and colleagues identified a component of *Leiurus quinquestriatus* venom, named chlorotoxin (ClTx), which inhibited a chloride conductance expressed in rat colonic epithelial cells and glial cells [294, 295]. However, the molecular identity of the channel that underlies this chloride conductance has never been identified; ClTx does not inhibit voltage-activated, cAMP-dependent, or Ca^{2+}-dependent chloride channels [296]. Sontheimmer and colleagues have shown that ClTx inhibits matrix metalloproteinase II, not a chloride channel [297].

The only peptide toxin found to inhibit a chloride channel of known molecular identity is GaTx1, which inhibits CFTR only from the intracellular side of the membrane. GaTx1, like other peptide toxins, inhibits CFTR with low nanomolar affinity, but in a strongly state dependent manner [295, 298, 299]. As described above, CFTR activity requires phosphorylation by PKA, as well as binding and hydrolysis of ATP at the nucleotide binding domains [298]. McCarty and coworkers showed that inhibition of CFTR channels by GaTx1 is greatly dependent upon channel open probability; GaTx1 inhibits channels with low P_O with greater efficacy than channels with high P_O. While this can be linked to alterations of [ATP], they showed that this was not directly due to

competition for ATP binding, as channels bearing mutations that greatly increase P_O were also inhibited poorly by GaTx1 [298, 299]. Analysis of single channel records showed that GaTx1 induced very long closed durations, silencing channels for tens of seconds to minutes. Thus, GaTx1 binds preferentially to the closed state of the channel, and modifies channel gating by stabilizing the closed state. This will be a very useful tool to study ATP-dependent gating of CFTR channels, providing a tool to assess conformational changes between closed and open states, as well as potentially identify sites within CFTR that are important for translating conformational changes within the nucleotide binding domains to the pore domain.

While CFTR is a very important chloride channel, there are many other chloride channels that lack quality inhibitors that can be used to study their activity. Included in this category are the channels in the ClC protein family, which, as described above, are critically involved in cell physiology. The need for these molecular tools is highlighted both by the lack of specific, high affinity inhibitors, and by the need for pharmacological tools that can aid in the characterization of channel gating and permeation.

1.7 Goal of the work presented in this dissertation

The goal of the work described in this dissertation was to: 1) determine if venom from the scorpion *Leiurus quinquestriatus hebraeus* contained a peptide component capable of inhibiting ClC-0, -1, or -2, and perform initial characterization of the inhibitory activity of venom, and 2) isolate the active component and characterize the inhibitory activity of the identified toxin.

PART 1

INHIBITION OF CLC-2 CHLORIDE CHANNELS BY A PEPTIDE COMPONENT OR COMPONENTS OF SCORPION VENOM

CHAPTER 2

INTRODUCTION

The phylogenetically ubiquitous Cl^- channel proteins within the ClC family are responsible for a multitude of physiological functions in organisms as varied as mammals, elasmobranchs, yeast, and green plants [28, 300]. Represented by nine mammalian variants, ClC proteins show widespread differential tissue distribution and provide regulatory control over numerous cellular functions ranging from the electrical excitability of skeletal muscles and neurons [29], to volume regulation of epithelial cells [28]. ClC channels are voltage-gated, and in some cases pH- or swelling-activated, as in ClC-2 [62, 301]. Mutations within these channels have been linked to such heritable human diseases as myotonia (ClC-1) [26], Dent's disease (ClC-5) [194], and Bartter's syndrome (ClC-Ka) [119]. ClC proteins such as ClC-2, ClC-5, and ClC-Kb are expressed in the kidney, where they play an important role in Cl^- transport in the ascending limbs of the loop of Henle, as well as the collecting duct [302]. Knockout mutants suggest that ClC-3 has a role in the formation of the hippocampus [147], and mutations in ClC-2 may be responsible for certain forms of generalized epilepsy [92], although this has not been conclusively proven. ClC-2 is also proposed to play a role in cystic fibrosis (CF).

CF is the most common lethal, autosomal recessive disease among Caucasians, and is caused by a defect in the Cystic Fibrosis Transmembrane conductance Regulator (CFTR). Both ClC-2 and CFTR are localized to epithelial cells in the lung and intestine [28, 76, 79, 80, 99, 303]. While CFTR is clearly localized to the apical membranes of

these epithelia, there is disagreement concerning the membrane localization of ClC-2. Contradictory studies have shown it localized to either the basolateral membrane [80, 81], or the apical membrane [76, 80, 304]. It has been proposed that ClC-2 may be a candidate channel for ameliorating the CF phenotype; it is possible that ClC-2 can provide the necessary Cl^- conductance at the apical membrane that is lacking when CFTR is defective. It also has been proposed, however, that disruption of ClC-2 can increase survivorship in CF patients [76, 99]. These contradictory studies make understanding ClC-2 very important, so that the role of ClC-2 in CF or treatment for CF can be better assessed.

Given the relative importance of ClCs, it is surprising that the fine structure and the underlying gating mechanisms of mammalian members of the ClC family remain unknown. In-depth structural analysis of membrane proteins is slow due to difficulty in successful formation of crystals for study. The recently solved structures of two bacterial ClC channel homologues have provided a roadmap for determination of pore structure of mammalian ClCs [14], but many questions remain unanswered. Despite considerable homology between bacterial and mammalian ClCs, the large cytoplasmic domains present in mammalian ClCs may have significant influence on both the function of those channels and their structure in comparison to the bacterial ClCs. A second problem is that crystal structures only capture a snapshot of molecular structure and may not describe the dynamic features of the gating process. ClC channels exhibit a fast gating process, which controls access to one of the two protopores, and a slow gating process, which controls access to both pores simultaneously. Although the ClC crystal structure provides some hints about residues involved in fast gating, it confers little other information about the

overall control of channel gating. Experiments utilizing structural probes in combination with site-directed mutagenesis are still necessary for the study of permeation and gating in ClC channels. Channel blockers such as DIDS and DNDS show little effect [71]; CPB and CPP have been used with some success in examining the gating processes of ClC-0 and ClC-1 [254, 257, 259], but they bind with relatively low affinity ($K_{1/2} \sim 15$ μM). DPC and NPPB ($K_{1/2} \sim 1$ mM) have been shown to be effective pore blockers of these channels, albeit with low affinity [71]. Heavy metal ions such as Zn^{2+} have been used in gating studies of ClC-0 [21]. However, high affinity probes of ClC channels have yet to be discovered. In order for detailed studies of ClC channel structure and dynamics to beperformed, new tools are needed which can address these issues.

Peptide toxins have been very useful for studying pore structure and gating mechanisms of voltage-gated cation channels [281, 289, 305]. They usually exhibit high affinity interactions and can act as either pore blockers or gating modifiers. These types of tools are lacking for chloride channel research. Recently, a component of scorpion venom has been shown to inhibit CFTR [295]. However, there are no known peptide inhibitors for the ClC family. Chlorotoxin (ClTx), a peptide toxin from the venom of *Leiurus quinquestriatus quinquestriatus*, has been shown to inhibit Cl^- current in channels reconstituted from rat intestinal cell membranes, although the molecular identity of this channel is not known [294, 306]. Studies have shown, however, that ClTx does not inhibit volume-regulated, calcium-activated, or cAMP- activated Cl^- channels from the extracellular side [296], or CFTR from the intracellular side [295]. Preliminary studies have shown that chlorotoxin has no inhibitory effect on ClC channels.

In this study, we asked whether scorpion venom contains a peptide component (or components) that may be an inhibitor of ClC Cl^- channels. The identification of a peptide inhibitor for ClC channels will provide an excellent tool for studying the structure and gating mechanisms of these complex proteins. We investigated the effects of partially-fractionated venom from the scorpion *L. quinquestriatus hebraeus* (Lqh) on the permeation and gating characteristics of ClC-0, ClC-1 and ClC-2. We show that one or more peptide components of venom interact in a voltage-dependent manner with ClC-2 from the extracellular side of the channel to inhibit Cl^- currents, while currents from ClC-0 and ClC-1 were not affected. Further, our data suggest that this peptide inhibitor acts as a gating modifier of ClC-2 channels.

CHAPTER 3

MATERIALS AND METHODS

3.1 Oocyte and cRNA Preparation

Xenopus oocytes were isolated as previously described [307] and incubated at 18^{o}C in a modified Liebovitz's L-15 medium (pH 7.5) with a cocktail of antibiotics (gentamicin, penicillin, streptomycin) and HEPES. For electrophysiological recording, cRNA was prepared for *Torpedo* ClC-0 and human ClC-1 using constructs in the pTLN vector, kindly donated by T. Jentsch (Institut für Molekulare Neuropathobiologie, Hamburg, Germany), and for rabbit ClC-2 using a construct in pSportI [71], donated by H.C. Hartzell (Emory University, Atlanta, GA). For two-electrode voltage clamp, oocytes were injected with 2.5 to 25 ng of either ClC-0, ClC-1, or ClC-2 cRNA, and data were collected 2-5 days after injection. For macropatch recordings 100 ng ClC-2 cRNA were injected per oocyte. All recordings were performed at room temperature.

3.2 Preparation of Venom, Chlorotoxin, DPC, and NPPB

Dried whole venom (Latoxan, France; or Sigma Chemical Co., Chicago, IL) was prepared at a stock concentration of 2 mg/mL in the appropriate bath solution (see below). The mucous portion of the venom was removed by processing the venom with four strokes in a Potter-Elvehjem tissue grinder, followed by centrifugation at 6000 × g for 30 minutes to pellet the mucous component. The supernatant was passed through a 10 kDa molecular weight cut-off filter (Millipore Corp; Bedford, MA) by centrifugation at

2000 × g for 40 minutes. The resulting partially fractionated venom "Lqh pf-venom" was then distributed into 1 mL aliquots and stored at -80^{o}C. Native chlorotoxin (Latoxan, isolated from Lqh venom), was prepared in the appropriate bath solution at a concentration of 1.2 μM, and used immediately.

Trypsinization was performed by incubating Lqh pf-venom solution with 0.0028% trypsin (Sigma, from porcine pancreas) overnight at room temperature. The solution was then boiled for 1 hour to deactivate the trypsin, and stored at -80^{o}C. For control experiments, undiluted Lqh pf-venom was boiled for 1 hour and allowed to cool before use. Boiled venom, with and without trypsinization, was then diluted to 0.1 mg/mL in recording solution.

DPC (Sigma) was dissolved directly in bath solution at a concentration of 1 mM, and stored at 4^{o}C. NPPB (Sigma) was dissolved in DMSO to a stock concentration of 100 mM and stored at 4^{o}C. Stock NPPB was diluted to 100 μM in bath solution for experiments and used immediately. The final concentration of DMSO in experimental solutions was no greater than 0.1%, which had no apparent effect on ClC-2 currents.

3.3 Two-Electrode Voltage Clamp Recordings

Standard two-electrode voltage clamp (TEVC) techniques were used to study whole cell currents. Currents were acquired using a GeneClamp 500B amplifier and pClamp software (Version 8.4; Axon Instruments, Union City, CA) at a corner frequency of 500 Hz. Electrodes were pulled from borosilicate glass (Sutter Instruments; Novato, CA) for a resistance that ranged from 0.3-1.3 MΩ when filled with 3 M KCl. Bath solution for whole cell experiments (ND96) was nominally Ca^{2+} free and contained (in

mM): 96 NaCl, 2 KCl, 1 $MgCl_2$, 1 $BaCl_2$ and 5 HEPES. For experiments with ClC-2, solutions also contained 20 mM mannitol to limit swelling-activated currents. For selectivity experiments, NaCl was replaced with the Na^+ salt of each of the anions studied, with 4 mM Cl^- remaining in the bath solution. Substitutions were always made in the same order (Br^-, I^-, aspartate) and bracketed with data for Cl^- (ND96 solution) before and after each substitute ion solution. Relative permeability (P_X/P_{Cl}) and relative conductance (G_X/G_{Cl}) for each substitute anion were calculated as previously shown using the average data for the bracketed exposure to Cl^- [307]. Relative conductance was calculated as $I_{Erev +25 mV (X^-)}/ I_{Erev + 25 mV (Cl^-)}$, where $I_{Erev +25 mV}$ denotes the current at 25 mV more depolarizing than the reversal potential. Slope conductance for Cl^- used was the average of the Cl^- recordings bracketing the recordings with the substitute anion. This procedure allowed the comparison of several ions in each experiment while controlling for changes in cell conditions. All solutions were adjusted with NaOH to pH 7.5. All experiments were performed using an agar bridge, and corrected for changes in junction potentials measured using a flowing KCl electrode [307].

3.4 Macropatch Recordings

Outside-out macropatches were used to assess the activity of trypsinized venom on ClC-2. The oocyte was placed in hypertonic stripping solution to allow the cell to shrink, and then the vitelline membrane was manually removed. Macropatch pipettes with resistances of 1-5 MΩ were pulled from borosilicate glass, fire-polished, and filled with solution containing (in mM): 150 NMDG-Cl, 5 $MgCl_2$, 10 TES and 2 Tris·EGTA (pH 7.4). Extracellular bath solution contained (in mM): 150 NMDG-Cl, 5 $MgCl_2$ and 10

TES (pH 7.4). Experiments were performed on patches with seal resistance >100 GΩ. Inside-out macropatches were used to test the effect of boiled venom on ClC-2. Pipettes were backfilled with 0.1 mg/mL boiled venom in extracellular solution; the tip of the pipette was filled with extracellular solution lacking venom. Recordings were made every five minutes while venom diffused to the tip until current reached steady-state. Data were acquired using an Axopatch 200B amplifier (Axon) operated by pClamp software. Data were filtered at 500 Hz, and acquired at 1 kHz.

3.5 Voltage Protocols

To determine the specificity of the venom for the different plasma membrane ClC channels, we individually tested ClC-0, ClC-1 and ClC-2 using step protocols with 13 test pulses for ClC-0, and 12 test pulses for ClC-1 and -2 (Fig. 7 *top*). For ClC-0, membrane potential was held at -140 mV for 5 seconds to activate the slow gate, and stepped to +60 mV for 150 ms to activate the fast gate. Voltage was then stepped to potentials ranging from -160 to +80 mV in 20 mV increments with a pulse duration of 300 ms, followed by a tail pulse to -100 mV for 100 ms. For ClC-1, V_M was held at -30 mV, and stepped to potentials ranging from -160 to +60 mV in 20 mV steps of 160 ms duration, with a tail pulse at -120 mV for 40 ms. The ClC-2 12-pulse voltage protocol used for initial experiments held V_M at -30 mV, and then stepped to potentials ranging from -160 to +60 mV in 20 mV steps, with a pulse duration of 3 s, and a tail pulse at +40 mV for 100 or 500 ms. The interpulse duration was 30 s for ClC-0, 15 s for ClC-1, and 45 s for ClC-2.

Voltage- and concentration-dependence of inhibition of ClC-2 were examined using a 5-pulse protocol stepping from -160 mV to +60 mV in +55 mV increments. The Lqh pf-venom was applied at concentrations ranging from 0.01 mg/mL to 0.3 mg/mL for 5 minutes prior to testing (concentrations of Lqh pf-venom hereafter are expressed as equivalent to the stated concentration of whole, unprocessed venom). Concentration-dependence was assessed by comparing maximal inhibition of quasi-steady-state currents at -160 mV or peak tail currents to pre-venom records for each concentration. Voltage-dependence was determined by comparing the I-V relationship for quasi-steady-state currents or peak tail currents to pre-venom records. For selectivity experiments cells were voltage clamped at -30 mV, stepped to -160 mV for 6 sec (to fully activate the channels) and rapidly ramped from -160 to +80 mV over a 50 ms period.

We compared the macroscopic kinetics between control cells and venom-treated cells using a single voltage pulse protocol of extended duration. V_M was held at -160 mV for 6 seconds, then stepped to +40 mV for 1.2 seconds. Time constants (τ) were calculated by fitting the quasi-steady-state activation currents and the tail currents to the sum of two exponential functions, using pClamp software.

Voltage protocols for ClC-2 in outside-out macropatches were similar to those for TEVC, with a holding membrane potential of -30 mV. One pulse of 1.5 s duration at V_M = -160 mV with a tail pulse +40 mV for 250 ms was used.

3.6 Data analysis

Data were analyzed using pClamp and SigmaPlot 7.0 (Jandel Scientific; San Raphael, CA). The percent inhibition was determined from the quasi-steady-state activation currents at the end of the pulse to V_M = -160 mV (after subtracting instantaneous currents) and the peak tail currents as:

$$\%Inhibition = 100 * \left(\frac{I_c - I_v}{I_c} \right)$$

where I_C and I_V are the control currents and currents in the presence of venom, respectively. Values for percent inhibition given in the text, therefore, specifically reflect inhibition of quasi-steady-state currents at -160 mV, or tail currents at +40 mV.

3.7 Statistics

Results are expressed as mean $\pm$ S.E.M. for *n* observations. Comparisons are by Student's t-test, with differences considered significant when $p \leq 0.05$. All statistical analysis was performed using SigmaStat 2.03 (Jandel Scientific; San Rafael, CA).

CHAPTER 4

RESULTS

4.1 Venom Selectively Inhibits ClC-2

It is well known that peptide toxins from venomous animals contain peptide inhibitors active against ion channels. None, however, have been shown to be active against members of the ClC voltage-gated chloride channel family. It was hypothesized that the peptide Chlorotoxin (ClTx), from the venom of the scorpion *Leiurus quinquestriatus hebraeus*, inhibited a chloride conductance. The molecular target of this toxin was later shown to be matrix metalloproteinase 2, not a chloride channel, although a chloride channel target may still exist [297]. However, due to the fact that this particular venom has been a rich source of peptide toxins active against cation channels, and it was thought to contain at least one peptide toxin active against a chloride channel, we screened this venom for activity against ClC channels. The effect of partially-fractionated scorpion venom (Lqh pf-venom) on ClC-0, human ClC-1, and rabbit ClC-2 expressed in *Xenopus* oocytes was examined using standard TEVC techniques (Fig. 7). While ClC-2 showed considerable inhibition both of the quasi-steady-state activation currents at hyperpolarizing potentials (58.0 $\pm$ 5.9% inhibition at 0.1 mg/mL and V_M = -160 mV, n = 16), and of the instantaneous tail currents (62.0 $\pm$ 6.7% inhibition), neither ClC-0 or ClC-1 showed significant reduction in currents despite using up to two-fold higher concentrations than used for ClC-2 (20-fold higher than the apparent IC_{50} for ClC-2). Native, purified chlorotoxin showed no inhibition of ClC-2 Cl^- currents (6.3 $\pm$ 7.6% at

1.2 μM, n = 2). These data indicate that a component (or components) of scorpion venom other than chlorotoxin selectively inhibited ClC-2, suggesting that the active toxin, once isolated, would potentially be a powerful tool for exploring structural aspects of this particular channel.

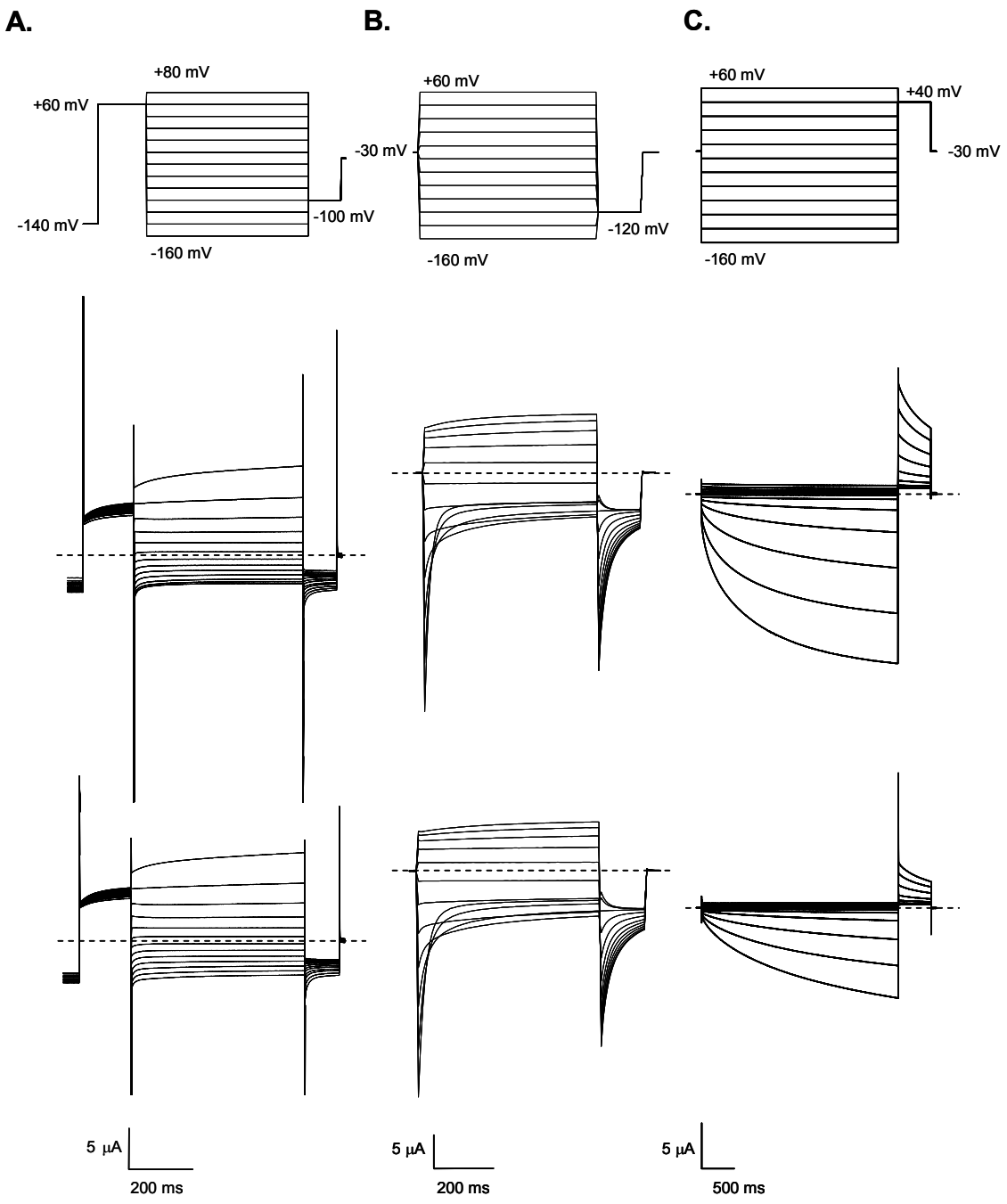

Figure 7: Effects of scorpion venom on macroscopic ClC currents. *Upper panels* are the TEVC voltage protocols, *center panels* are representative currents in the absence of venom and the *lower panels* show representative currents from the same oocytes in the presence of venom for **(A)** ClC-0 (0.2 mg/mL pf-venom), **(B)** ClC-1 (0.2 mg/mL pf-venom), and **(C)** ClC-2 (0.1 mg/mL pf-venom). Note that inhibition occurred only for ClC-2 with maximum inhibition ~50% in this example. The dashed line indicates the zero-current level for all traces.

One potential problem with studying ClC-2 channels expressed in *Xenopus* oocytes arises from the fact that currents from endogenous oocyte channels may resemble currents from ClC-2 [308, 309], as endogenous channels are also activated by prolonged pulses to hyperpolarizing potentials. Because activity of these endogenous channels may be enhanced when the cells are injected with large volumes of cRNA, it was important to determine whether the currents we identified as ClC-2 actually arose from ClC-2 channels. To address this problem, we periodically tested batches of ClC-2 cRNA-injected oocytes for permeability and conductance sequences by replacing Cl^- with Br^-, I^- or aspartate. One distinguishing feature of these two channel types is that the endogenous channels show a selectivity sequence of $I^- > Cl^-$ while all ClCs have the selectivity sequence of $Cl^- > Br^- > I^-$ for both permeability and conductance [28]. Selectivity was testing using ramp protocols described in the Materials and Methods. Each substitute anion was bracketed by recordings with normal Cl^- containing solution, to account for any rundown that may occur during the course of the experiment. The results of selectivity experiments (Table 4) showed that the currents elicited in ClC-2 injected oocytes had a permeability sequence of $Cl^- > Br^- > I^-$ > aspartate, and a conductivity sequence of $Cl^- > Br^-$ > aspartate > I^-, which is consistent with ClC channel currents [28]. Representative I/V plots are shown in Figure 8.

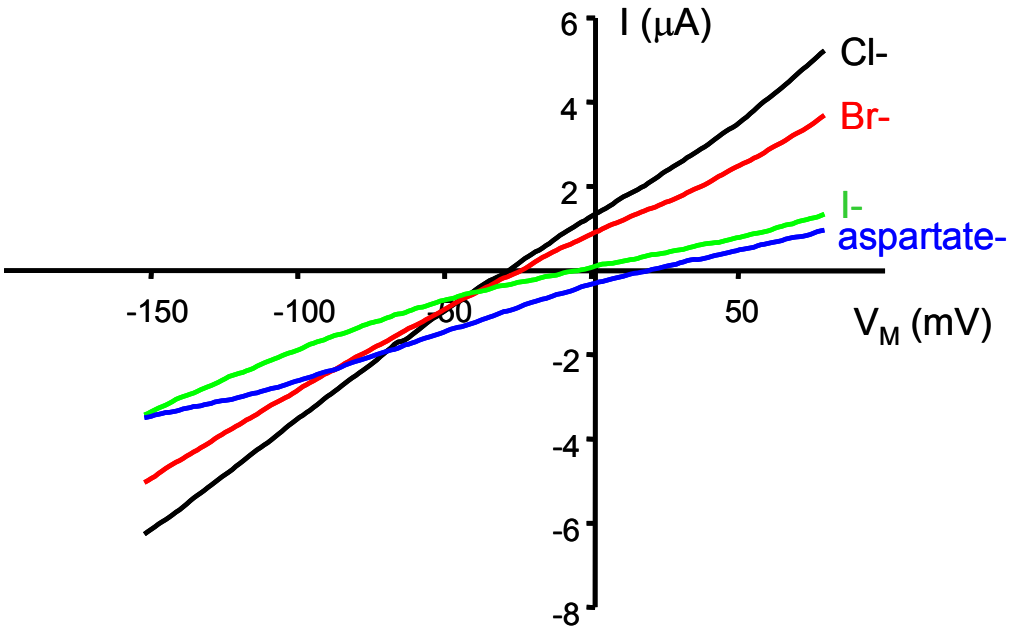

Figure 8: Ion selectivity of ClC-2. The current-voltage relationship was obtained by comparing depolarizing ramps from -160 to +80 mV. Representative currents from one oocyte, in the presence of Cl^-, Br^-, I^-, and aspartate, are shown. A shift in reversal potential to more positive membrane potentials indicates the substitute ion is less permeable than chlrodide. Thus, for ClC-2, the permeability sequence is $Cl^- > Br^- > I^-$ > aspartate.

Table 4: Anion selectivity of ClC-2 currents in oocytes. Reversal potential, relative permeability, and relative conductance for Cl^-, Br^-, I^-, and aspartate as obtained from experiment shown in Figure 8. (*) indicates $p < 0.05$ compared to Cl^-

Table 4: Anion Selectivity of ClC-2 currents in oocytes			
	$E_{rev}(mV)$	P_X/P_{Cl}	G_X/G_{Cl}
Cl^-	-36.8 ± 2.52	1.0	1.0
Br^-	-30.0 ± 2.21*	0.76 ± 0.004*	0.85 ± 0.02*
I^-	-12.9 ± 2.78*	0.37 ± 0.02*	0.27 ± 0.03*
Aspartate	9.14 ± 3.62*	0.15 ± 0.01*	0.35 ± 0.02*

4.2 Inhibition by Venom is Reversible

Many very high affinity peptide toxins show relatively slow kinetics for both the on-rate of the toxin, as well as the off-rate, showing return to baseline currents over many minutes. Also, it is important to demonstrate that venom activity is reversible upon return to non-venom containing recording solution in order to rule out possible non-specific effects. Therefore, to determine if inhibition of ClC-2 by venom is reversible, we measured the amount of inhibition over the duration of an experiment, including during exposure to venom and subsequent washout. Time series of currents at V_M = -160 mV in one-minute intervals during exposure to 0.1 mg/mL Lqh pf-venom (n = 3), and subsequent washout, show the progression of inhibition to be relatively slow and completely reversible (Fig. 9). Maximum inhibition occurred after ~5 minutes of exposure, though the majority of inhibition occurred within the first two minutes, which is the period during which the solution in the recording chamber should be entirely exchanged. Activity returned to pre-venom values after ~10 minutes of washout. However, in some cases washout took considerably longer than 10 minutes, implying that the off-rate of the venom is slow, consistent with other peptide inhibitors.

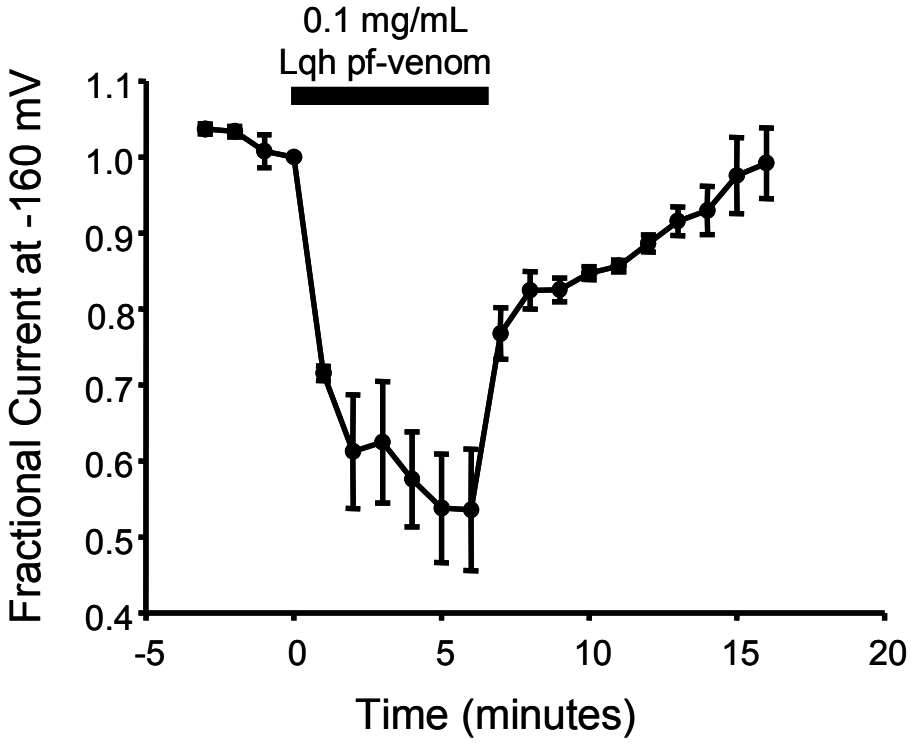

Figure 9: Inhibition of ClC-2 by venom. Time series for the inhibitory effect of venom (0.1 mg/mL, n = 3) on ClC-2 currents using a single pulse voltage protocol (fractional activation currents at V_M = -160 mV) taken at one-minute intervals. Venom flow was initiated at t = 0 and continued for 6 minutes. Maximum inhibition occurred at ~5 minutes of exposure. Inhibition was reversible within ~ 10 minutes.

4.3 The Inhibitory Component (or Components) is a Peptide

Many of the most potent and selective inhibitors of voltage-gated channels are peptide toxins isolated from animal venom [249]. Peptide components of a wide variety of venoms have provided useful tools in the study of cation channels to determine aspects of both pore structure and gating processes [280, 286, 310]. We tested the hypothesis that the active component(s) of scorpion venom is a peptide by incubating Lqh pf-venom with the protease trypsin to digest any proteins within the venom, and then boiling the mixture to inactivate the enzyme. However, when applied to whole oocytes under TEVC, the trypsinized venom produced significant leak current. It is possible that the trypsinization process released bound calcium ions, which in turn activated calcium-activated chloride channels, although the addition of chelating agents such as EGTA into our solutions did not resolve this problem. In contrast, outside-out macropatches from oocytes expressing ClC-2 remained stable during exposure both to Lqh pf-venom and trypsinized Lqh pf-venom. Macropatch currents showed no significant inhibition by 0.1 mg/mL trypsinized Lqh pf-venom (Fig. 10B,E), while strong inhibition was observed in response to untreated Lqh pf-venom (Fig. 10B,C). As a control we asked whether boiled untrypsinized Lqh pf-venom inhibited ClC-2 currents using TEVC. Boiled Lqh pf-venom at 0.1 mg/mL inhibited ClC-2 quasi-steady-state currents in TEVC experiments to the same degree as unboiled Lqh pf-venom at the same concentration (62.0 $\pm$ 4.38% inhibition, n = 3; Fig. 10B). Boiled venom also inhibited ClC-2 in inside-out macropatches in experiments where the pipette solution contained 0.1 mg/mL boiled venom (36.9% inhibition; *see Methods*), as shown in Figure 10D. Macropatch currents elicited by a pulse to V_M = -160 mV were allowed to stabilize as the boiled venom

solution diffused to the patch, and currents showed no change over 20 minutes after maximal inhibition by boiled venom was reached. The difference in degree of inhibition between TEVC and macropatch recordings could be attributed to the differing cytoplasmic chloride concentrations. These data suggest that the lack of inhibition with trypsinized venom is due to the peptide being degraded by trypsin, and not denaturation by boiling. Since heat stability is a common feature of peptide toxins, which usually have multiple intrapeptide disulfide bridges [311], this supports the hypothesis that the active component(s) is a heat stable peptide.

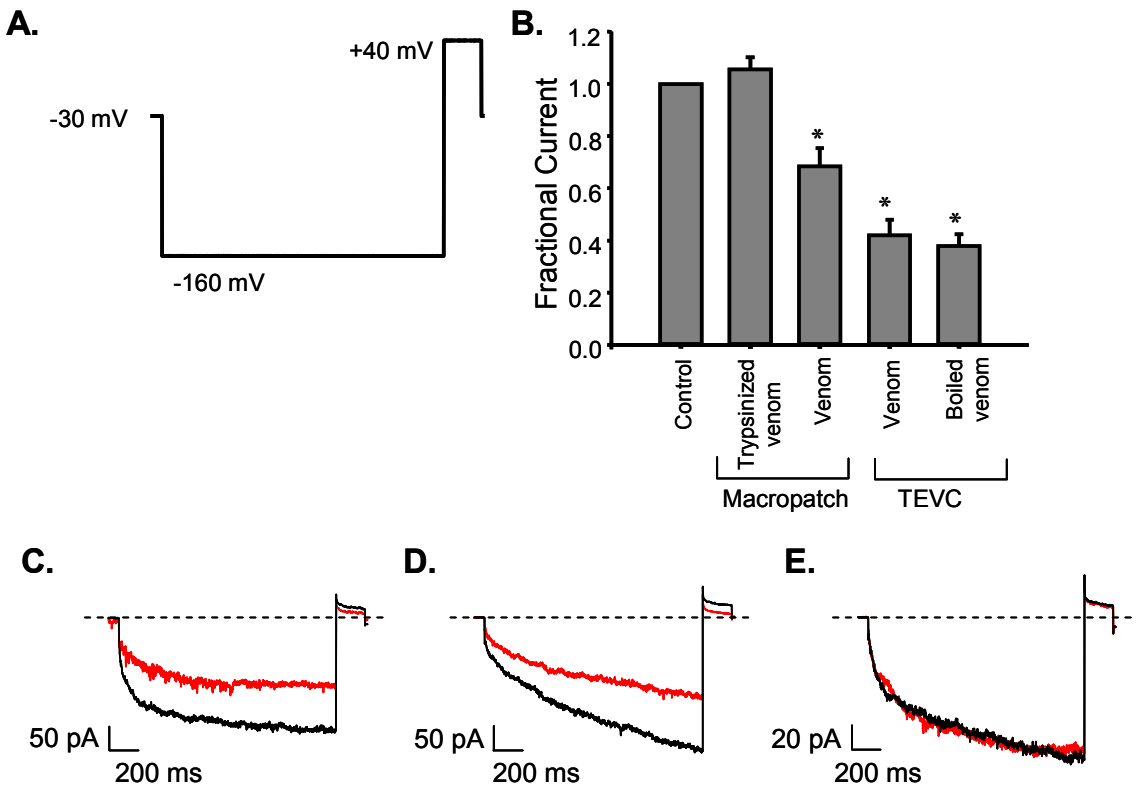

Figure 10: Trypsinization destroys activity of pf-venom. **(A)** Voltage protocol for excised, outside-out macropatch recordings. **(B)** Normalized current remaining for currents at V_M = -160 mV for control, trypsinized venom (105.7 $\pm$ 10.0%, p = 0.31, n = 5), and pf-venom (68.5 $\pm$ 6.2%, p < 0.015, n = 3) in outside-out macropatches, as well as pf-venom (42.0 $\pm$ 4.9%, p < 0.001, n = 16) and boiled pf-venom (38.0 $\pm$ 4.38%, p = 0.006, n = 3) for TEVC recordings. Venom concentration was 0.1 mg/mL for all of these experiments. (*) indicates p < 0.05. **(C)** Macropatch currents at V_M = -160 mV in the absence (*black trace*) and presence (*red trace*) of untreated pf-venom. **(D)** Inside-out macropatch current at V_M = -160 mV in the absence (*black trace*) and presence (*red trace*) of boiled pf-venom that was backfilled in the patch pipette. **(E)** Macropatch current at V_M = -160 mV in the absence (*black trace*) and presence (*red trace*) of trypsinized pf-venom. The dashed line indicates the zero-current level for all traces.

4.4 Inhibition is Concentration-Dependent

Peptide toxins typically inhibit their targets with very high affinity, usually in the nanomolar range [249, 312, 313], which makes them valuable tools for in depth studies of channel structure and gating processes [280, 286, 310]. Inhibition of ClC-2 currents by scorpion venom was clearly concentration-dependent, for both the quasi-steady-state current (Fig. 11A), and the tail current (Fig. 11B). The dose-response curve for inhibition of quasi-steady-state current at V_M = -160 mV for each Lqh pf-venom concentration (Fig. 11C) was fit to a three parameter Hill equation (r^2 = 0.91; p = 0.08). The data show clear concentration-dependent inhibition up to 0.1 mg/mL with saturation occurring at concentrations above 0.1 mg/mL. The apparent IC_{50} was 0.01 mg/mL, and the Hill coefficient was 0.97. This likely represents a high affinity interaction between the active component(s) and ClC-2, because it is not likely that the active component is present at very high abundance in the venom mixture, which may contain hundreds of individual components.

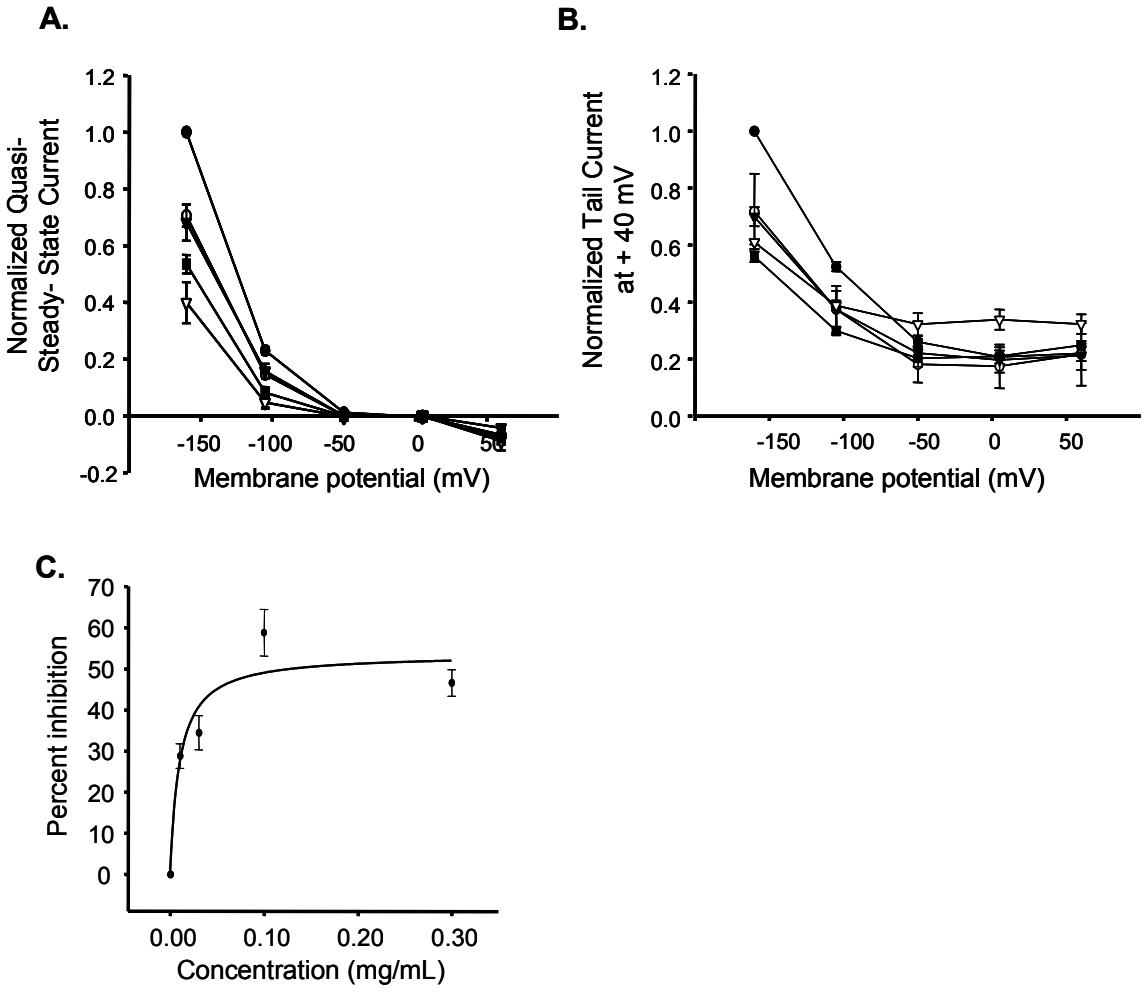

Figure 11: Voltage- and dose-dependence of inhibition of ClC-2 by venom. Voltage dependence of the **(A)** quasi-steady-state activation currents and **(B)** tail currents of ClC-2 at zero (filled circles), 0.01 (open circles), 0.03 (filled triangles), 0.1 (open triangles), and 0.3 (filled squares) mg/mL pf-venom using a 5 pulse voltage protocol. **(C)** Concentration dependence of inhibition at V_M = -160 mV. All concentrations include 3-16 replicates. The line was fit to the mean at each concentration using a three parameter Hill equation.

4.5 Venom Shifts Apparent Voltage-Dependence of Activation

The mechanism of inhibition may be assessed by analyzing the effects of Lqh pf-venom on the voltage dependence of activation of ClC-2. ClC-2 currents display a high degree of inward rectification due to poor activation at potentials more depolarizing than -30 mV. This form of current-voltage relationship is seen for both quasi-steady-state currents and tail currents at +40 mV. Peptide inhibitors may inhibit channels by either blocking channel conductance through the pore by physically occluding the pore, or by alter channel gating, such that the energy required for channel activation is higher; thus a stronger stimulus is required to achieve channel activation. These mechanisms of inhibition would therefore have different effects on the relationship between channel activation and voltage. Pore blockers would lower the maximum current, leaving the voltage-dependence of activation unchanged, while gating modifiers would shift the voltage-dependence of activation. In the presence of venom the apparent voltage-dependence of activation for quasi-steady state currents is shifted to more hyperpolarizing potentials (Fig. 12A). This may be caused by voltage dependent occlusion of the pore. However, this relationship was also seen for tail currents elicited when the voltage was stepped to +40 mV (Fig. 12B). The voltage-dependence of activation for tail currents may be converted to a P_O/V curve if maximal conductance is assumed to have a P_O ~1. In the case of ClC-2, the P_O/V curve does not saturate within the voltage range applied; however, maximal P_O may be estimated, and the $V_{1/2}$ can be calculated from the fit. A shift in the $V_{1/2}$ for channel activation in the presence of venom would imply that the active component of venom acts as a gating modifier. Analysis of voltage-dependence of activation from tail currents of multiple experiments reveals that

venom does indeed shift the $V_{1/2}$ of channel activation from 126 $\pm$ 2 mV to 176 $\pm$ 20 mV (Fig. 13), suggesting that the active component of venom acts as a gating modifier.

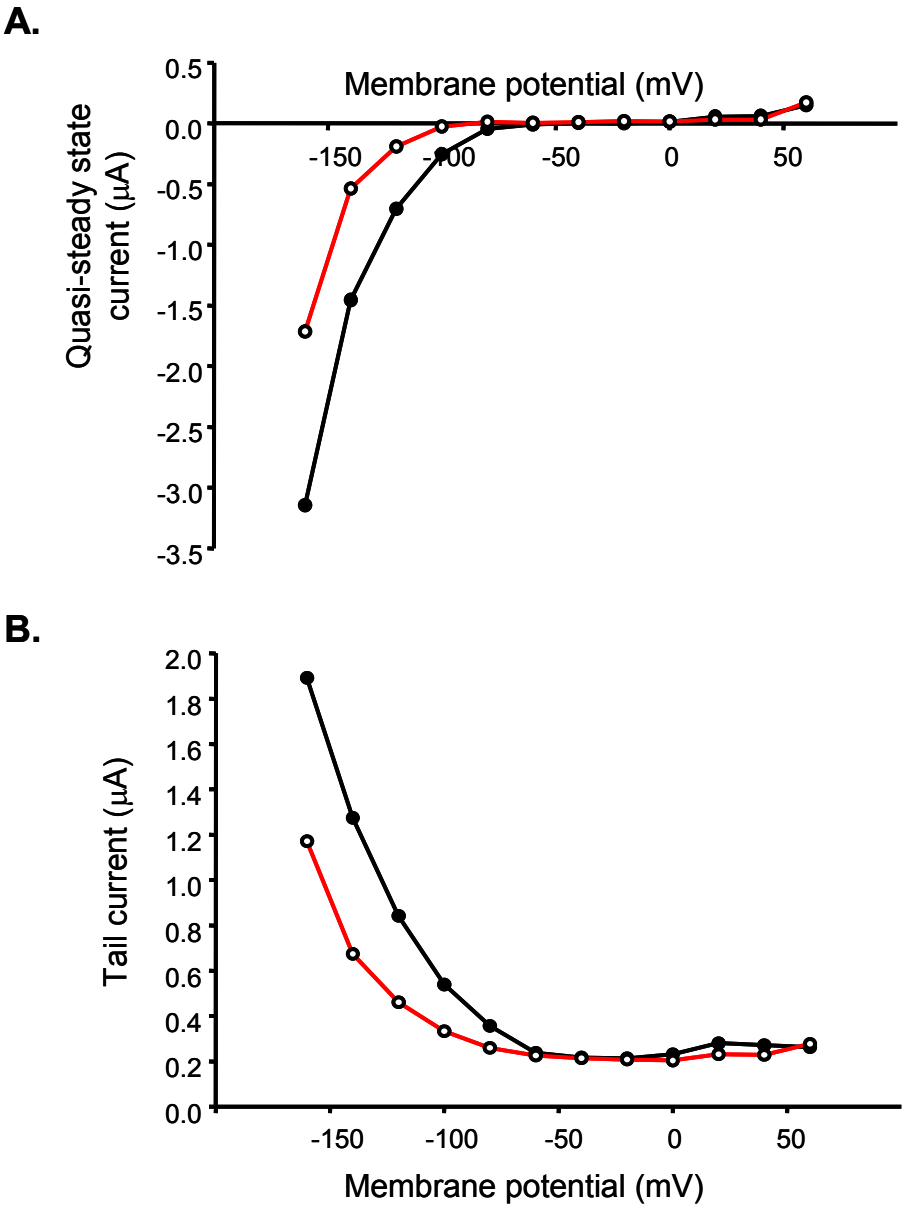

Figure 12: Effect of venom on ClC-2 macroscopic currents. Voltage dependent inhibition by pf-venom (0.1 mg/mL) of the **(A)** quasi-steady-state and **(B)** tail currents of ClC-2 in a representative experiment using the 12-pulse protocol described in Figure 7.

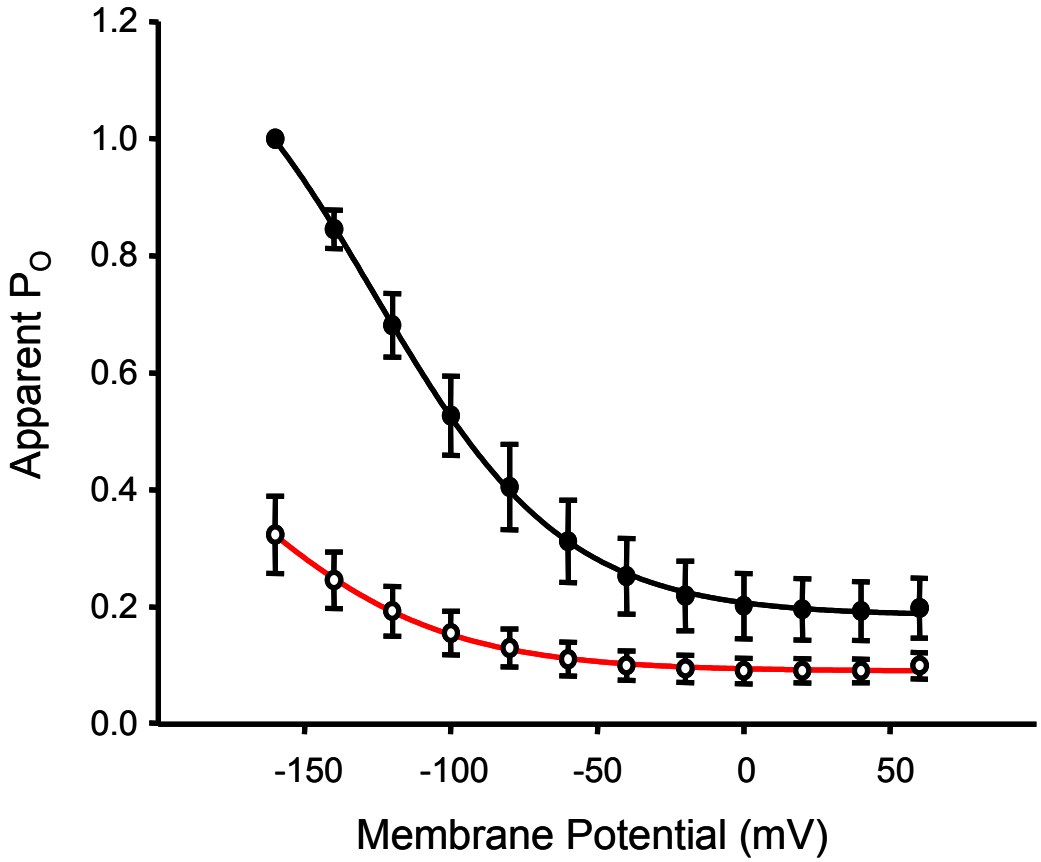

Figure 13: Venom shifts the ClC-2 activation curve. The P_O/V curve of ClC-2 that the half-maximal activation voltage is shifted to the left in the presence of 0.1 mg/mL. P_O was normalized to current at V_M = -160 mV in the absence of venom. Each point represents measurements from 8 experiments.

4.6 Voltage-Dependence of Inhibition

We examined the voltage-dependence of inhibition of quasi-steady-state currents with voltage step protocols, as well as inhibition of tail currents at +40 mV (Fig. 14). Inhibition of quasi-steady-state current showed significant voltage dependence. There was increasing inhibition of quasi-steady-state currents as the membrane potential became more depolarizing (Fig. 14A *left*). Comparison of current remaining at -160 mV to that at -60 mV showed a significant difference ($p = 0.03$, $n = 8$). Plotting I/I_o for tail currents, however, showed no voltage dependence when comparing tail current remaining following steps to -160 mV versus that following steps to -60 mV ($p = 0.34$). This is likely due to small contaminating currents at positive membrane potentials that are due to activation of endogenous channels in the oocyte.

To further clarify the mechanism of inhibition, we compared inhibition of ClC-2 by Lqh pf-venom with inhibition by small organic molecules known to be pore blockers of a variety of Cl^- channels. Inhibition by DPC was voltage-dependent (Fig 14B); however, as the I/I_o plot indicates, inhibition decreased with more depolarizing potentials throughout the voltage protocol. Inhibition by NPPB followed the same trend as inhibition by DPC for both activation and tail currents (Fig. 14C). Indeed, both DPC and NPPB led to an increase in current at weakly hyperpolarizing potentials. These results were unlike the results for Lqh pf-venom, suggesting that venom inhibits ClC-2 channels via a mechanism different from that underlying inhibition by DPC or NPPB.

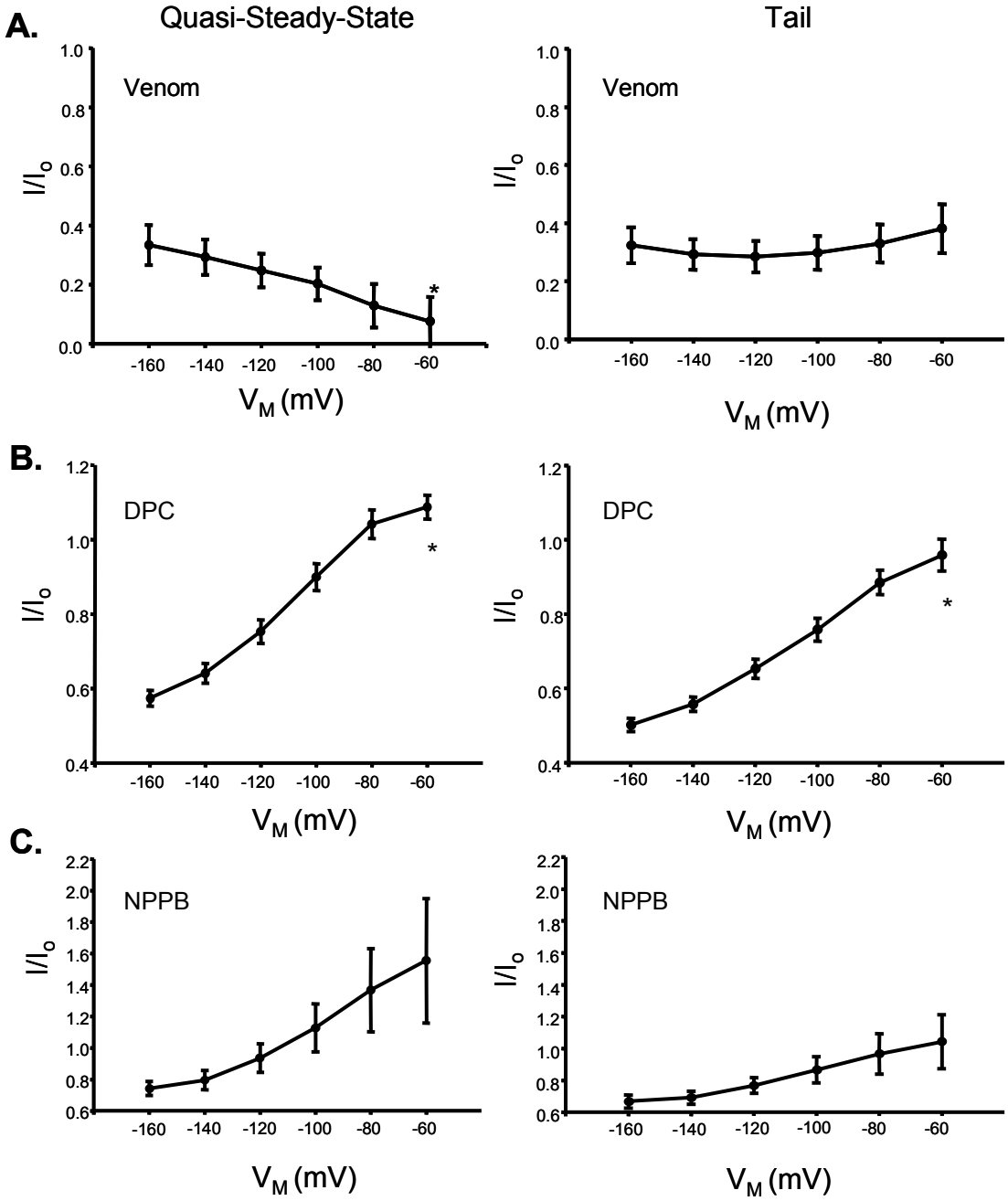

Figure 14: Comparison of inhibition of ClC-2 by venom and known pore blockers. Effect of **(A)** pf-venom (0.1 mg/mL, n = 8), **(B)** DPC (1 mM, n = 6), and **(C)** NPPB (100 μM, n = 4) on normalized ClC-2 activation currents (*left panels*) and tail currents (*right panels*). (*) indicates statistical difference between current remaining at V_M = -60 mV compared to current remaining at V_M = -160 mV.

4.7 Kinetics of ClC-2 Gating

Another way to assess the mechanism of inhibition is to examine effects of the inhibitor on the kinetics of either channel activation of deactivation. Open channel pore blockers should have no effect on the kinetics of either channel activation, or deactivation, because they simply reduce the number of channels that are able to conduct. Due to the fact that open channel blockers may bind or unbind at any time, no effect on channel kinetics should be observed. Gating modifiers, on the other hand, may alter channel activation kinetics or deactivation kinetics due to the fact that they intrinsically alter either the opening rate or the closing rate of the channel. This may be reflected as a change in the macroscopic kinetics of activation or deactivation. Using this approach to determine if an inhibitor is a gating modifier may be difficult, because a state-dependent pore blocker that can only bind in the closed state will also appear to slow channel activation. Channel kinetics were examined by using a prolonged voltage step protocol to obtain values for the time constant of activation ($\tau_{activation}$) at V_M = -160 mV, as well as the time constant for deactivation ($\tau_{deactivation}$) from the tail pulse at V_M = +40 mV (Fig. 15). Both of these relaxations were fit best by the sum of two exponential functions. In the presence of venom, inhibition of ClC-2 was exhibited as an increase (2.50 $\pm$ 0.35 fold, n = 7, p= 0.008, at 0.03 mg/mL venom) in the time constant for the fast component of $\tau_{activation}$ (Fig. 15C). At a higher concentration, both time constants of activation were significantly affected. The slow component showed a 1.92 $\pm$ 0.18 fold increase (n = 11, p < 0.001), while the fast component showed a 2.89 $\pm$ 0.49 fold increase (n = 11, p < 0.001) (Fig. 15C). There was no change in the time constants of deactivation for ClC-2 when exposed to venom at a concentration of 0.1 mg/mL (*data not shown*). This indicates that

the activation of the channel is significantly slowed in the presence of venom, which is consistent with the action of a gating modifier. There were no significant changes in fractional area contributed by each time constant for activation (Fig. 15D) or deactivation (*data not shown*) in the presence of 0.03 or 0.1 mg/mL venom. This suggests that fast and slow gating may be highly coupled in ClC-2, as one would expect that the contribution of one time constant would change if it were affected more than the other. This coupling of fast and slow gating in ClC-2 has been described previously by Zuniga [67], and more recently by de Santiago *et al.* [68].

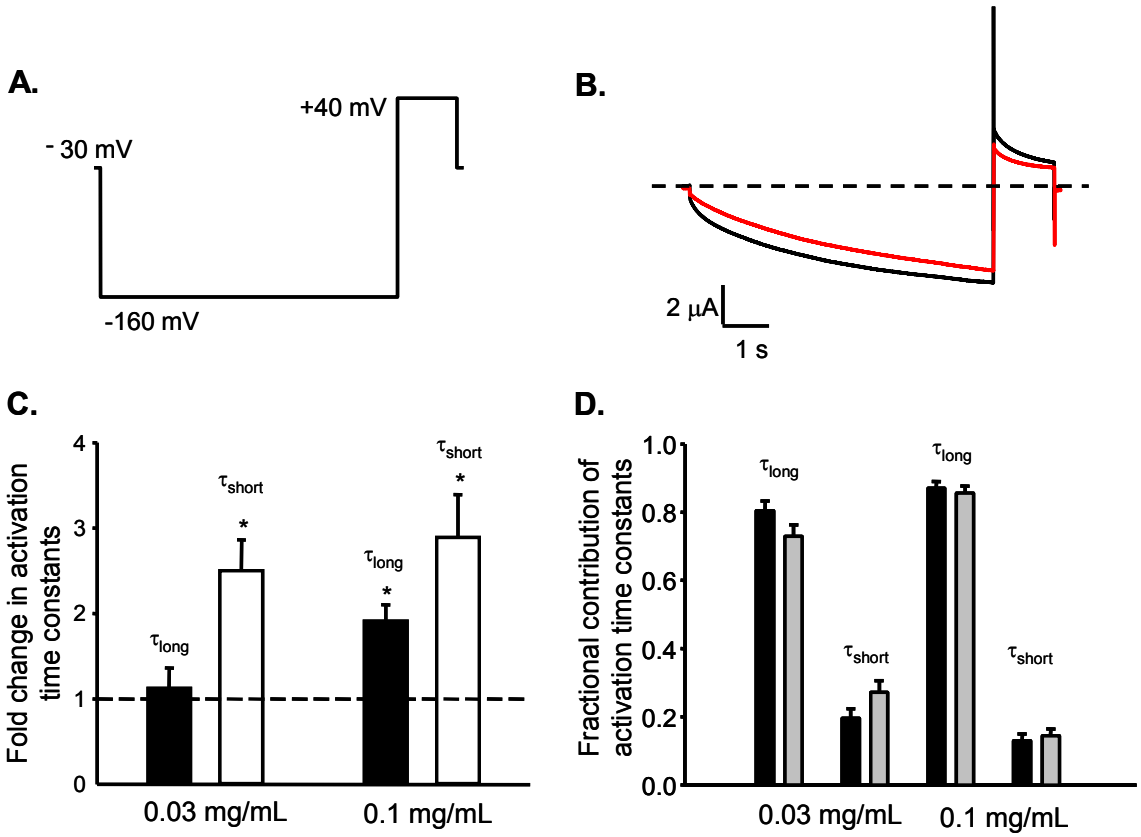

Figure 15: Venom alters channel activation kinetics. Effect of pf-venom (0.03 mg/mL and 0.1 mg/mL) on the activation kinetics of ClC-2. **(A)** Extended TEVC voltage protocol. The step potential was held for six seconds; tail potential was held for 1.2 seconds. **(B)** Representative TEVC recording, at V_M = -160 mV, before pf-venom (*black trace*) and with 0.1 mg/mL pf-venom (*red trace*). Data were fit with a second-order exponential and the time constants (τ) were normalized to values before pf-venom. The dashed line indicates zero-current level. **(C)** Effect of pf-venom on the long (τ_1, filled bars) and short (τ_2, open bars) time constants for activation. Values above the dashed line represent increased time constants while values below represent a decrease. The fractional contributions to the fit from τ_1 and τ_2 for channel activation are shown in panel **(D)**. Pre-venom results are represented by the *black bars*, while results with pf-venom are represented by the *gray bars*. Statistical analysis was performed on non-transformed data. (*) indicates $p < 0.05$.

4.8 State Dependence

Inhibition appears to be independent of the activation state of the channel. By plotting the degree of relative inhibition over time during the three-second activation pulse, we found no significant change in the percent decrease in the current (Fig. 16). In order for a state-dependent pore-blocker to appear to slow channel activation kinetics, it must unbind during channel activation. This would appear as more inhibition at the beginning of the voltage pulse, with reduced inhibition at the end. The degree of inhibition did not change significantly over the duration of the pulse. However, even though the current remaining at the beginning of the pulse is not statistically different from the current remaining at the end of the pulse, it does trend toward significance ($p = 0.09$, $n = 16$), hence, the trend suggests more inhibition at the end of the pulse than at the beginning. Therefore it is unlikely that the active component acts as a state-dependent pore blocker.

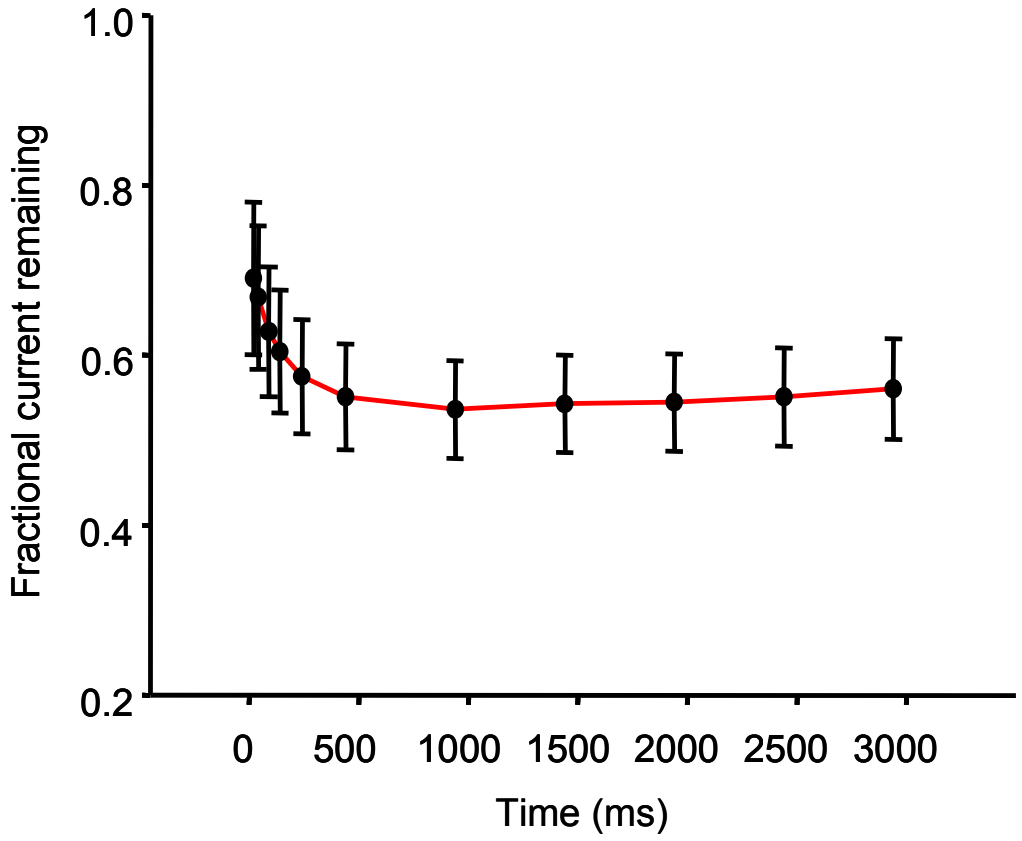

Figure 16: Inhibition of ClC-2 does not change over the voltage pulse. Fractional current remaining is shown for specific time point during a three second voltage pulse to V_M = -160 mV. There is no change in inhibition of ClC-2 currents over the course of the voltage pulse (n = 16).

4.9 Effect of Venom on Swelling Activated Currents

It has been shown that ClC-2 channels can be activated in several different ways, including pH-dependent activation, swelling activation, and voltage-dependent gating [300]. We have shown above that venom acts as a gating modifier by slowing voltage-dependent activation of ClC-2. We next tested for effects of venom on swelling induced activation of ClC channels by swelling oocytes expressing the channel by exposure to ND96 with 10 mM mannitol. We observed a 1.25 $\pm$ 0.05 fold increase in currents as a result of swelling (n = 7, p = 0.01). To test if venom inhibits the induction of swelling activated currents, we exposed ClC-2 channels to 0.1 mg/mL Lqh pf-venom in ND96 with 20 mM mannitol, and then exposed the channels to 0.1 mg/mL Lqh pf-venom in ND96 with 10 mM mannitol to induce swelling activated currents. When the channels were swollen with 10 mM mannitol in the presence of 0.1 mg/mL Lqh pf-venom, we observed a 1.36 $\pm$ 0.09 fold increase in currents (n = 7, p = 0.007) (Fig. 17A). This is not a significant change in the fold increase in currents as a result of swelling (p = 0.33), indicating that venom has no effect on the induction of swelling activated currents. This trend was maintained with tail currents, where control cells showed a 1.22 $\pm$ 0.05 fold increase (n = 7, p = 0.03), and cells swollen in the presence of venom showed an increase of 1.10 $\pm$ 0.05 fold (n = 7, p = 0.05) (Fig. 17B). When the percent apparent inhibition of steady-state currents was compared for venom with 20 mM mannitol, and venom with 10 mM mannitol, there was a significant decrease in the amount of inhibition observed under swelling conditions, compared to control (57.51 $\pm$ 0.05 % vs. 42.81 $\pm$ 0.05% p = 0.008) (Fig. 17C). Tail currents however, showed no significant change in the amount of inhibition observed for Lqh pf-venom with 10 or 20 mM mannitol. The lack of effect on

swelling-induced ClC-2 currents suggests that the effect of cell swelling on ClC-2 is not a direct gating mechanism, consistent with the suggestion that swelling-induced currents only reach steady-state after a period of > 10 minutes.

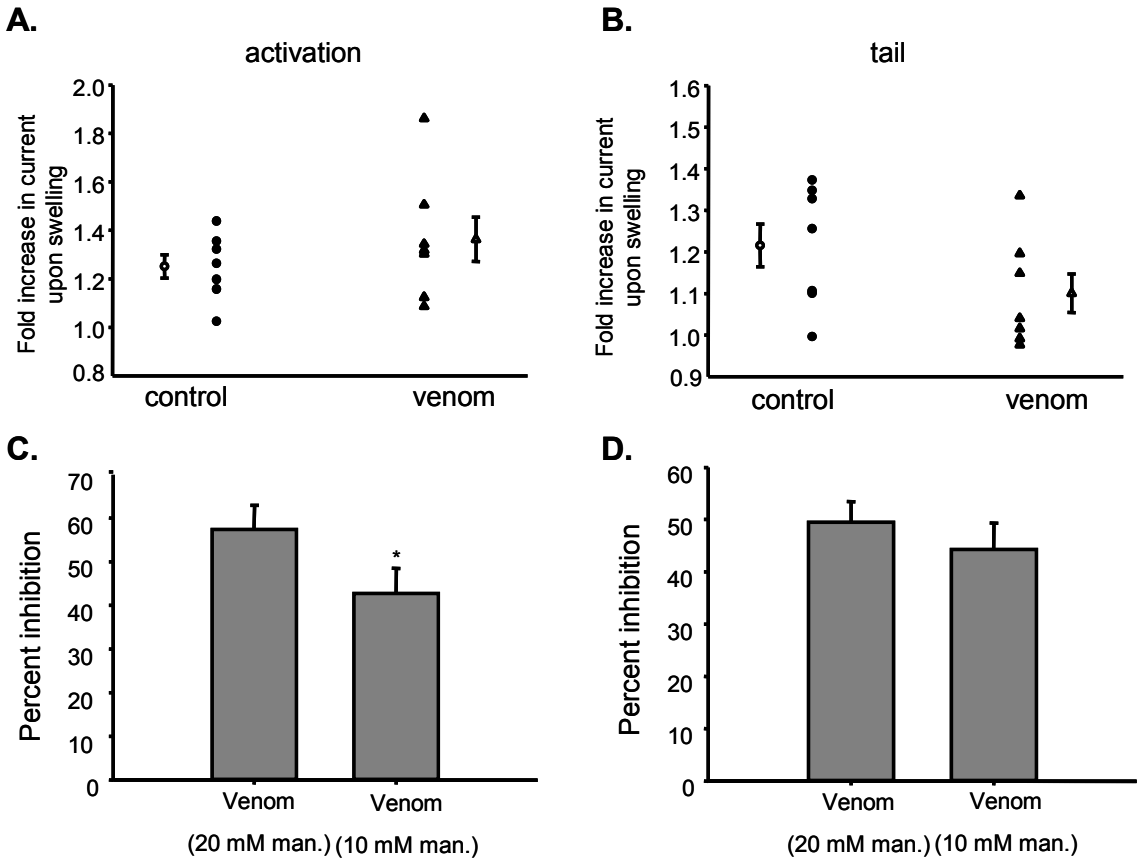

Figure 17: Effect of pf-venom on swelling induced ClC-2 currents. Data are plotted as fold increase of **(A)** activation currents and **(B)** tail currents upon induction of swelling. Closed circles represent fold increase in currents upon swelling for individual experiments, while open circles are mean $\pm$ SEM for control cells. Closed triangles are individual experiments for fold increase in current upon swelling in the presence of 0.1 mg/mL venom, and open triangles are mean $\pm$ SEM for cells in the presence of venom. **(C)** Percent inhibition of ClC-2 time-dependent activation currents at V_M = -160 mV, for venom prepared with 20 or 10 mM mannitol. **(D)** Percent inhibition of ClC-2 tail currents at V_M = +40 mV, for venom prepared with 20 or 10 mM mannitol.

CHAPTER 5

DISCUSSION

Peptide toxins have proven to be indispensable tools in studying pore structures and gating mechanisms in a variety of voltage-gated channels [249, 280, 312, 314]. In this study, we investigated the inhibitory effects of venom isolated from the scorpion *L. quinquestriatus hebraeus* on three plasma membrane members of the ClC family. Of the three channels studied, the venom showed a strong inhibitory effect only on ClC-2. This suggests that the inhibition is not due to the action of heavy metal ions such as Zn^{2+} or Cd^{2+}, which could be contaminants carried in venom, that are known to inhibit ClC-0 and ClC-1, as well as ClC-2 [21]. Thus, unlike the inhibitory effects of other organic molecules such as DPC, 9-AC, and members of the clofibric acid family [71, 257], and despite the relatively high homology in the primary sequence of the three channels [315], the selective nature of the venom suggests that it could not only be a powerful tool for understanding the structure of ClC-2 but may also offer insight into the functional relevance of the structural differences between various ClC members.

Our results have shown that a peptide component (or components) of scorpion venom inhibits ClC-2. The toxin is slow to bind to the channel, taking approximately five minutes to show maximum inhibition, at 0.1 mg/mL equivalent concentration, and is relatively tenacious once bound, taking approximately ten minutes to fully restore pre-venom current levels during washout. In addition, macropatch data have shown that trypsinization of the Lqh pf-venom removes the inhibitory effect, strongly suggesting that

the active component(s) is a peptide. The possibility remains that multiple components of the venom are acting in concert, and that trypsinization of the partially fractionated venom disrupts the interaction of the components responsible for inhibition. Experiments have shown that native ClTx (Latoxan) does not inhibit ClC-2. Lqh venom contains several components that are similar to components of *L. quinquestriatus quinquestriatus* venom, the source of ClTx [316], and given the large number of peptide toxins that have been identified, it is possible that the active component(s) of this venom is a peptide that has already been characterized. However, it is also possible that the active component is a novel peptide. Once the toxin is isolated, sequence analysis will allow for an evaluation of evolutionary relationships to other toxins.

Determining the underlying mechanism of inhibition is complicated, since permeation and gating are tightly coupled in ClC family channels [28, 317]. However, two lines of evidence suggest that the venom acts as a gating modifier. First, ClC-2 channel activity is clearly voltage-dependent and venom shifts the voltage-dependence of activation to more hyperpolarizing potentials. However, at the test potentials used in this study, ClC-2 currents never apparently reach full activation, even at extremely hyperpolarizing potentials (*e.g.*, -160 mV) that are barely tolerated by the cell. Hence, estimation of maximal P_o, and its potential decrement in the presence of venom, is difficult [62]. Secondly, inhibition by venom alters channel activation kinetics; this is observed as a slowing of both time constants of activation for ClC-2 in the presence of venom. This effect also appears to be dose-dependent, with more pronounced effects at higher concentrations of venom. This slowing of activation could represent a stabilization of the closed state, which is not uncommon for gating modifiers. Gating in ClC channels

is complicated, in that there are both fast and slow gating processes, and in that gating and permeation are linked, with Cl^- acting as both the gating charge and the permeant ion [28]. It is possible that the active component(s) has some effect on permeation that is not evident in our assays, but these results taken together provide convincing evidence that the main effect of the venom is modification of channel gating. Whether the venom acts on the fast or slow gate presently is unknown. In ClC-2, it is difficult to separate the fast and slow gates at the macroscopic level. It may be that single channel recordings, in association with the purified toxin, can differentiate between these possibilities, but the low single channel conductance of these channels [62] will make those experiments difficult to perform.

The finding that the active component(s) of venom behaves as a gating modifier suggests that it must function to prevent some conformational change that is necessary for gating. In voltage-gated K^+ channels the S4 region responsible for the detection of voltage is linked to the movement of S5 and S6, which are the pore lining helices [237]. Binding of voltage-sensing toxin (VSTx) prevents the movement of the S4 region, and thus inhibits gating [288]. Although the domain movements associated with gating of ClC channel proteins are not known, it is proposed that the movement of a conserved glutamate residue that lies within the pore regulates fast gating [66-68, 239]. The mechanism underlying the slow gate is still unknown, although the slower kinetics of this gate would suggest that large movements of the protein are necessary. Given that the ClC-2 activation rates are slowed by venom, it is possible that this peptide is directly interacting with one of the gates. The dose response indicates a Hill coefficient of 0.97, which would suggest that the toxin is interacting with the channel with a 1:1

stoichiometry. This would indicate either an interaction with the single slow gate, or an allosteric interaction that may affect all gates. Interaction with the two fast gates would provide two binding sites, and possibly give a Hill coefficient significantly different than one, assuming binding of the toxin to each of the fast gates is an independent event. It has been shown that Cl^- can act as the principle gating charge in ClC channels; ClC-2 relies on intracellular Cl^- to gate the channel [18]. Since the venom works from the extracellular side of the channel, venom-induced disruption of intracellular Cl^- binding sites through a direct interaction is unlikely.

Purification of a single peptide that inhibits ClC-2 would provide a powerful tool in the study of gating for ClC channels. Once the active component or components are isolated a functional map of the channel can be made, so that the protein movements necessary for gating can be identified. This report provides the basis for the identification of a tool that will lead to a better structural understanding of mammalian ClC channels.

PART 2

ISOLATION OF A NOVEL PEPTIDE INHIBITOR OF CLC-2 CHLORIDE CHANNELS

CHAPTER 6

INTRODUCTION

ClC proteins form a family of voltage-gated Cl^- channels and Cl^-/H^+ exchangers that are found in animals, plants, and bacteria [28]. These proteins are expressed on the plasma membrane and some intracellular membranes in both excitable and non-excitable cells [28, 301]. There are nine mammalian members of the ClC family which perform functions as varied as maintenance of membrane potential in neuronal cells (for ClC-2) [92], Cl^- transport across plasma membranes of epithelial and skeletal muscle cells (ClC-1, ClC-2, ClC-Ka/b) [28, 318], and participation in lysosomal acidification (ClC-5, ClC-6) [301]. Defects in the genes encoding ClC proteins are linked to a number of diseases including myotonia, epilepsy, Dent's disease, and Bartter's syndrome [28, 92, 301, 319]. It has recently been suggested that ClC-2 may play a role in constipation-associated irritable bowel disease as well as in atherosclerosis [84, 86]. Most ClC channels show localized tissue expression; ClC-1 for example is expressed solely in skeletal muscle, while ClC-Ka/b is localized to the kidney. ClC-2, on the other hand, is expressed nearly ubiquitously, suggesting that this channel plays an important, yet largely undefined, physiological role [28, 301].

ClC proteins are structurally unrelated to cation channels, with the functional unit being a homodimer [12]. In 2002, the crystal structure of a bacterial ClC protein was solved, revealing a very complicated membrane topology consisting of 18 α-helical units per subunit, some of which fully traverse the membrane, while some do not [14].

Examination of the crystal structure revealed no obvious pore, as is evident in K^+ channel structures, even though bound Cl^- ions were evident [14, 237]. Shortly after the crystal structure was solved it was shown that the bacterial ClC protein was actually a Cl^-/H^+ exchanger, and not a channel [126, 127]. Molecular dynamics studies have revealed a tortuous transmembrane permeation pathway through the ClC protein [247]. Comparison of the amino acid sequence of the *S. typhimurium* ClC protein with that of the eukaryotic ClC channels ClC-0, -1, and -2 revealed only 22%, 16%, and 19% identity overall (*data not shown*). This divergence is largely in the cytoplasmic domains, which are absent in bacterial ClC proteins; sequence identity is much higher in the transmembrane domains.

Gating in ClC proteins is complicated, involving both fast and slow gating processes which are thought to involve separate regions of the protein [28]. Fast gating controls the opening and closing of both protopores independently; these gates operate on the millisecond timescale or faster. Through examination of the crystal structure, and subsequent electrophysiological analysis, the fast gating process was revealed to involve a conserved glutamate residue deep within each pore [239]. This glutamate residue lies near a Cl^- binding site and moves slightly to open the pathway in response to changes in membrane voltage and subsequent changes in occupancy of that site, thus providing the link between permeation and gating observed in ClC channels [237, 318]. In contrast, slow gating controls both pores simultaneously, operating on the hundreds of milliseconds to seconds timescale. Unlike fast-gating, the regions of the ClC protein involved in slow gating are still unknown, despite the availability of the crystal structure. It is believed that the dimer interface contributes to slow gating, as well as the long cytoplasmic C-terminal domain, an isolated version of which was recently crystallized

[23, 38, 39, 69, 243, 245]. However, the conformational changes involved in the fast and slow gating processes are still largely unknown. Also, in both ClC-1 and -2, fast and slow gating are linked through an undetermined mechanism [33, 68].

Despite the availability of the bacterial ClC protein crystal structure, our understanding of gating mechanisms and structural rearrangements of ClC proteins has lagged behind that of their cation channel counterparts. This is due in large part to a lack of useful pharmacological agents, such as peptide toxins, that may be used as tools. Toxins from venomous animals such as scorpions, snakes, and cone snails have been used for a number of years to define the permeation pathways and gating processes of cation channels [320]. However, no peptide toxins have been isolated that inhibit a ClC channel, and only one toxin has been isolated that inhibits a Cl^- channel of known molecular identity [298]. We recently showed that the venom from the scorpion *L. quinquestriatus hebraeus* contains a peptide component that inhibits the ClC-2 chloride channel [61]. Here, we report the isolation of this peptide toxin, and its initial proteomic and pharmacological characterization.

CHAPTER 7

MATERIALS AND METHODS

7.1 Oocyte and cRNA Preparation

Xenopus oocytes were isolated as previously described [61] and incubated at 18^{o}C in a modified Liebovitz's L-15 medium (pH 7.5) with a cocktail of antibiotics (gentamicin, penicillin, streptomycin) and HEPES. cRNA was prepared from rabbit ClC-2 using a construct in pSportI, donated by H.C. Hartzell (Emory University, Atlanta, GA). For two-electrode voltage clamp experiments (TEVC), oocytes were injected with 2.5 - 50 ng of cRNA encoding ClC-1, -2, -3, or -4, 0.06 - 1 ng ShB-IR cRNA, 50 - 100 ng $GABA_C$-rho subunit cRNA, or 2 - 20 ng cRNA encoding wild type Cystic Fibrosis Transmembrane Conductance Regulator (WT-CFTR). For patch recordings, oocytes were injected with 0.5 - 2 ng ClC-2 cRNA or Flag cut-Δ-R-CFTR. Data were collected at room temperature 2 - 5 days post injection. Methods for animal handling are in accordance with the NIH guidelines and the protocol was approved by the Animal Use and Care Committee of the Georgia Institute of Technology and Emory University.

7.2 Venom Preparation and Toxin Purification

Venom from Leiurus quinquestriatus hebraeus was obtained from Latoxan (France), and prepared as described [61]. Dried whole venom was prepared at a stock concentration of 2 mg/mL in the appropriate bath solution (see below) for electrophysiological recording. For toxin purification venom was prepared at a

concentration of 5 mg/mL in solution that contained (in mM): 150 NMDG-Cl, 5 $MgCl_2$, 10 TES, and 10 Tris·EGTA, pH 7.5. Subsequent fractions were resuspended in ND96. All venom and fraction concentrations are stated as equivalent to the dried weight of whole venom.

Reversed-phase HPLC was performed on Lqh pf-venom prepared as described above. RP-HPLC was performed on a Waters 1525 binary HPLC coupled to a Waters 2487 dual wavelength absorbance detector, utilizing a Zorbax 300SB-C3 column (4.6 mm x 250 mm) or Zorbax SB-C18 column (4.6 mm x 250 mm). Lqh pf-venom or venom fraction was applied to the column in 500 mL aliquots. Samples were eluted with gradients of aqueous acetonitrile. Elution gradients were designed to optimize protein separation, and absorbance was monitored at 220 nm. Separations on the C3 column were performed using an elution gradient which ramped from 0- 95% acetonitrile over 50 minutes, with brief periods where the percent acetonitrile was held constant. The protocol then ramped back to 0% acetonitrile over 5 minutes and this condition was held constant for another 5 minutes. The first round of separations on the C18 column were performed using an elution gradient that ramped from 0-25% acetonitrile over 50 minutes, held at 25% acetonitrile for 5 minutes, and then ramped back to 0% acetonitrile over 5 minutes. For final peak collection using the C18 column, the percent acetonitrile was held at 5% for 5 minutes, then ramped to 20% over 55 minutes. All collected fractions were dried via SpeedVac and were resuspended in volumes of the appropriate bath solution equivalent to the total volume of Lqh pf-venom injected onto the column. Resuspended fractions were stored at -80^{o}C

7.3 Electrophysiology

Standard TEVC techniques were used to study whole cell ClC-2 currents expressed in *Xenopus* oocytes. Currents were acquired using a GeneClamp 500B amplifier and pClamp 8.4 software (Axon Instruments, Union City, CA). Data were acquired at 2 kHz and filtered at a corner frequency of 500 Hz. Bath solutions and voltage protocols for TEVC experiments with ClC channels were as previously described in Chapter 3. Currents were measured in the absence and presence of venom fractions, or isolated toxin, with percent inhibition being assessed at the end of the activation pulse. For ShB-IR experiments, leak currents were subtracted using a P/4 protocol. $GABA_C$ and CFTR recordings were performed at a holding potential of V_M = -60 mV.

Inside-out multi-channel and single-channel patch clamp experiments were performed as previously described [299]. All data were recorded to DAT tape at 10 kHz and were subsequently filtered at 100 Hz and acquired by computer at 500 Hz. For inside-out patches in the presence of toxin, the toxin was backfilled into the pipette and allowed to diffuse to the surface of the patch. Multi channel patch recordings of Flag cut-Δ-R-CFTR were performed by application of 0.2 mM ATP or 0.2 mM ATP + 60 nM toxin to the intracellular face of patches containing CFTR; currents were recorded at V_M = -80 mV. Unless otherwise stated, all single channel traces depicted in the figures were recorded at V_M = -100 mV. For all electrophysiological data shown, the horizontal dashed line indicates the zero-current level.

In order to prevent loss of material, all toxin containing solutions were prepared immediately prior to experiments from a 20 μM stock. All solution lines and recording

chambers were coated with BSA to prevent loss of material due to sticking to plastic or glass.

7.4 Protein Analysis

The active toxin was analyzed via MALDI-MS at the Georgia Institute of Technology Bioanalytical Mass Spectrometry Facility. Edman degradation was performed at the Emory University Microchemical and Proteomics Facility. Sequence analysis of the natural and modified (reduced and alkylated) peptides was performed using Applied Biosystems model Procise-cLC automated protein sequencer (Applied Biosystems 491cLC CLC capillary protein sequencing system; Foster City, CA) using the manufacturer's cycles with slight modifications. Prior to sequencing, natural and modified samples were de-salted and purified via RP-HPLC.

7.5 Homology Modeling

The homology model of the GaTx2 toxin was created using the Modeller 8v2 program, using Neurotoxin P01 as the template structure [321]. The GaTx2 homology model was then minimized via a 5 ps, 2500 step simulation with NAMDv2 utilizing the charmm22 force field. Prior to minimization, disulfide bridges were patched in order to ensure that the disulfide bonds remained intact during energy minimization.

7.6 GaTx2 Synthesis

Methods for peptide synthesis, purification, and folding have been previously described [322, #325]. Solid phase synthesis was performed by Fmoc chemistry, using the HBTU/HOBT/DIPEA method on an Applied Biosystems 431A synthesizer. Oxidative cyclization of the crude linear peptide was performed under equilibrating conditions. The cyclized peptide was then purified from the reaction mixture via RP-HPLC and characterized by MALDI-MS and analytical HPLC.

7.7 Statistics

Data are expressed as mean $\pm$ SEM for *n* obervations. Differences were determined to be significant when $p < 0.05$, using paired and unpaired Student's *t*-tests.

CHAPTER 8

RESULTS

8.1 Isolation of the Active Toxin

We recently showed that a peptide component of scorpion venom is capable of specifically inhibiting the ClC-2 chloride channel [61]. In order to isolate the active component of this venom, we used reversed-phase HPLC (RP-HPLC) to separate the components of partially-fractionated venom (Lqh pf-venom), which contains only components smaller than 10 kDa. We tested each fraction for inhibition of ClC-2 currents using two-electrode voltage clamp (TEVC). With initial separation performed using a C3 column, we observed that the fraction collected from 0 - 10 minutes, Fraction A, retained activity similar to Lqh pf-venom (Fig. 18A, 45.7 $\pm$ 6% inhibition, fraction concentration 0.1 mg/mL equivalent, n = 3, p = 0.01).

The brief retention time of the active component on the C3 column suggests that the toxin is very hydrophilic.; therefore, further separation of components was not feasible using the C3 column. In order to increase the retention time of the active component so that it no longer co-eluted with the salt peak, further isolation and purification of the active toxin was achieved through two successive rounds of RP-HPLC using a C18 column, as summarized in Figure 18B and 18C. The isolated toxin, peak #3, eluted at ~5% acetonitrile using this elution gradient, and was sufficient to fully recapitulate the activity observed for Lqh pf-venom when diluted to the same equivalent concentration (64.2 $\pm$ 5.3% inhibition at 0.1 mg/mL equivalent, n = 4, p = 0.025). Amino

acid analysis performed during protein sequencing (*see* Fig. 3) revealed that this toxin was present at very low abundance, with 0.1 mg/mL venom containing only 10 nM toxin. A dose-response curve constructed using native purified toxin showed that the K_D at V_M = -160 mV is only 80 pM, which represents the highest affinity interaction of any ClC channel inhibitor identified to date (Fig. 18D).

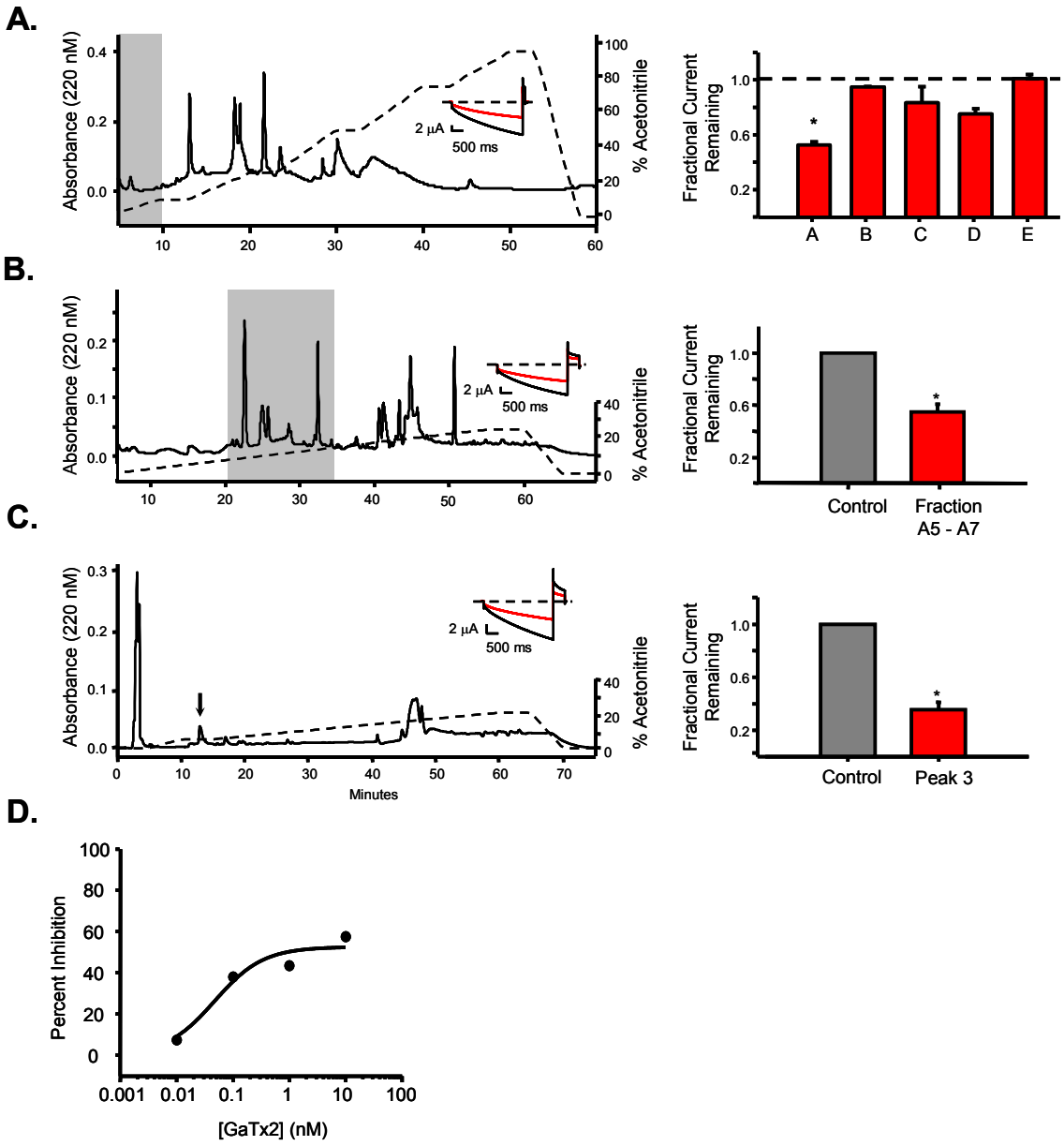

Figure 18: Isolation of the active toxin. (*A* - *C*) *Left:* Representative RP-HPLC chromatograms of Lqh pf-venom (*A*) or active fractions (*B, C*) The area included in the gray boxes, or indicated by an arrow, contains the active fraction or peak. The elution gradient is represented by a dashed line. The *right* panel presents summary data for fraction activity. Bars show mean ± SEM for 3-10 observations. The *inset* shows representative traces from TEVC experiments in the absence (*black* trace) or presence (*red* trace) of the active fractions or isolated peak at V_M = -160 mV stepped from –30 mV. (*D*) Dose-response curve from a single TEVC experiment for inhibition of ClC-2 at V_M = -160 mV by 0.01, 0.1, 1, or 10 nM native toxin.

8.2 Proteomic Characterization of GaTx2

Peak #3 was then subjected to MALDI-TOF mass spectrometric analysis to determine the molecular mass of the intact compound, and to ensure that the collected chromatographic peak contained only one component. This analysis revealed that peak #3 contained one component with an apparent mass of 3.19 kDa (Fig. 19A); a doubly charged species of the same component was also apparent. This is within the mass range of many short-chain peptide inhibitors isolated from *Leiurus quinquestriatus* venom.

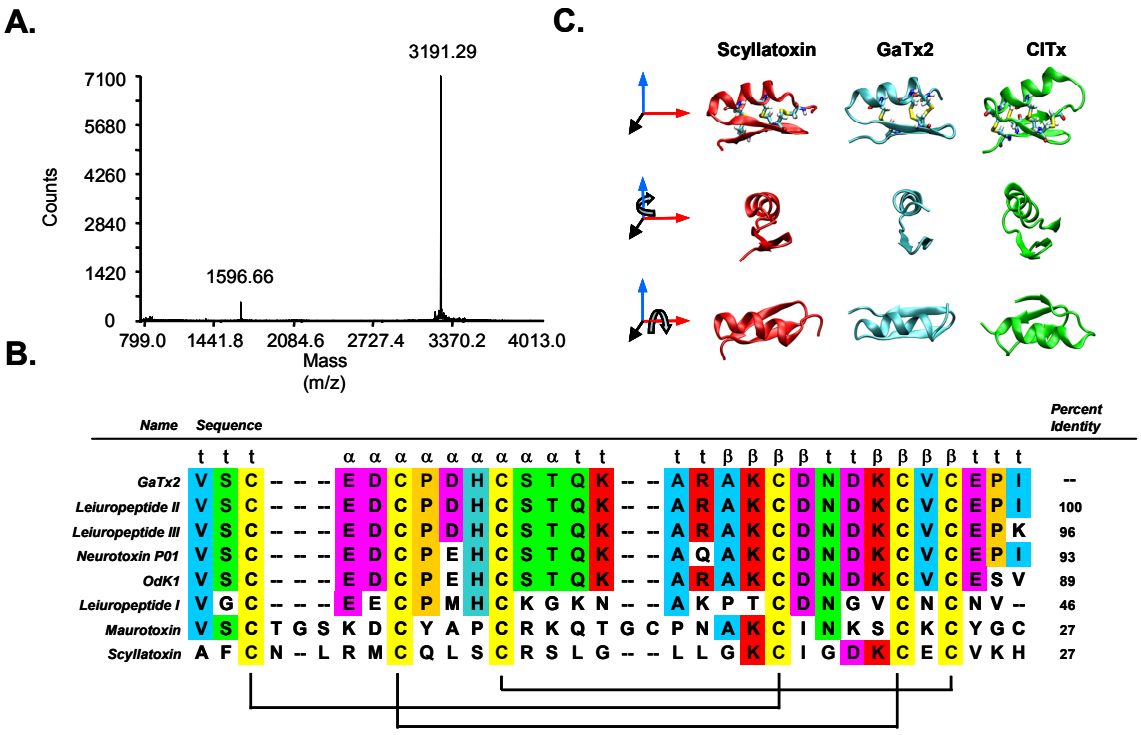

Figure 19: Proteomic characterization of GaTx2. (*A*) MALDI-MS analysis of peak 3. (*B*) Sequence alignment of GaTx2 with other previously identified, highly related toxins. Disulfide bridge connectivity (specifically for GaTx2) is shown below the sequence alignment, while the predicted secondary structure for GaTx2 is shown above the sequence. (*C*) Homology model of GaTx2 (*middle*) shown with the NMR structures of Scyllatoxin (*left*) and Chlorotoxin (*right*), in three orientations. The top panel shows disulfide bridges in bond representation.

Initial attempts to determine the primary sequence of the active toxin were performed via MS/MS; however no fragmentation of the toxin was observed, even under very harsh conditions such as Xenon bombardment, likely due to the presence of multiple disulfide bonds. Additionally, attempts to sequence a reduced form of the toxin via MS/MS failed because of the very low abundance of the active component. Reduction of the active toxin with DTT followed by carboxamidomethylation induced a mass shift (3191.6 to 3539.5 kDa), as determined by MALDI-MS, that corresponded to the modification of 6 cysteine residues, indicating that the intact protein contained 3 disulfide linkages. Due to the difficulties obtaining primary sequence information from MS methods, the primary sequence of the toxin was determined via Edman degradation; however, only a few residues of the intact toxin could be sequenced using this process. Therefore, the reduced/carboxamidomethylated toxin was sequenced using Edman degradation and amino acid analysis, providing the complete primary sequence: **^{1}VSCEDCPDHCSTQKARAKCDNDKCVCEPI^{29}**. The identity of the C-terminal residue, I29, was determined by amino acid analysis. This sequence was confirmed by Edman sequencing of Lys-C protease digested, reduced/carboxamidomethylated toxin. We have isolated this toxin from venom on three separate occasions, as confirmed by MS analysis of the active fraction from these isolations. Sequence comparisons revealed that this primary sequence exactly matches the sequence of Leiuropeptide II (LPII) (Fig. 19B), a peptide isolated in 1997 from the same scorpion which was not shown to have any lethal effects when injected into mouse brain or insects [323]. In fact, LPII was proposed to be a potassium channel inhibitor based on cysteine alignment and the

presence of a lysine residue at position 18, which is in the same position in the folded protein as the critical lysine (Lys27) of charybdotoxin. Lysine 27 is part of a critical dyad, with its partner being an aromatic residue located ~6Å away [324]. In LPII, however, this aromatic residue is absent. No target for LPII has ever been identified. Because this toxin actually inhibits a chloride channel, instead of a K^+ channel as originally proposed, we have renamed it Georgia anion toxin 2 (GaTx2) to avoid confusion. GaTx2 is also very similar in primary sequence to a number of other toxins; the most relevant are shown in Figure 19B. Of these toxins, only four have been shown to be active against ion channels: neurotoxin P01, which is weakly toxic [325], scyllatoxin, which inhibits Ca^{2+}-activated K^+ (K_{Ca}) channels [326], and maurotoxin and OdK1, both of which inhibit $K_V1.2$ [327, 328].

Short-chain peptide toxins from scorpion venoms tend to adopt a roughly similar tertiary structure, and many of these structures have been solved via NMR or X-ray crystallography. The NMR structure of GaTx2 (leiuropeptide II) has been previously solved [323]; however, the coordinates are unavailable. Therefore, created a homology model of GaTx2 based on the NMR structure of neurotoxin P01 [321], in order to make structural comparisons of GaTx2 to other known scorpion toxins (Fig. 19C *middle*). Neurotoxin P01 is 93% identical to GaTx2, providing an excellent template for an accurate homology model. This model predicts that GaTx2 is composed of 2 β-strands and one α-helix, which are connected via 3 disulfide bonds. The basic fold and disulfide connectivity are consistent with the NMR structure of LpII [323]. This basic fold is highly conserved among numerous toxins isolated from various scorpion species [275]. GaTx2 is noticeably more compact than both scyllatoxin (Fig. 19C *left*) and chlorotoxin

(Fig. 19C *right*), a toxin isolated from a related scorpion that is thought to inhibit an unidentified Cl^- channel in rat brain when reconstituted into lipid bilayers [294, 326]. The primary and secondary structures of GaTx2 are also very different from GaTx1, a recently isolated peptide inhibitor active against the CFTR Cl^- channel [298]. GaTx2 is ~400 Da smaller than GaTx1 and has one fewer disulfide bond. GaTx2 has a calculated pI of just 4.51, which accounts for the large negative electrostatic potential that is associated with the protein and could possibly explain the lack of activity against cation channels.

8.3 Inhibition of ClC-2 by Synthetic GaTx2

In order to determine if the component that was isolated from venom is truly responsible for the observed inhibitory activity, we produced GaTx2 via solid-phase chemical synthesis, as has been done for many other peptide inhibitors [322, 329]. The folded synthetic toxin shows the same mass as the purified native toxin, indicating that no post-translational modifications were associated with the native toxin other than the three disulfide bonds (Fig. 20A). Activity of the synthetic form of GaTx2 was tested initially via TEVC using the same voltage protocols applied during the isolation of the toxin. TEVC experiments showed that synthetic GaTx2 inhibited ClC-2 mediated currents by 61.41 ± 8.02 % at V_M = -160 mV (n = 3) (Fig. 20B, C). This activity was almost exactly the same as that observed by the native toxin (64.24 ± 5.37, n = 4) (Fig. 20C).

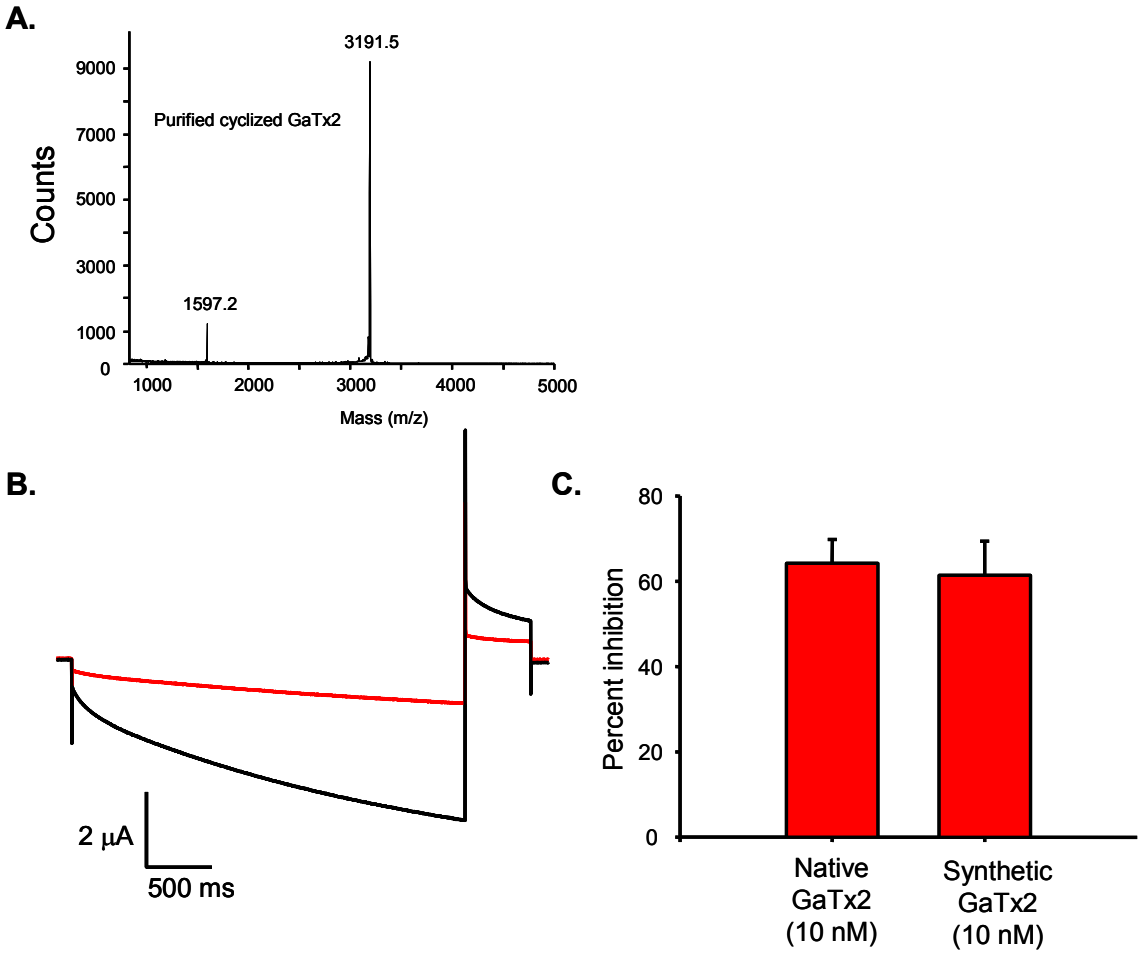

Figure 20: Inhibition of ClC-2 macroscopic currents by synthetic GaTx2.*(A)* MALDI-MS of the folded synthetic GaTx2 matches the mass spectra of the native toxin *(B)* TEVC experiment at V_M = -160 mV in the absence (*black* trace) or presence (*red* trace) of 10 nM synthetic GaTx2. *(C)* Comparison of percent inhibition by native and synthetic GaTx2 at the same concentration at V_M = -160 mV. The native and synthetic toxins inhibit ClC-2 currents to the same degree (Native GaTx2, n = 4; Synthetic GaTx2, n = 3).

8.4 Kinetics of Inhibition of ClC-2 by GaTx2

In order to gain a better understanding of inhibition of ClC-2 by GaTx2, we measured the rate of both onset of, and recovery from inhibition of ClC-2 currents using TEVC; solution exchange in these experiments was complete within ~10 seconds. In order to allow sufficient channel activation, and maximal deactivation between pulses, channels were activated every 15 seconds with a 1 second voltage pulse to V_M = -100 mV, followed by a tail pulse to +40 mV. Evaluation of inhibition of ClC-2 currents by 1 mM Zn^{2+}, as a control, showed that inhibition occurred very rapidly, with a time constant for recovery from inhibition of ~38 seconds (Fig. 21A, C). Time-dependent currents were inhibited by ~95% by 1 mM Zn^{2+}, as expected [250]. These experiments were then repeated using GaTx2 over a broad concentration range. Data obtained in the presence of 100 pM GaTx2 show a fast onset of inhibition and a slow recovery from inhibition (Fig. 21B, D). Using this protocol, we were able to construct a dose-response curve for inhibition of ClC-2 time-dependent currents by synthetic GaTx2 at V_M = -100 mV. Fitting the data with a three-parameter Hill function gave a K_D = 22 $\pm$10 pM and a Hill coefficient of ~1 (Fig. 22A), consistent with the very high affinity interaction observed for native GaTx2. Furthermore, we observed that the first order on-rate of GaTx2 increased as a function of [GaTx2], while the off-rate was independent of toxin concentration. The very slow off-rate (K_{Off} = 0.0034 s^{-1}) is consistent with an intimate interaction between toxin and channel. The fit of the first order on-rates gave a second order rate constant of 43×10^6 $M^{-1}s^{-1}$ (K_{on}) (Fig. 22B). This value is likely an underestimate of the true rate constant, which is impacted by the solution exchange time and interpulse duration of the voltage protocol. These values are consistent, however,

with values that have been reported for other channel/toxin interactions [279].

Calculation of the K_D from the rate constants, given as K_{off}/K_{on}, gave a value of 80 pM.

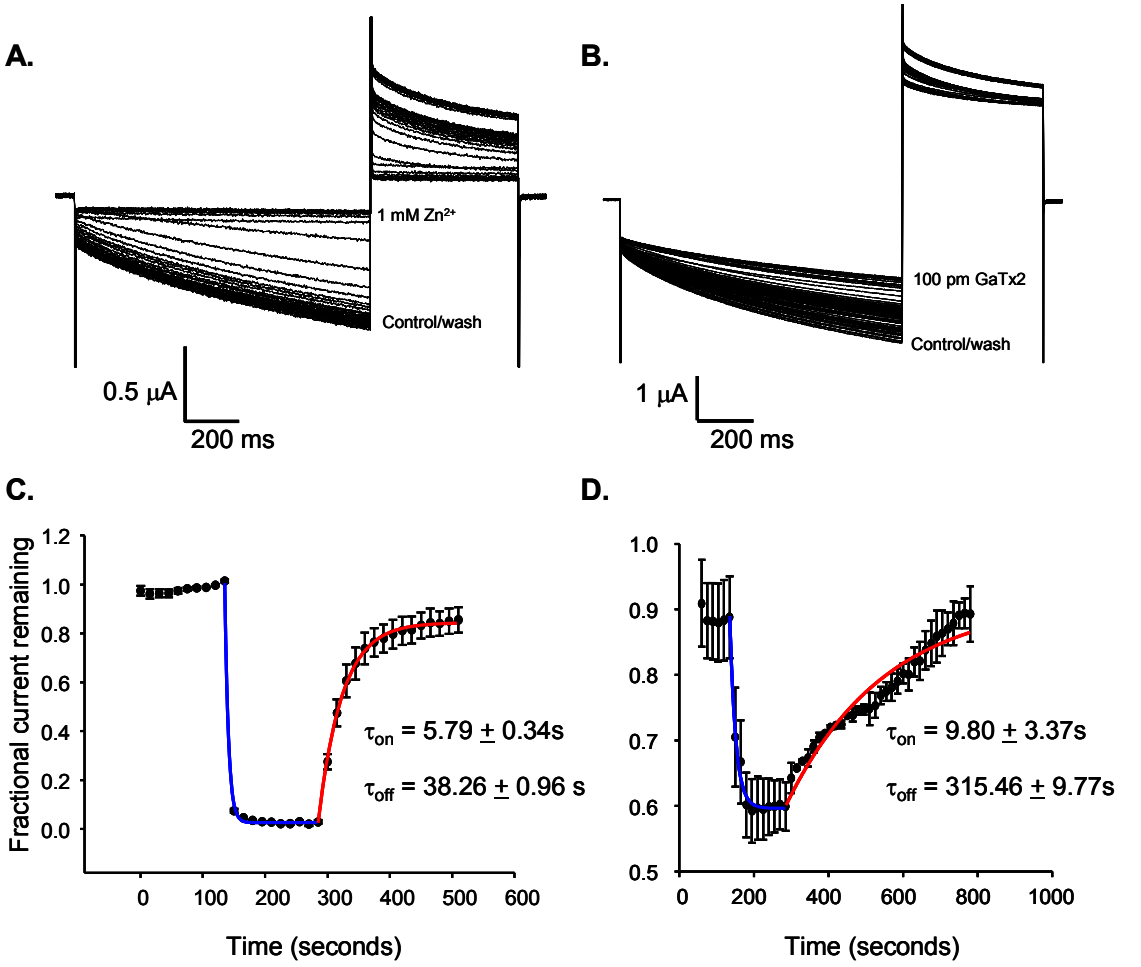

Figure 21: Time-course of inhibition of ClC-2 by synthetic GaTx2. *(A)* Control recording of ClC-2 in the presence of 1 mM Zn^{2+}, a well characterized inhibitor of ClC-2 channels. Channels were activated every 15 seconds by a 1 second voltage pulse to -100 mV, followed by a tail pulse to +40 mV. Zn^{2+} was applied after channel activity had stabilized. *(B)* Experiment in the presence of 100 pM GaTx2 using the protocol just described. Note that time-dependent currents were inhibited by ~40%. *(C)* Summary data for five experiments in the presence of 1 mM Zn^{2+}. Time dependent currents were inhibited by ~95% very rapidly, and returned to near baseline within 2 minutes. *(D)* Summary data for experiments in the presence of 100 pM GaTx2. Onset of inhibition occurred rapidly (n = 5), while recovery from inhibition was very slow (n = 2 for this concentration), taking > 7 minutes to return to baseline.

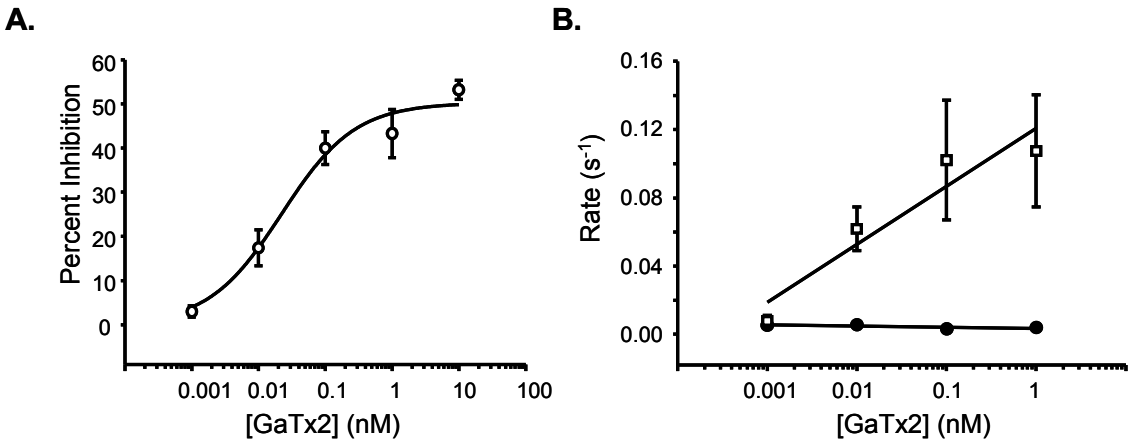

Figure 22: GaTx2 inhibits ClC-2 with very high affinity. *(A)* Dose-response curve for inhibition of ClC-2 currents by synthetic GaTx2 at V_M = -100 mV. Data were fit with a three parameter Hill equation, giving a $K_D = 22 \pm 10$ pM. Each point represents data from 3 -5 TEVC experiments. *(B)*. Plot of first order rate constants for the onset of inhibition (open squares), and recovery from inhibition (filled circles). The rate of onset of inhibition was concentration dependent, with a second order rate constant of 43×10^6 $M^{-1}s^{-1}$ (n = 3-5 for each point), obtained from the slope of the line for the fit of the data. Recovery from inhibition was concentration independent with a rate of 0.0034 s^{-1} (n = 2 - 3 each point; some error bars are smaller than the symbols).

8.5 Inhibition of ClC-2 by GaTx2 is voltage dependent

In order to further characterize the activity of synthetic GaTx2, we recorded from inside-out multi-channel patches, where the pipette was backfilled with varying concentrations of synthetic toxin. The pipette was backfilled in such a way as to allow 10 minutes of control recording (at V_M = -100 mV or -60 mV), followed by 10 minutes of recording in the presence of GaTx2. We then calculated the average window current from five separate four-minute windows in both control and experimental conditions. When no toxin was backfilled into the pipette, we observed no change in average window current over the course of the experiment (Fig. 23A). However, when 2 nM synthetic GaTx2 was backfilled into the pipette, average window currents were drastically reduced at the end of the experiment (Fig. 23A, B; 80.4 $\pm$ 2.0% decrease). We repeated these experiments with varying concentrations of GaTx2 to obtain a dose-response curve, which provided K_D = 12 $\pm$ 5 pM and a Hill coefficient of ~1 at -100 mV using this protocol (Fig. 23B). This value is not significantly different from the K_D measured using TEVC at the same membrane potential.

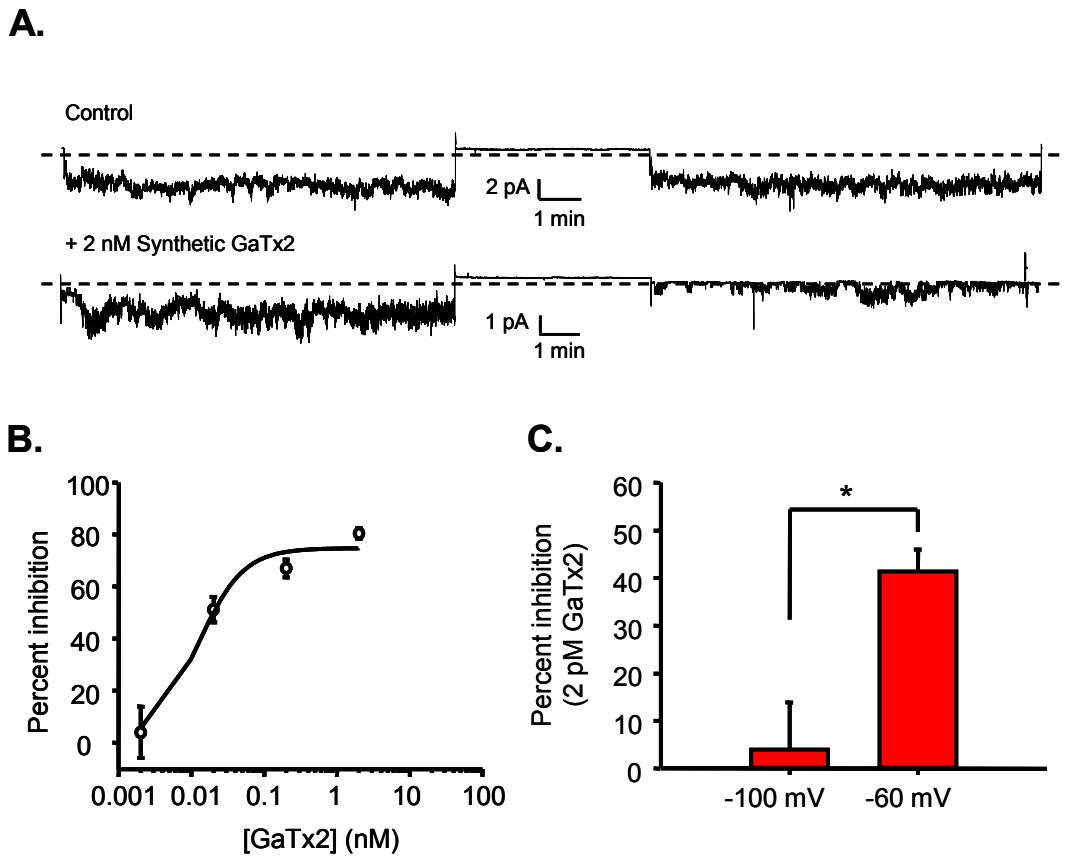

Figure 23: Synthetic GaTx2 inhibits ClC-2 in a voltage-dependent manner. (*A*) Multi-channel inside-out patch recording of ClC-2 at V_M = -100 mV in the presence of control extracellular solution (*top*), or 2 nM synthetic GaTx2 (*bottom*). The record at the left is from the beginning of the experiment, while the record at the right is from the end of the experiment, after the backfilled toxin had time to diffuse to the patch at the tip of the electrode. (*B*) Dose-response curve for inhibition of ClC-2 currents from multi-channel patches by GaTx2 at concentrations of 2 pM, 20 pM, 200 pM, and 2 nM; V_M = -100 mV. All points contain data from 6 - 17 measurements of window current at each concentration. (*C*) Comparison of inhibition of ClC-2 by 2 pM GaTx2 when currents were measured at V_M = -60 or -100 mV, in multichannel patches as shown in part A; * indicates $p < 0.001$.

Our previous experiments with Lqh-pf venom indicated that inhibition of ClC-2 was voltage-dependent, with improved inhibitory efficacy at less hyperpolarizing potentials [61]. The experiment shown in Figure 18D provided a K_D of 80 pM at V_M = -160 mV; in contrast, the experiments shown in Figure 23 provided a K_D of 12 pM. This suggests that the binding affinity of GaTx2 is voltage-dependent. In order to further characterize this phenomenon, we compared the degree of inhibition of ClC-2 current by 2 pM synthetic GaTx2 at V_M = -100 and -60 mV using multi-channel patches (Fig. 23C). At V_M = -100 mV, 2 pM toxin did not inhibit ClC-2 significantly (4.0 $\pm$ 9.9 % inhibition, n = 11 windows); however, at V_M = -60 mV, ClC-2 currents were inhibited 41.4 $\pm$ 4.1 % (n = 17 windows) by 2 pM toxin, confirming the notion that inhibition of ClC-2 by GaTx2 is voltage-dependent.

8.6 Effect of GaTx2 on Single ClC-2 Channels

Understanding the mechanism of inhibition of ClC-2 by GaTx2 will be essential for using this toxin as a tool to probe ClC channel structure and function. Peptide toxins may either inhibit channels by acting as pore blockers, which fully or partially occlude the pore, or by acting as gating modifiers, making it more difficult for the channel to open [249]. In order to determine if GaTx2 alters the single channel conductance of ClC-2, which may bee indicative of pore block, we created all-points amplitude histograms from segments of records with only 1-2 open channels, in the absence and presence of GaTx2. In the presence of 2 nM GaTx2, the single protopore amplitude at -100 mV was unchanged from control (0.25 $\pm$ 0.01 pA vs. 0.26 $\pm$ 0.01 pA, n = 3, p = 0.45) (Fig. 24A) as measured from the difference between levels O1 and O2 from the amplitude

histograms created from 2-minute sections of record in the absence and presence of toxin. This suggests that GaTx2 does not induce partial conductances, although this does not discount the possibility of inhibition via a pore block mechanism. We next performed patch clamp experiments with either one or two channels in the patch and 20 pM GaTx2 backfilled into the pipette. Measuring channel activity as NP_O/N, we observed that NP_O/N was reduced by 59.5 $\pm$ 8% (Fig. 24D, n = 2) at –100 mV, which is consistent with the reduction of window current observed in multichannel patches for this concentration of toxin (Fig. 23B). Some toxins act via a pore block mechanism by inducing long closed states within a channel burst [278, 295]. Expanded recordings of bursts (Fig. 24C) show that there appear to be no toxin-induced intraburst closures that would be consistent with a pore block mechanism.

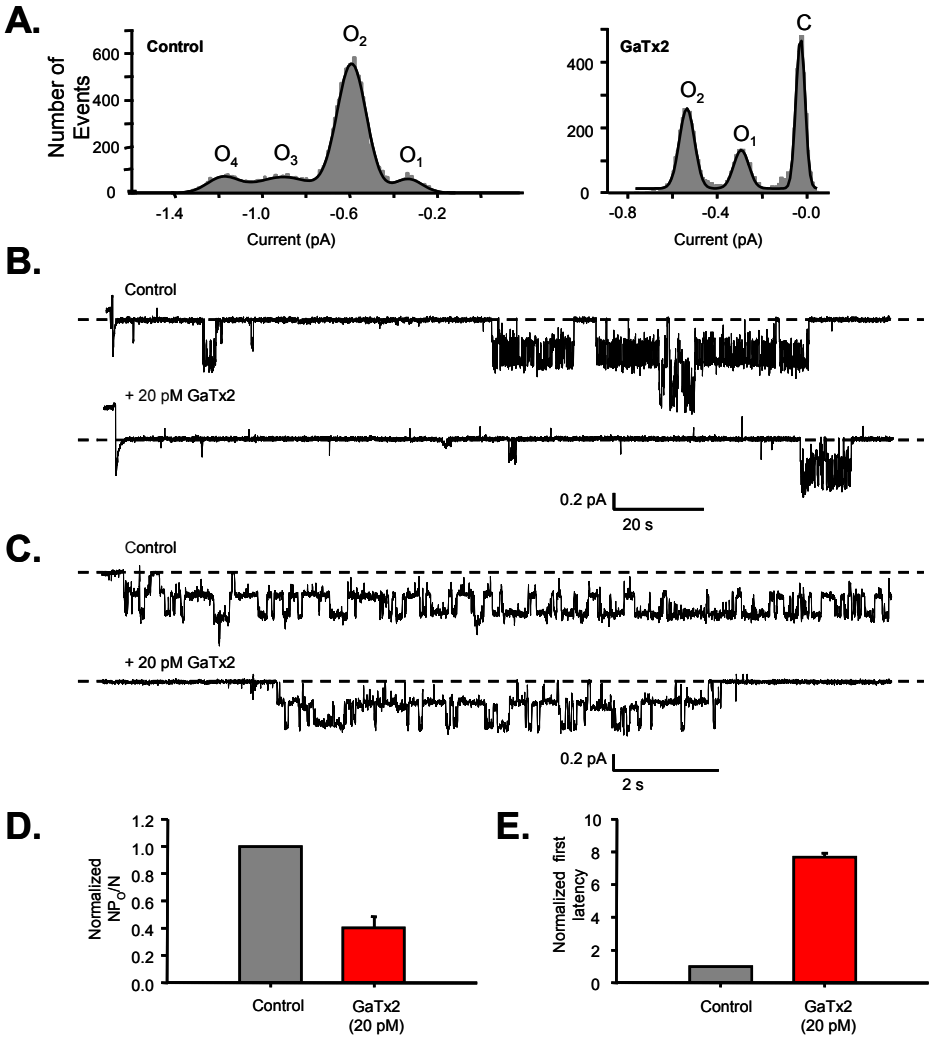

Figure 24: GaTx2 inhibits ClC-2 by slowing channel opening. (*A*) All-points amplitude histograms in the absence (*left*) and presence (*right*) of 2 nM GaTx2. (*B*) Representative single channel trace of ClC-2 with and without 20 pM synthetic toxin at V_M = -100 mV. (*C*) Expanded single channel trace of a ClC-2 burst in the absence and presence of 20 pM GaTx2. (*D*) Comparison of channel activity (as NP_O/N) in the absence and presence of 20 pM GaTx2. (*E*) Comparison of latency to opening of the first double-barreled burst after stepping from 0 to -100 mV, in the absence and presence of 20 pM GaTx2.

Prior experiments with Lqh pf-venom led us to propose that ClC-2 is inhibited by this toxin via modification of channel gating; channel activation was slowed in the presence of venom [61]. We reasoned that this effect may be apparent as a change in the latency to first opening of single ClC-2 channels. In the presence of 20 pM GaTx2, we observed a 7.67 $\pm$ 0.25 fold increase (from 13 $\pm$ 5 s to 107 $\pm$ 40 s) (Fig. 24E, n = 2) in the latency to first opening upon stepping from V_M = 0 to -100 mV, which is consistent with a modification of channel gating.

8.7 GaTx2 is not an Open Channel Blocker

Thus far, our experiments have suggested that GaTx2 acts to slow channel opening via modification of channel gating. To provide further evidence for this mechanism, we tested the effect of GaTx2 on channels that had reach steady-state activation using outside-out macropatches. We reasoned that if GaTx2 modifies channel gating, application of toxin to open channels should not reduce current amplitude, or would reduce currents very slowly. If the toxin inhibited via an open channel pore block mechanism, then currents should be reduced even if toxin was applied when channels are open. To test this, we activated ClC-2 channels with a pulse to -100 mV, and allowed current to reach steady-state (Fig. 25). After steady-state had been achieved, usually after several minutes, 2 nM GaTx2 was applied for at least 1 minute using a fast perfusion system with a solution exchange time constant of ~20 ms [61]. Application of toxin did not inhibit open channel currents (1.02 $\pm$ 0.02 fold change, n = 5, p = 0.15) (Fig. 25A, B), although application of toxin before steady state was reached led to substantial inhibition (Fig. 25A *inset*). In contrast, application of 1 mM DPC for 30 seconds to open channels

resulted in 44.90 + 3.00 % inhibition ($n = 9$, $p < 0.01$) (Fig. 25 B, D). This suggests that DPC inhibited ClC-2 channels via an open channel pore block mechanism, while GaTx2 was not capable of inhibiting open channels. This also suggest that GaTx2 does not alter channel fast gating, as slowing of this process should resemble open channel block of macroscopic currents. Therefore, it seems likely that GaTx2 inhibits ClC-2 channel activation by inhibiting slow gating.

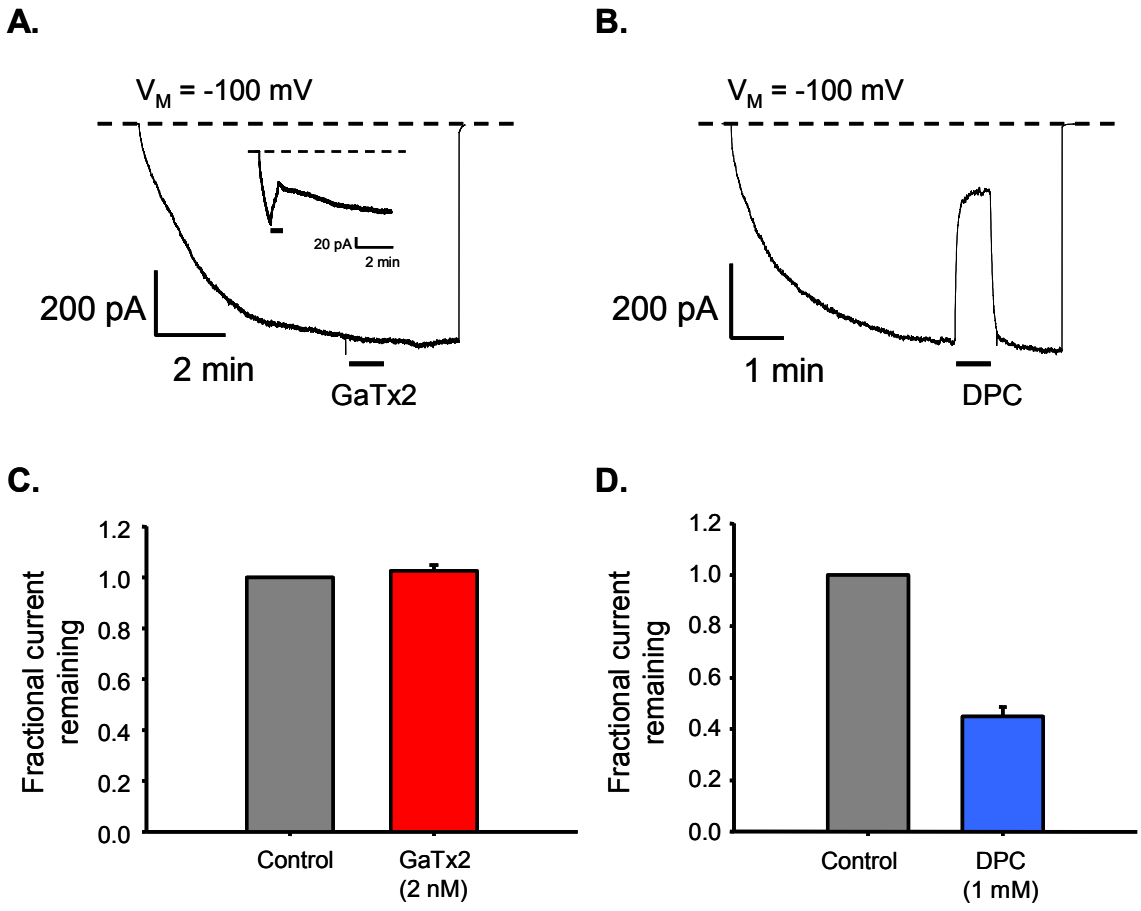

Figure 25: GaTx2 cannot inhibit open ClC-2 channels. ClC-2 channels were studied using outside-out macrpatches activate by a voltage step to V_M = -100 mV. Channel activity was allowed to reach steady-state. Patches were then exposed to either 2 nM GaTx2 *(A)*, or 1 mM DPC. Summary data shown in *(C)* and *(D)* shows that while GaTx2 is unable to inhibit ClC-2 steady-state currents (n = 5) *(C)*, DPC is able to inhibit very well (n = 9) *(D)*. The inset in *(A)*, on the other hand shows that if GaTx2 is applied to channels during the activation phase, then currents are inhibited.

8.8 Specificity of GaTx2

Most peptide toxins are usually highly specific for their respective targets, although not always perfectly selective. Charybdotoxin (ChTx), for example, is known to inhibit both K_{Ca}, and K_V channels [278, 279]. Although ClC-2 is a very broadly expressed Cl^- channel, many other Cl^- channel types are expressed in excitable and non-excitable cells. Most inhibitors available for Cl^- channels are very non-specific. In order to develop GaTx2 into a useful tool, we first needed to determine if GaTx2 is specific for ClC-2 or if it is capable of inhibiting other anion-selective channels. We first asked whether GaTx2 is capable of inhibiting any other members of the ClC channel family. We previously showed that venom had no effect on the skeletal muscle Cl^- channel ClC-1 [61]. To confirm this we asked whether synthetic GaTx2 could inhibit ClC-1. We compared currents in the presence of toxin to those after washout of toxin in order to account for channel rundown. In the presence of 10 nM GaTx2, tail currents at V_M = -120 mV from pulses to +60 mV were 1.036 $\pm$ 0.012 fold larger than currents after washout of toxin, implying no inhibition of ClC-1 (Fig. 26A). Application of 10 nM GaTx2 to ClC-3 likewise did not alter currents at V_M = +80 mV (Fig. 26B, 0.90 $\pm$ 0.05 fold, n = 3, p = 0.18). GaTx2 also was not capable of inhibiting ClC-4 mediated Cl^- transport measure at V_M = +80 mV (10 nM GaTx2, 0.97 $\pm$ 0.02 fold, n = 3, p = 0.42) (Fig. 26C), indicating that GaTx2 does not inhibit a ClC protein that functions as a transporter. We also know from previous experiments that Lqh pf-venom does not inhibit ClC-0 [61]. Thus, GaTx2 is not capable of inhibiting currents mediated by any other ClC channel on which we have tested it.

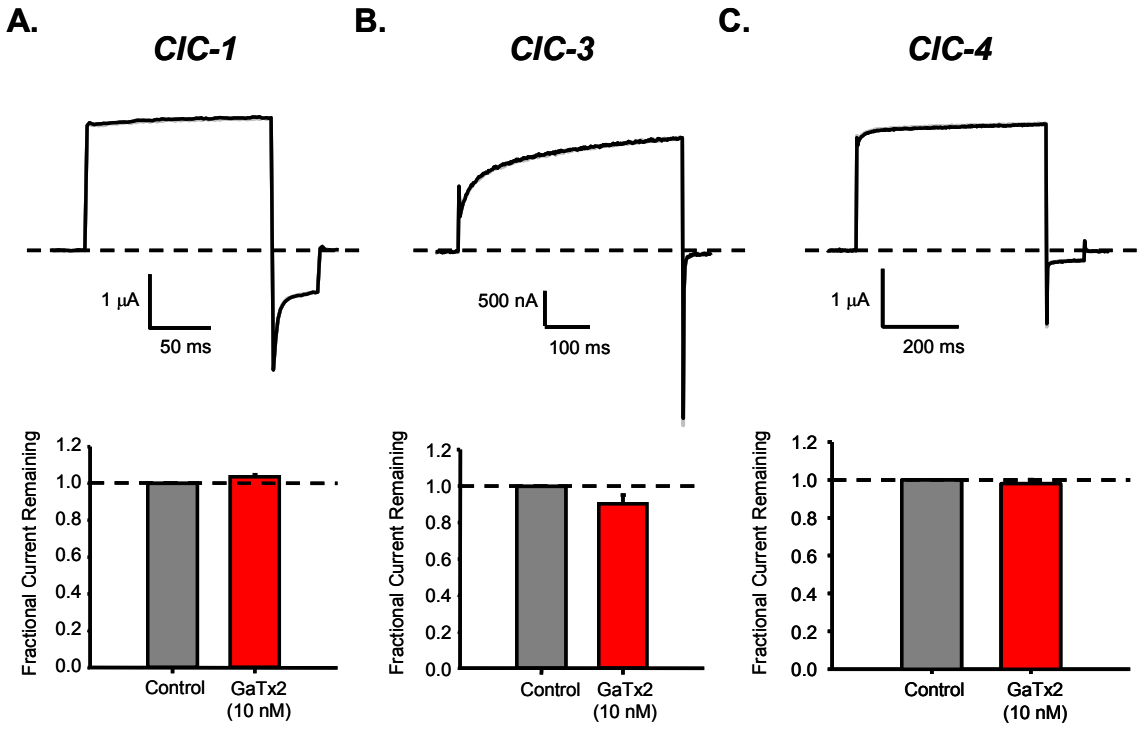

Figure 26: GaTx2 cannot inhibit other ClC proteins. In TEVC experiments, GaTx2 was applied to oocytes expressing either ClC-1 *(A)*, ClC-3 *(B)*, or ClC-4 *(C)*. Representative currents in the absence and presence of toxin are shown in the *top* panels, while summary data is presented in the *bottom* panel. GaTx2 was unable to inhibit any other ClC protein. n = 3 - 4 for each type.

We have recently identified and characterized a peptide inhibitor of currents mediated by CFTR chloride channels. CFTR was not inhibited by the venom fraction that contains GaTx2 [295]. However, in order to corroborate these results we tested the effect of synthetic GaTx2 on CFTR. We first tested GaTx2 on CFTR currents by application of toxin to the extracellular face of the channels using TEVC. Channels were activated by 200 mM IBMX + 25 mM db-cAMP. After steady-state activation was achieved, 20 nM GaTx2 was applied for 5 minutes. No change in current was observed during the application of toxin (Fig. 27A, 0.95 $\pm$ 0.02 fold, n = 2), consistent with the notion that Lqh pf-venom could not inhibit CFTR currents from the extracellular fact. Due to the fact that GaTx1 only inhibited CFTR from the intracellular face [298], we applied 60 nM GaTx2 to the intracellular face of the channel using multi-channel patches. For these experiments we used Flag-cut ΔR-CFTR, a mutant CFTR lacking the R-domain, rendering it independent of phosphorylation by PKA insensitive to dephosphorylation-mediated rundown. Channels were activated with 0.2 mM ATP, then reactivated with 0.2 mM ATP + 60 nM GaTx2. No inhibition of channels currents was observed (Fig. 27B, 0.91 $\pm$ 0.13 fold, n = 10 windows, p=0.74). Therefore, GaTx2 also is not capable of inhibiting CFTR from either the extracellular or intracellular face.

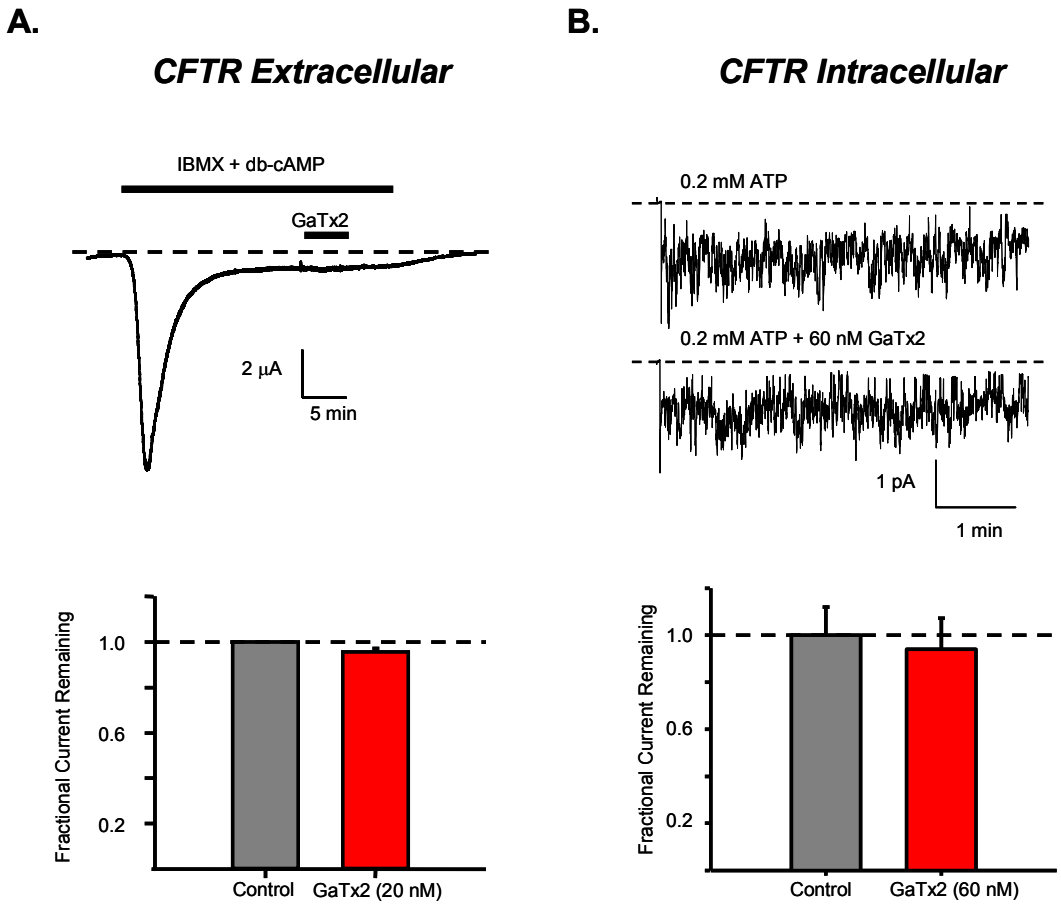

Figure 27: GaTx2 cannot inhibit CFTR. *(A)* TEVC experiment in which WT-CFTR channels were activated by a mixture of IBMX and db-cAMP. Channel activity increased rapidly, then decayed and settled to steady state level. Channels were then exposed to 20 nM extracellular GaTx2 for 5 minutes. Summary data presented in the *bottom* panel show that GaTx2 cannot inhibit ClC-2 from the extracellular side (n =2). *(B)* Inside-out multi-channel patch recording of Flag-cut-ΔR-CFTR, V_M = -80 mV. Channels were activated by application to the intracellular face of CFTR either 0.2 mM ATP or 0.2 mM ATP + 60 nM GaTx2. Window currents for multiple 3-minute windows were analyzed in the absence and presence of GaTx2 for multiple patches. Summary data in the *bottom* panel show that GaTx2 cannot inhibit CFTR from the intracellular side (n = 10 windows).

We next asked whether GaTx2 is capable of inhibiting currents from ligand-gated chloride channels formed by $GABA_C$ receptors. $GABA_C$ currents were measured by TEVC both in the absence and presence of GaTx2 (Fig. 28A). Comparison of current in the presence of 10 μM GABA to currents in the presence of 10 μM GABA plus 10 nM GaTx2 showed no change (13 $\pm$ 9.4 % increase, n = 3, p = 0.32). GABA-induced Cl^- currents also did not significantly increase upon removal of toxin from the bath solution (14 $\pm$ 19% increase, p = 0.74). This suggests that GaTx2 is not capable of inhibiting $GABA_C$ receptors.

Xenopus oocytes contain a large number of endogenous calcium-dependent chloride channels (Cl_{Ca}). Application of 10 mM Ca^{2+} to the face of an excised inside-out patch rapidly activates these channels, which rundown over the course of the experiment. Therefore, control records and records in the presence of GaTx2 were obtained from different patches. In order to access toxin activity, we measured current decay over the course of three pulsed exposures to high [Ca^{2+}]; toxin was applied between the 1st and 2nd Ca^{2+} pulses. If GaTx2 inhibited channel currents, we expected to observe a greater degree of rundown in toxin-containing patches versus control patches. However, the decay between pulses was the same with and without 10 nM GaTx2 (Fig. 28B, 25.67 $\pm$ 3.65% (control, n = 5), vs. 34.11 $\pm$ 5.26, (+GaTx2, n=6), p = 0.24), suggesting that GaTx2 is not capable of inhibiting these channels from the intracellular side. We were unable to test the effect of GaTx2 on Cl_{Ca} when applied to the extracellular face because receptor-mediated activation of these channels exhibits irreversible desensitization after one exposure to receptor ligand (not shown).

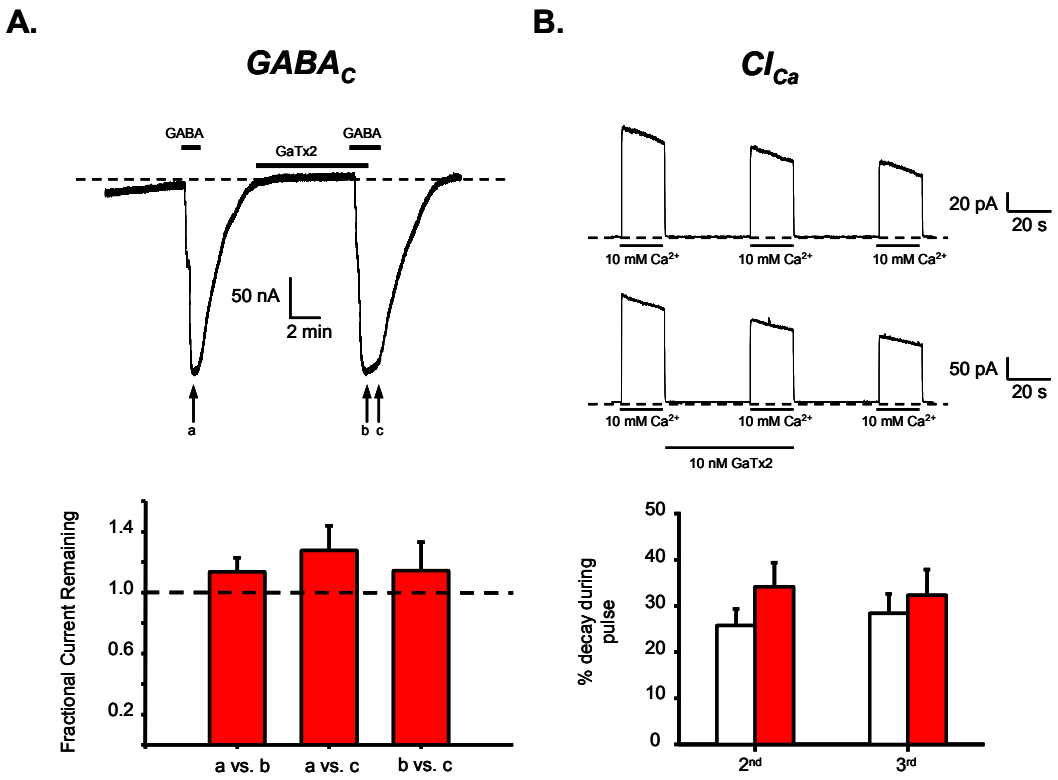

Figure 28: GaTx2 does not inhibit other major Cl^- channel types. *(A)* TEVC recording of oocytes expressing $GABA_C$ channels activated by 10 μM GABA (V_M = -60 mV). Channels were exposed to 20 nM GaTx2 for 5 minutes then activated by GABA again. GaTx2 was then removed, while the oocyte was still exposed to GABA. The bottom panel shows that GaTx2 does not inhibit $GABA_C$ currents (n = 3), and GABA-activated current does not increase when GaTx2 is removed. *(B)* Inside out macropatch recording of endogenous *Xenopus* Ca^{2+}-dependent Cl^- channels, V_M = -50 mV. Channels were activated by multiple applications of 10 mM Ca^{2+}, and the amount of rundown was quantified. Toxin was applied to some patches between the first and second application by Ca^{2+}. The degree of rundown between the 1st and 2nd application of Ca^{2+} did not differ between control patches and patches exposed to toxin (control, n = 5; GaTx2, n = 6).

Finally, because the toxin bearing the sequence of GaTx2 was originally predicted to be a K^+ channel inhibitor, we sought to determine if this toxin could inhibit the voltage-gated *Drosophila Shaker* K^+ channel B variant with inactivation-removed (ShB-IR), by exposing oocytes expressing ShB-IR to 20 nM GaTx2, a concentration that strongly inhibits ClC-2 currents (Fig. 29A). We observed no inhibition of ShB-IR currents, indicating that GaTx2 does not interact with this channel (1.00 + 0.007 fold, n = 2). We similarly tested the effect of GaTx2 on the mammalian Shaker equivalent $K_V1.2$, and observed no change in K^+ currents (Fig. 29B, 0.99 $\pm$ 0.03 fold, n = 4, p=0.55). It is possible that GaTx2 may inhibit these channels at a much higher concentration, but it had no effect in the concentration range that effectively inhibits ClC-2 mediated currents. Thus, we have shown that GaTx2 is a specific ClC-2 inhibitor, being unable to inhibit other members of the ClC family, CFTR, $GABA_C$, Cl_{Ca}, or major voltage-dependent K^+ channels.

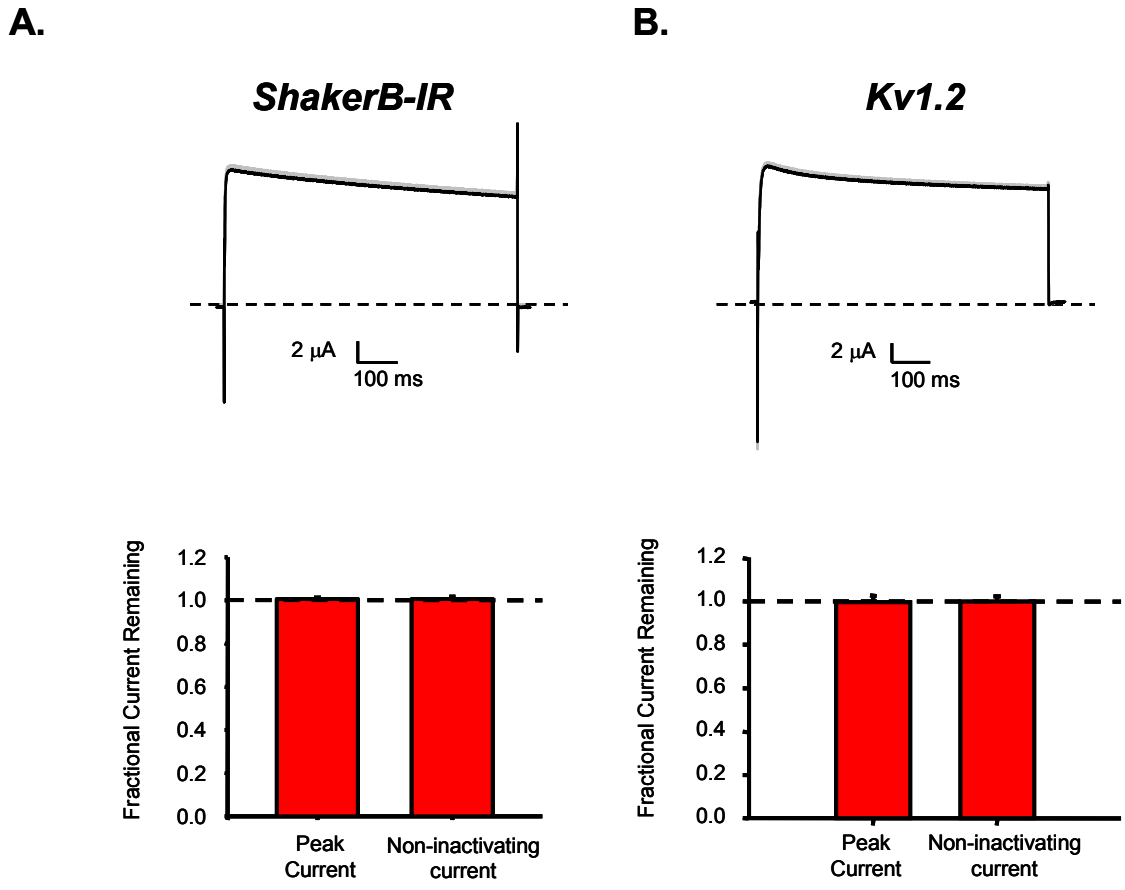

Figure 29: GaTx2 does not inhibit voltage-dependent K^+ channels. TEVC recording of *Shaker* ShB-IR K^+ channels *(A)*, and $K_V1.2$ channels *(B)*. Channels were activated by a voltage pulse to 0 mV from a holding potential of $V_M = 90$ mV. Channels were exposed to either 20 nM GaTx2 *(A)*, or 10 nM GaTx2 *(B)*. Summary data show that GaTx2 is not capable of inhibiting *Shaker* ShB-IR K^+ channels (n = 2), or $K_V1.2$ (n = 4).

CHAPTER 9

DISCUSSION

We previously showed that Lqh pf-venom contained a peptide component that inhibited the ClC-2 chloride channel [61]. Here we describe the successful isolation and initial characterization of this toxin, which we have named GaTx2. This toxin is a 3.2 kDa peptide with three disulfide bonds which hold together a secondary structure composed of one α-helix and two β-strands. Although the sequence of GaTx2 has been previously described [323], this is the first description of its molecular target. The target for this toxin was predicted to be a K^+ channel based solely on sequence alignments with other known or putative K^+ channel toxins. Therefore, this is also the first toxin that has been shown to be misclassified, raising the possibility that a number of other toxins capable of inhibiting anion-selective channels have already been sequenced.

The crystal structure of a bacterial ClC protein has been very useful for directing experiments aimed at gaining further understanding of the pore structures and fast gating mechanisms of ClC channel proteins [239, 242]. Although the crystal structure has not been as useful for understanding slow gating, some progress has been made through mutagenesis studies [23, 38, 39, 69, 243]. The new crystal structures of the isolated C-terminal domain from ClC-0 will likely be very helpful in this regard [245]. However, many of the conformational changes associated with channel gating are still unknown, and are unlikely to be elucidated strictly by studying available structures, which do not capture the dynamic nature of these proteins. The GaTx2 toxin will allow the biophysical

study of these gating processes in greater detail. GaTx2 inhibits ClC-2 with higher affinity than any other available drug and, in fact, is the best inhibitor of any chloride channel. The previously best available ClC inhibitor, a pentameric DIDS hydrolysis product, inhibits ClC-Ka with a K1/2 of 0.5 μMwhile GaTx1 inhibits CFTR with a K_D of 25 nM at -100 mV [264, 298]. The apparent dissociation constant of GaTx2 for ClC-2 at -100 mV is ~ 15 pM (Fig. 22A, 23B). Consistent with this high affinity interaction, recovery of ClC-2 currents from inhibition is very slow, with a time constant of ~300s.

Interestingly, inhibition of ClC-2 by GaTx2 seems to be protocol dependent. Application of toxin to channels that have reached steady state activation did not reduce currents. However, significant inhibition was observed when channels were allowed to close in the presence of toxin, as observed for both TEVC recording and inside-out multi-channel patches. Therefore, GaTx2 does not mediate a simple open channel block mechanism such as that seen for some peptide toxins. Inhibition of GaTx2 is also voltage-dependent, with stronger inhibition at more physiological membrane potentials. It is presently unclear why maximal inhibition is ~60% for TEVC, while 80% inhibition can be achieved using patch clamp techniques. It is possible that the differences in recording conditions, such as chloride concentrations, may affect the inhibitory activity of GaTx2. Details regarding the exact mechanism of inhibition still need to be addressed. The voltage-dependence and protocol dependence suggest that the mechanism by which GaTx2 inhibits ClC-2 is a complicated one.

The physiological role of ClC-2 is still largely undefined. It is thought that ClC-2 may play a role in vascular smooth muscle cells and may be expressed on the apical membrane of epithelial cells along with CFTR, although this is still controversial [99,

303]. GaTx2 will be useful in determining the role of ClC-2 in these cells and may aid in determining the membrane localization of ClC-2 in specific cell types. Also, mutations in ClC-2 have been implicated in epilepsy [92], while under-activity of WT ClC-2 has been implicated in constipation-associated inflammatory bowel disease [86]. Therefore, GaTx2 may serve as a lead compound for peptidomimetic drugs that target ClC-2.

CHAPTER 10

PERSPECTIVES AND FUTURE DIRECTIONS

10.1 Summary of Presented Work

The goal of the work presented in this dissertation was to identify and characterize a peptide inhibitor targeting a member of the ClC family of voltage-gated chloride channels and chloride/proton exchangers. Initial experiments showed that venom from the scorpion *Leiurus quinquestriatus hebraeus* was able to inhibit currents mediated by the ClC-2 chloride channel from the extracellular side when expressed in *Xenopus* oocytes. The data presented in Chapters 2 - 9 provide a description of the first peptide toxin inhibitor of any ClC protein, specifically ClC-2. As a first step towards isolation of the active toxin, we characterized the effect of Lqh pf-venom on ClC-2 mediated Cl^- currents using a combination of TEVC and macropatch techniques. The active component was then isolated using multiple rounds of RP-HPLC with columns of varied hydrophobicity. Proteomic characterization of the toxin was then carried out using a combination of MALDI mass spectrometry, N-terminal protein sequencing, and amino acid analysis. The active toxin, which we named Georgia anion toxin 2 (GaTx2), is composed of 29 amino acids, has a molecular mass of 3.2 kDa, and contains three disulfide bridges. We have also produced this toxin using solid-phase chemical synthesis. Finally, basic pharmacological characterization of the active toxin was performed using a combination of TEVC, macropatch, and single channel recording.

ClC proteins are expressed in nearly all cell types, where they are involved in maintenance of membrane potential, electrical excitability, endocytosis, and acidification of intracellular compartments. While there is a large base of general knowledge regarding these proteins, many of the biophysical characteristics for most ClC family members remain vague, in large part due to the lack of specific pharmacological tools that can be used to study ClC protein structure/function relationships. Peptide toxins isolated from animal venoms have provided just such tools for many cation channels. However, there is only one peptide toxin available that inhibits a chloride channel of known molecular identity; GaTx1 inhibits the CFTR chloride channel [298]. Our initial studies showed that Lqh pf-venom contained a peptide component capable of inhibiting ClC-2 mediated Cl^- currents, but not currents mediated by ClC-0 or ClC-1. Peptide toxins active against cation channels inhibit channel activity by two distinct mechanisms; they may physically occlude the ion permeation pathway, or they may modifiy channel gating in such a way that increases the energy required for channel activation. Our data suggest that ClC-2 channel activation was shifted to more hyperpolarizing potentials in the presence of venom, supporting the hypothesis that the active component may be a gating modifier. Consistent with this hypothesis, channel activation kinetics were slowed in the presence of venom. While ClC-2 is a voltage-dependent channel, it is also activated by cell swelling and extracellular acidification. Interestingly, the active component of venom appears to act solely on the voltage-dependent gating mechanism, as swelling activation of ClC-2 was unaltered in the presence of venom.

Isolation of this active component via RP-HPLC led to the purification of a 3.2 kDa protein, which we have named Georgia anion toxin 2 (GaTx2). A toxin with the

same primary sequence was previously isolated in 1997, but no target was identified, and no further studies using this toxin have been carried out since the original isolation. In the present work, we showed that GaTx2 is a specific inhibitor of ClC-2 chloride channels. This toxin cannot inhibit currents other members of the ClC family, CFTR from the extracellular or intracellular side, $GABA_C$ Cl^- channels, Ca2+-dependent chloride channels from the intracellular side, or the voltage-dependent K^+ channels *Shaker* and $K_V1.2$. GaTx2 inhibited ClC-2 currents with very high affinity (K_D ~ 15 pM at -100 mV) and, like venom, in a voltage-dependent manner; the toxin inhibited with high affinity at more physiological membrane potentials, i.e. higher affinity at -60 mV versus -100 mV. Importantly, synthetic GaTx2 was able to inhibit ClC-2 currents in the same manner as native GaTx2. This is important because not only does this prove that the toxin isolated from venom was the active component, but it also makes future studies using this toxin more feasible, as isolation of the toxin from venom is both time consuming and difficult.

GaTx2 appears to alter channel gating in a manner similar to that of venom; channel activation kinetics are slowed in the presence of toxin. Our data suggest that this toxin is not a simple open channel blocker because it is unable to inhibit ClC-2 mediated currents when applied to channels that have reached steady-state activation with a P_O ~1, consistent with the notion that this toxin is a gating modifier. A state-dependent pore blocker that binds only when the channel is closed would yield similar results; however, if GaTx2 inhibited ClC-2 currents via this mechanism then toxin would unbind during the course of a voltage pulse. Our data examining the effect of Lqh pf-venom on ClC-2 currents suggest that the amount of inhibition does not decrease over the course of the voltage pulse. The trend actually shows greater inhibition at the end of the pulse than at

the beginning, although there is no statistical significance. Thus, it is unlikely that GaTx2 acts as a state-dependent pore blocker, leaving modification of channel gating the only likely mechanism of inhibition.

10.2 Future Directions and Implications

GaTx2 represents the first peptide toxin inhibitor of ClC channels, and is the highest affinity inhibitor of any chloride channel. The experiments described in this dissertation have provided a basis for the development of this toxin as a pharmacological tool that may be used to study ClC channel structure/function relationships. While this toxin represents the first of a new class of peptide inhibitors, it is important to point out that this is likely not the only peptide toxin active against ClC proteins. Thousands of peptide toxins exist in nature when the components of venoms from other scorpion, spider, snake, and cone snail species are taken into account [249]. Although many, but by no means all, of these toxins have been purified from these animal venoms, most are characterized solely based on sequence alignments and disulfide bridge connectivity, as was the case originally for GaTx2 [323]. This simply emphasizes the need for experimental confirmation for conclusions based on *in silico* methods.

Many future studies utilizing this toxin are possible. One of the first that needs to be undertaken is to determine if GaTx2 can inhibit ClC-2 in a cell line which natively expresses this channel. Most cell types exhibit several types of chloride currents. While ClC-2 RNA has been shown to be nearly ubiquitously expressed via Northern blot analysis [60], there is still a question of whether the protein is expressed in all of these cells. If GaTx2 is able to inhibit endogenous ClC-2 channel activity, the pattern of

functional protein expression may be established. Furthermore, there is still some controversy regarding membrane localization of ClC-2 in cells where protein expression has been well established [76, 78, 80, 303]. GaTx2 can be used in Ussing chamber experiments to establish either apical or basolateral localization for ClC-2 where the issue remains unclear. This toxin may also be critical for determination of the physiological role of ClC-2, which is still undefined in many cell types. Studies have indicated that ClC-2 may be involved in migration of glioblastoma cells, possibly playing a role in regulatory volume decrease [330]. Inhibition of endogenous Cl^- current using the non-specific Cl^- channel inhibitor NPPB reduced cell migration; this was corroborated by similar effects of knock-down of ClC-2 using siRNA [330]. Preliminary studies from our lab suggest that GaTx2 can also inhibit migration of U87 glioblastoma cells. An invasion assay using transwell inserts showed that when cells were allowed to invade for 20 hours in the absence of toxin, a large number of cells were able to migrate through the insert; this migration was reduced when the experiment was performed in the presence of 500 nM GaTx2 (Fig. 30A). Additionally, preliminary experiments examining proliferation of Caco-2 cells suggest that proliferation is slowed when grown in the presence of GaTx2. Using transepithelial resistance as a measure of cell proliferation, cells were grown either in the absence or presence of 4 nM GaTx2. In the absence of toxin cells reached confluency quickly both before and after wounding by a high voltage pulse. However, when cultured in the presence of toxin both initial growth and wound healing were slowed (Fig. 30B). This provides strong evidence that ClC-2 is involved in both migration of U87 cells and proliferation of Caco-2 cells, but these studies need to be

repeated, and performed in combination with whole-cell recording to examine the GaTx2 sensitive current to establish that this current is indeed mediated by ClC-2.

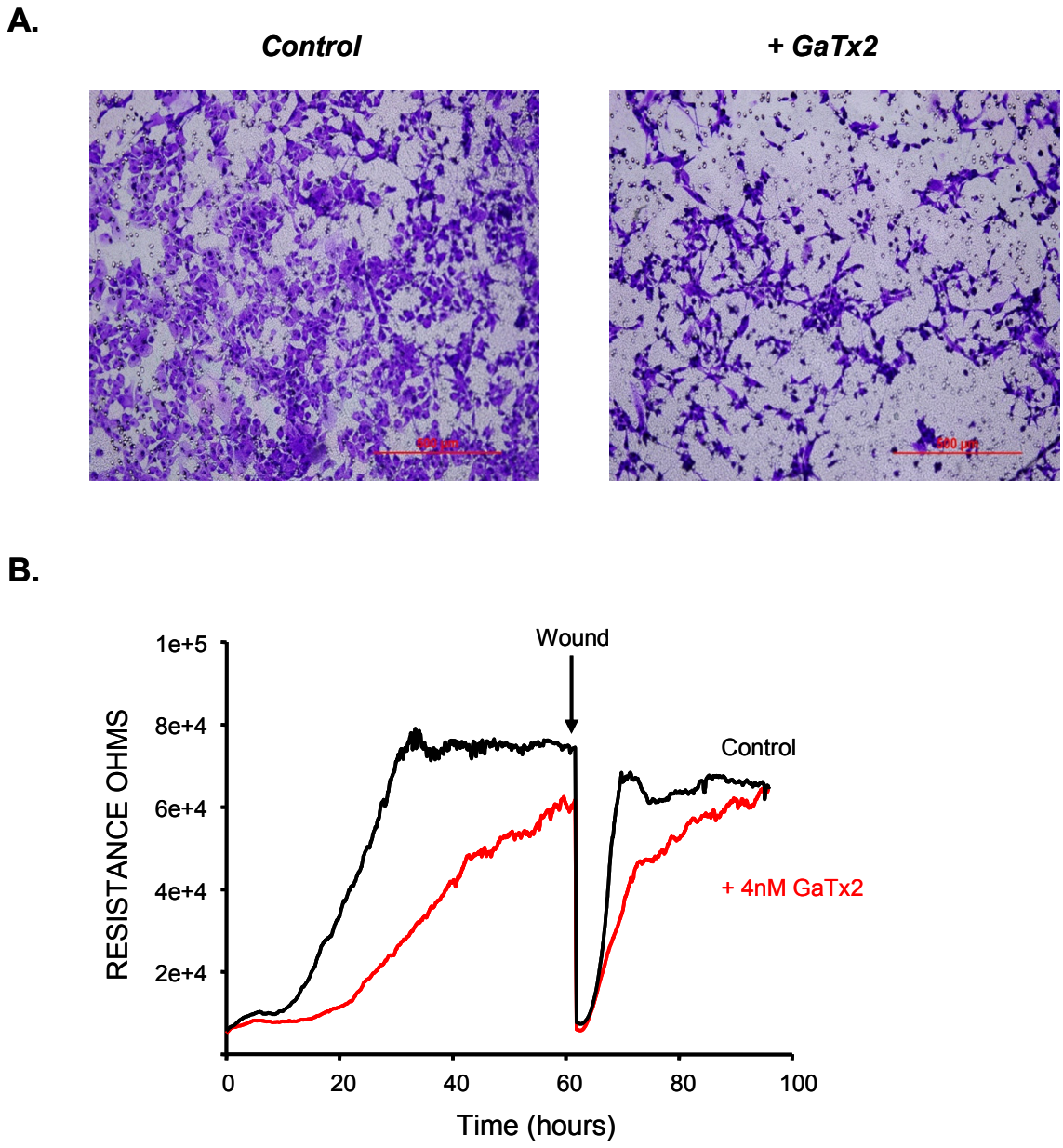

Figure 30: GaTx2 alters cell migration and proliferation. *(A)* Migration assay of U87 glioblastoma cells that have been allowed to migrate for 20 hours either in the absence (left) or presence of 500 nM GaTx2 (right). *(B)* Wound healing assay examining Caco-2 cell growth. Cells were allowed to proliferate either in the absence (*black* trace) or presence (*red* trace) of 4 nM GaTx2. Once a tight epithelium was established, cells were wounded by a high voltage pulse, and allowed to proliferate again. Membrane resistance is used as a measure of confluency; high resistance indicates a tight epithelium.

As outlined in Chapter 1, ClC-2 is believed to be involved in epilepsy, with one specific mutation, G715E, shifting the voltage-dependence of ClC-2 activation to more depolarizing potentials, leading to overexcitability of neurons [92]. It has also been proposed that ClC-2 is involved in constipation-associated inflammatory bowel disease . In the intestine it has been well established that ClC-2 has a basolateral localization, thus aiding in chloride efflux and water absorption. Inhibition of basolaterally localized ClC-2 would prevent excess water reabsorption, and relieve constipation. Finally, ClC-2 is expressed in the same lung epithelial cells that express CFTR, the chloride channel dysfunctional in cystic fibrosis (CF). It has been postulated that ClC-2 may serve as an alternate Cl^- pathway in these cells, thereby alleviating the loss of Cl^- transport associated with cystic fibrosis. Recently, peptide toxins have become very useful as lead compounds for pharmaceuticals, including a conotoxin derivative that is used to treat chronic pain [331]. It may therefore be possible to use GaTx2 as a lead compound for drugs that can be used to treat the diseases associated with altered ClC-2 activity. If GaTx2 can be developed in such a way as to promote ClC-2 activation, then this toxin may also serve as a platform to develop drugs that activate alternative Cl^- transport in patients suffering from CF.

In addition to the experiments that can be performed to examine the physiological role of ClC-2, GaTx2 will most likely be an excellent tool for ClC-2 structure/function studies. One of the first steps that must be taken is the identification of the binding site for GaTx2. Peptide toxins that bind to cation channels bind their targets in regions that are critical for channel function, i.e. the pore domain or voltage sensor, and these toxins have been used to dissect both ion permeation and voltage-dependent gating [267, 274,

281]. For ClC channels, while it is largely accepted that the available crystal structure provides an excellent template for structural studies of ClC proteins from higher organisms, there is little doubt that there must be some critical differences between the bacterial and eukaryotic proteins. One important discovery was the determination that the bacterial ClC protein is a Cl^-/H^+ exchanger, not an ion channel [126, 127]. This suggests that the permeation pathway may be different between the two classes of proteins, and also that the gating mechanisms will likely be very different. In fact, the ClC transporter ClC-ec1 appears only to have a fast gating mechanism, as determined by Q_{10} measurements of the transport rate . While fast gating may be similar for both ClC channels and transporters, slow-gating appears to be non-existent in the transporters, and is very poorly understood from a structural standpoint for ClC channels . Our data suggest that GaTx2 acts as a gating modifier that may alter slow gating of ClC-2. The protocol dependent activity of GaTx2 suggests that this toxin is very sensitive to the conformation of the channel; therefore, GaTx2 will likely serve to report the structural changes that ClC-2 undergoes during voltage-dependent gating. This makes identification of the binding site a necessary step. This should first be undertaken by using specific mutations of the ClC-2 channel that are known to affect gating, such as deletion of the N-terminus, and the G715E mutation, as well as the E217A and C256S mutations to determine the effect that these mutations have on toxin activity, and to examine which gating mechanism is more strongly affected by GaTx2. The effect of GaTx2 on ClC-2 gating can also be assessed using specific voltage protocols designed to isolate the fast and slow gating processes, such as those successfully used by de Santiago and coworkers [68]. A third approach that would unambiguously address this question is to

quantitatively examine the effect of GaTx2 on ClC-2 single channels, although the very slow off-rate of the toxin would make these experiments very difficult.

Chimeric channels will likely be very useful for the identification of the toxin binding site due to the fact that GaTx2 has no effect on currents mediated by ClC-0 or ClC-1. Therefore, ClC-0/ClC-2 or ClC-1/ClC-2 chimeras could be used to identify the general region to which the toxin binds. Once this region is identified, point mutations can be made to identify the specific residues involved in binding. Likewise, the residues on GaTx2 that contribute to toxin efficacy must be identified. Due to the fact that WT-GaTx2 can be successfully synthesized, making mutant GaTx2 is a simple matter of replacing a specific residue during the synthesis process. Each mutant toxin can then be tested to determine if the introduced mutation alters toxin activity. The residues that contribute to toxin activity will likely line one face of the toxin. Once both sides of the toxin/channel interaction interface are identified, thermodynamic mutant cycle analysis (TMCA) can be used to determine which residues interact with each other. TMCA has been very successfully used to map the interaction interface between agitoxin2 and the *Shaker* K^+ channel. This process systematically tests combinations of wild type and mutant toxins and channels, and provides a measurement for the interaction energy for the specific combinations. In this way, the exact orientation of the toxin within the binding site can be determined. This will be important to assess why GaTx2 inhibits ClC-2 channels, but not other ClC proteins. There must be critical differences between the ClC members within the binding site. Also, once the binding site is identified, researchers can determine what effect mutations of the toxin binding site have on ClC-2 gating, and if mutation of analogous residues in other ClC proteins also alters channel gating. It would

also be interesting to determine if the GaTx2 binding site can be transferred to other ClC proteins, and if this new chimeric protein has altered biophysical characteristics.

Finally, a detailed study aimed at in depth examination of the inhibitory mechanism of GaTx2 needs to be performed. Our data suggest that GaTx2 acts as a gating modifier, but these results will only serve as a starting point for more directed study. We have shown that inhibition of ClC-2 currents by GaTx2 is voltage dependent, but a more detailed analysis is needed to determine if the membrane potential affects toxin on-rate or off-rate. It also needs to be determined if GaTx2 activity is affected by either intracellular or extracellular chloride concentration. Our data show a maximal inhibition of ~60% using TEVC, while ~80% inhibition can be achieved using multi-channel patches. The most notable difference in the experimental conditions is that of the solution composition, with the bath solutions for the patch experiments containing 150 mM chloride compared to 100 mM for TEVC experiments; the difference is even larger when comparing the intracellular chloride concentration, ~30 mM for TEVC versus 150 mM for patch recording. Thus, it is possible that chloride concentration may play a role in the activity of the toxin. If this is the case, however, it will need to be determined if this is a direct effect of chloride concentration on toxin binding, or if changing chloride concentration simply shifts channel P_O such that toxin activity is altered, especially considering that permeation and gating are linked in ClC channels [11]. As a gating modifier, GaTx2 is sensitive to channel open probability, making it likely that anything that changes channel open probability, such as changing chloride concentration, will also likely alter toxin activity. The effect of GaTx2 on swelling activation, pH-dependent gating, and PKA activation also needs to be investigated.

10.3 Closing

Identification of this toxin is a major step forward for the pharmacology of ClC channels. This will open the way for detailed study of ClC structure/function relationships using pharmacological tools, and be very useful for physiological study of ClC-2. Finally, this toxin has the potential to be a lead compound for the development of therapeutics to treat inflammatory bowel disease, epilepsy, and possibly CF. Future work utilizing GaTx2 will lead to a deeper understanding of ClC protein biophysics and physiology, and this toxin will hopefully only be the first in a new family of peptide toxin inhibitors of ClC proteins.

LITERATURE CITED

1. White MM & Miller C, A voltage-gated anion channel from the electric organ of Torpedo californica. *J Biol Chem*, 1979. **254**: p. 10161-10166.

2. Miller C & White MM, A voltage-dependent chloride conductance channel from Torpedo electroplax membrane. *Ann N Y Acad Sci*, 1980. **341**: p. 534-551.

3. Miller C & White MM, Dimeric structure of single chloride channels from Torpedo electroplax. *Proc Natl Acad Sci U S A*, 1984. **81**: p. 2772-2775.

4. Hanke W & Miller C, Single chloride channels from Torpedo electroplax. Activation by protons. *J Gen Physiol*, 1983. **82**: p. 25-45.

5. Middleton RE, Pheasant DJ, & Miller C, Purification, reconstitution, and subunit composition of a voltage-gated chloride channel from Torpedo electroplax. *Biochemistry*, 1994. **33**: p. 13189-13198.

6. Catalan M*, et al.*, ClC-2 in guinea pig colon: mRNA, immunolabeling, and functional evidence for surface epithelium localization. *Am J Physiol Gastrointest Liver Physiol*, 2002. **283**: p. G1004-1013.

7. Jentsch TJ, Steinmeyer K, & Schwarz G, Primary structure of Torpedo marmorata chloride channel isolated by expression cloning in Xenopus oocytes. *Nature*, 1990. **348**: p. 510-514.

8. White MM & Miller C, Probes of the conduction process of a voltage-gated Cl^- channel from Torpedo electroplax. *J Gen Physiol*, 1981. **78**: p. 1-18.

9. Richard EA & Miller C, Steady-state coupling of ion-channel conformations to a transmembrane ion gradient. *Science*, 1990. **247**: p. 1208-1210.

10. Bauer CK, Steinmeyer K, Schwarz JR, & Jentsch TJ, Completely functional double-barreled chloride channel expressed from a single Torpedo cDNA. *Proc Natl Acad Sci U S A*, 1991. **88**: p. 11052-11056.

11. Pusch M, Ludewig U, Rehfeldt A, & Jentsch TJ, Gating of the voltage-dependent chloride channel CIC-0 by the permeant anion. *Nature*, 1995. **373**: p. 527-531.

12. Middleton RE, Pheasant DJ, & Miller C, Homodimeric architecture of a ClC-type chloride ion channel. *Nature*, 1996. **383**: p. 337-340.

13. Ludewig U, Pusch M, & Jentsch TJ, Independent gating of single pores in CLC-0 chloride channels. *Biophys J*, 1997. **73**: p. 789-797.

14. Dutzler R*, et al.*, X-ray structure of a ClC chloride channel at 3.0 Åreveals the molecular basis of anion selectivity. *Nature*, 2002. **415**: p. 287-294.

15. Pusch M, Ludewig U, & Jentsch TJ, Temperature dependence of fast and slow gating relaxations of ClC-0 chloride channels. *J Gen Physiol*, 1997. **109**: p. 105-116.

16. Swartz KJ, Towards a structural view of gating in potassium channels. *Nat Rev Neurosci*, 2004. **5**: p. 905-916.

17. Chen TY & Miller C, Nonequilibrium gating and voltage dependence of the ClC-0 Cl^- channel. *J Gen Physiol*, 1996. **108**: p. 237-250.

18. Pusch M, Jordt SE, Stein V, & Jentsch TJ, Chloride dependence of hyperpolarization-activated chloride channel gates. *J Physiol*, 1999. **515 (Pt 2)**: p. 341-353.

19. Chen TY, Chen MF, & Lin CW, Electrostatic control and chloride regulation of the fast gating of ClC-0 chloride channels. *J Gen Physiol*, 2003. **122**: p. 641-651.

20. Chen MF & Chen TY, Different fast-gate regulation by external Cl(-) and H(+) of the muscle-type ClC chloride channels. *J Gen Physiol*, 2001. **118**: p. 23-32.

21. Chen TY, Extracellular zinc ion inhibits ClC-0 chloride channels by facilitating slow gating. *J Gen Physiol*, 1998. **112**: p. 715-726.

22. Lin YW, Lin CW, & Chen TY, Elimination of the slow gating of ClC-0 chloride channel by a point mutation. *J Gen Physiol*, 1999. **114**: p. 1-12.

23. Estevez R*, et al.*, Functional and structural conservation of CBS domains from CLC chloride channels. *J Physiol*, 2004. **557**: p. 363-378.

24. Li Y, Yu WP, Lin CW, & Chen TY, Oxidation and reduction control of the inactivation gating of Torpedo ClC-0 chloride channels. *Biophys J*, 2005. **88**: p. 3936-3945.

25. Steinmeyer K, Ortland C, & Jentsch TJ, Primary structure and functional expression of a developmentally regulated skeletal muscle chloride channel. *Nature*, 1991. **354**: p. 301-304.

26. Koch MC*, et al.*, The skeletal muscle chloride channel in dominant and recessive human myotonia. *Science*, 1992. **257**: p. 797-800.

27. Gronemeier M*, et al.*, Nonsense and missense mutations in the muscular chloride channel gene Clc-1 of myotonic mice. *J Biol Chem*, 1994. **269**: p. 5963-5967.

28. Jentsch TJ, Stein V, Weinreich F, & Zdebik AA, Molecular structure and physiological function of chloride channels. *Physiol Rev*, 2002. **82**: p. 503-568.

29. Steinmeyer K*, et al.*, Inactivation of muscle chloride channel by transposon insertion in myotonic mice. *Nature*, 1991. **354**: p. 304-308.

30. Pusch M, Steinmeyer K, & Jentsch TJ, Low single channel conductance of the major skeletal muscle chloride channel, ClC-1. *Biophys J*, 1994. **66**: p. 149-152.

31. Steinmeyer K*, et al.*, Multimeric structure of ClC-1 chloride channel revealed by mutations in dominant myotonia congenita (Thomsen). *EMBO J*, 1994. **13**: p. 737-743.

32. Fahlke C, Rhodes TH, Desai RR, & George AL, Jr., Pore stoichiometry of a voltage-gated chloride channel. *Nature*, 1998. **394**: p. 687-690.

33. Saviane C, Conti F, & Pusch M, The muscle chloride channel ClC-1 has a double-barreled appearance that is differentially affected in dominant and recessive myotonia. *J Gen Physiol*, 1999. **113**: p. 457-468.

34. Fahlke C*, et al.*, Mechanism of voltage-dependent gating in skeletal muscle chloride channels. *Biophys J*, 1996. **71**: p. 695-706.

35. Rychkov GY*, et al.*, Concentration and pH dependence of skeletal muscle chloride channel ClC-1. *J Physiol*, 1996. **497 (Pt 2)**: p. 423-435.

36. Accardi A & Pusch M, Fast and slow gating relaxations in the muscle chloride channel CLC-1. *J Gen Physiol*, 2000. **116**: p. 433-444.

37. Bennetts B, Roberts ML, Bretag AH, & Rychkov GY, Temperature dependence of human muscle ClC-1 chloride channel. *J Physiol*, 2001. **535**: p. 83-93.

38. Hebeisen S*, et al.*, The role of the carboxyl terminus in ClC chloride channel function. *J Biol Chem*, 2004. **279**: p. 13140-13147.

39. Duffield M, Rychkov G, Bretag A, & Roberts M, Involvement of helices at the dimer interface in ClC-1 common gating. *J Gen Physiol*, 2003. **121**: p. 149-161.

40. Accardi A, Ferrera L, & Pusch M, Drastic reduction of the slow gate of human muscle chloride channel (ClC-1) by mutation C277S. *J Physiol*, 2001. **534**: p. 745-752.

41. Pedersen TH, Nielsen OB, Lamb GD, & Stephenson DG, Intracellular acidosis enhances the excitability of working muscle. *Science*, 2004. **305**: p. 1144-1147.

42. Palade PT & Barchi RL, Characteristics of the chloride conductance in muscle fibers of the rat diaphragm. *J Gen Physiol*, 1977. **69**: p. 325-342.

43. Pedersen TH, de Paoli F, & Nielsen OB, Increased excitability of acidified skeletal muscle: role of chloride conductance. *J Gen Physiol*, 2005. **125**: p. 237-246.

44. Bennetts B*, et al.*, Cytoplasmic ATP-sensing domains regulate gating of skeletal muscle ClC-1 chloride channels. *J Biol Chem*, 2005. **280**: p. 32452-32458.

45. Bennetts B, Parker MW, & Cromer BA, Inhibition of skeletal muscle ClC-1 chloride channels by low intracellular pH and ATP. *J Biol Chem*, 2007. **282**: p. 32780-32791.

46. Tseng PY, Bennetts B, & Chen TY, Cytoplasmic ATP inhibition of CLC-1 is enhanced by low pH. *J Gen Physiol*, 2007. **130**: p. 217-221.

47. Zifarelli G & Pusch M, The muscle chloride channel ClC-1 is not directly regulated by intracellular ATP. *J Gen Physiol*, 2008. **131**: p. 109-116.

48. Gurnett CA, Kahl SD, Anderson RD, & Campbell KP, Absence of the skeletal muscle sarcolemma chloride channel ClC-1 in myotonic mice. *J Biol Chem*, 1995. **270**: p. 9035-9038.

49. Papponen H*, et al.*, Regulated sarcolemmal localization of the muscle-specific ClC-1 chloride channel. *Exp Neurol*, 2005. **191**: p. 163-173.

50. Pusch M, Myotonia caused by mutations in the muscle chloride channel gene CLCN1. *Hum Mutat*, 2002. **19**: p. 423-434.

51. Lipicky RJ & Bryant SH, Sodium, potassium, and chloride fluxes in intercostal muscle from normal goats and goats with hereditary myotonia. *J Gen Physiol*, 1966. **50**: p. 89-111.

52. Bryant SH & Morales-Aguilera A, Chloride conductance in normal and myotonic muscle fibres and the action of monocarboxylic aromatic acids. *J Physiol*, 1971. **219**: p. 367-383.

53. Zifarelli G & Pusch M, CLC chloride channels and transporters: a biophysical and physiological perspective. *Rev Physiol Biochem Pharmacol*, 2007. **158**: p. 23-76.

54. Cho DH & Tapscott SJ, Myotonic dystrophy: emerging mechanisms for DM1 and DM2. *Biochim Biophys Acta*, 2007. **1772**: p. 195-204.

55. Klocke R, Steinmeyer K, Jentsch TJ, & Jockusch H, Role of innervation, excitability, and myogenic factors in the expression of the muscular chloride

channel ClC-1. A study on normal and myotonic muscle. *J Biol Chem*, 1994. **269**: p. 27635-27639.

56. Beck CL, Fahlke C, & George AL, Jr., Molecular basis for decreased muscle chloride conductance in the myotonic goat. *Proc Natl Acad Sci U S A*, 1996. **93**: p. 11248-11252.

57. Rhodes TH*, et al.*, A missense mutation in canine C1C-1 causes recessive myotonia congenita in the dog. *FEBS Lett*, 1999. **456**: p. 54-58.

58. Fahlke C*, et al.*, An aspartic acid residue important for voltage-dependent gating of human muscle chloride channels. *Neuron*, 1995. **15**: p. 463-472.

59. Pusch M, Steinmeyer K, Koch MC, & Jentsch TJ, Mutations in dominant human myotonia congenita drastically alter the voltage dependence of the CIC-1 chloride channel. *Neuron*, 1995. **15**: p. 1455-1463.

60. Thiemann A, Grunder S, Pusch M, & Jentsch TJ, A chloride channel widely expressed in epithelial and non-epithelial cells. *Nature*, 1992. **356**: p. 57-60.

61. Thompson CH*, et al.*, Inhibition of ClC-2 chloride channels by a peptide component or components of scorpion venom. *J Membr Biol*, 2005. **208**: p. 65-76.

62. Jordt SE & Jentsch TJ, Molecular dissection of gating in the ClC-2 chloride channel. *EMBO J*, 1997. **16**: p. 1582-1592.

63. Ramjeesingh M*, et al.*, Quaternary structure of the chloride channel ClC-2. *Biochemistry*, 2000. **39**: p. 13838-13847.

64. Nobile M, Pusch M, Rapisarda C, & Ferroni S, Single-channel analysis of a ClC-2-like chloride conductance in cultured rat cortical astrocytes. *FEBS Lett*, 2000. **479**: p. 10-14.

65. Weinreich F & Jentsch TJ, Pores formed by single subunits in mixed dimers of different CLC chloride channels. *J Biol Chem*, 2001. **276**: p. 2347-2353.

66. Niemeyer MI*, et al.*, A conserved pore-lining glutamate as a voltage- and chloride-dependent gate in the ClC-2 chloride channel. *J Physiol*, 2003. **553**: p. 873-879.

67. Zuniga L*, et al.*, The voltage-dependent ClC-2 chloride channel has a dual gating mechanism. *J Physiol*, 2004. **555**: p. 671-682.

68. de Santiago JA, Nehrke K, & Arreola J, Quantitative analysis of the voltage-dependent gating of mouse parotid ClC-2 chloride channel. *J Gen Physiol*, 2005. **126**: p. 591-603.

69. Yusef YR*, et al.*, Removal of gating in voltage-dependent ClC-2 chloride channel by point mutations affecting the pore and C-terminus CBS-2 domain. *J Physiol*, 2006. **572**: p. 173-181.

70. Grunder S, Thiemann A, Pusch M, & Jentsch TJ, Regions involved in the opening of CIC-2 chloride channel by voltage and cell volume. *Nature*, 1992. **360**: p. 759-762.

71. Furukawa T, Ogura T, Katayama Y, & Hiraoka M, Characteristics of rabbit ClC-2 current expressed in Xenopus oocytes and its contribution to volume regulation. *Am J Physiol*, 1998. **274**: p. C500-512.

72. Arreola J, Begenisich T, & Melvin JE, Conformation-dependent regulation of inward rectifier chloride channel gating by extracellular protons. *J Physiol*, 2002. **541**: p. 103-112.

73. Hinzpeter A*, et al.*, Membrane cholesterol content modulates ClC-2 gating and sensitivity to oxidative stress. *J Biol Chem*, 2007. **282**: p. 2423-2432.

74. Suh BC & Hille B, PIP_2 is a necessary cofactor for ion channel function: how and why? *Annu Rev Biophys*, 2008. **37**: p. 175-195.

75. Britton FC*, et al.*, Molecular distribution of volume-regulated chloride channels (ClC-2 and ClC-3) in cardiac tissues. *Am J Physiol Heart Circ Physiol*, 2000. **279**: p. H2225-2233.

76. Gyomorey K*, et al.*, Expression of the chloride channel ClC-2 in the murine small intestine epithelium. *Am J Physiol Cell Physiol*, 2000. **279**: p. C1787-1794.

77. Mohammad-Panah R*, et al.*, ClC-2 contributes to native chloride secretion by a human intestinal cell line, Caco-2. *J Biol Chem*, 2001. **276**: p. 8306-8313.

78. Blaisdell CJ*, et al.*, pH-regulated chloride secretion in fetal lung epithelia. *Am J Physiol Lung Cell Mol Physiol*, 2000. **278**: p. L1248-1255.

79. Cuppoletti J*, et al.*, ClC-2 Cl^- channels in human lung epithelia: activation by arachidonic acid, amidation, and acid-activated omeprazole. *Am J Physiol Cell Physiol*, 2001. **281**: p. C46-54.

80. Lipecka J*, et al.*, Distribution of ClC-2 chloride channel in rat and human epithelial tissues. *Am J Physiol Cell Physiol*, 2002. **282**: p. C805-816.

81. Pena-Munzenmayer G*, et al.*, Basolateral localization of native ClC-2 chloride channels in absorptive intestinal epithelial cells and basolateral sorting encoded by a CBS-2 domain di-leucine motif. *J Cell Sci*, 2005. **118**: p. 4243-4252.

82. Hinzpeter A*, et al.*, Association between Hsp90 and the ClC-2 chloride channel upregulates channel function. *Am J Physiol Cell Physiol*, 2006. **290**: p. C45-56.

83. Britton FC*, et al.*, Functional characterization of novel alternatively spliced ClC-2 chloride channel variants in the heart. *J Biol Chem*, 2005. **280**: p. 25871-25880.

84. Cheng G, Kim MJ, Jia G, & Agrawal DK, Involvement of chloride channels in IGF-I-induced proliferation of porcine arterial smooth muscle cells. *Cardiovasc Res*, 2007. **73**: p. 198-207.

85. Tewari KP, Malinowska DH, Sherry AM, & Cuppoletti J, PKA and arachidonic acid activation of human recombinant ClC-2 chloride channels. *Am J Physiol Cell Physiol*, 2000. **279**: p. C40-50.

86. Cuppoletti J*, et al.*, SPI-0211 activates T84 cell chloride transport and recombinant human ClC-2 chloride currents. *Am J Physiol Cell Physiol*, 2004. **287**: p. C1173-1183.

87. Smith RL*, et al.*, Differential expression of an inwardly rectifying chloride conductance in rat brain neurons: a potential mechanism for cell-specific modulation of postsynaptic inhibition. *J Neurosci*, 1995. **15**: p. 4057-4067.

88. Staley K*, et al.*, Alteration of $GABA_A$ receptor function following gene transfer of the CLC-2 chloride channel. *Neuron*, 1996. **17**: p. 543-551.

89. Bosl MR*, et al.*, Male germ cells and photoreceptors, both dependent on close cell-cell interactions, degenerate upon ClC-2 Cl(-) channel disruption. *EMBO J*, 2001. **20**: p. 1289-1299.

90. Blanz J*, et al.*, Leukoencephalopathy upon disruption of the chloride channel ClC-2. *J Neurosci*, 2007. **27**: p. 6581-6589.

91. Kajita H, Omori K, & Matsuda H, The chloride channel ClC-2 contributes to the inwardly rectifying Cl^- conductance in cultured porcine choroid plexus epithelial cells. *J Physiol*, 2000. **523 Pt 2**: p. 313-324.

92. Haug K*, et al.*, Mutations in CLCN2 encoding a voltage-gated chloride channel are associated with idiopathic generalized epilepsies. *Nat Genet*, 2003. **33**: p. 527-532.

93. Niemeyer MI*, et al.*, Functional evaluation of human ClC-2 chloride channel mutations associated with idiopathic generalized epilepsies. *Physiol Genomics*, 2004. **19**: p. 74-83.

94. Stogmann E*, et al.*, Mutations in the CLCN2 gene are a rare cause of idiopathic generalized epilepsy syndromes. *Neurogenetics*, 2006. **7**: p. 265-268.

95. Everett K*, et al.*, Linkage and mutational analysis of CLCN2 in childhood absence epilepsy. *Epilepsy Res*, 2007. **75**: p. 145-153.

96. McCarty NA, Permeation through the CFTR chloride channel. *J Exp Biol*, 2000. **203**: p. 1947-1962.

97. Ostedgaard LS*, et al.*, Processing and function of CFTR-DeltaF508 are species-dependent. *Proc Natl Acad Sci U S A*, 2007. **104**: p. 15370-15375.

98. Riordan JR, CFTR function and prospects for therapy. *Annu Rev Biochem*, 2008. **77**: p. 701-726.

99. Zdebik AA*, et al.*, Additional disruption of the ClC-2 Cl(-) channel does not exacerbate the cystic fibrosis phenotype of cystic fibrosis transmembrane conductance regulator mouse models. *J Biol Chem*, 2004. **279**: p. 22276-22283.

100. Uchida S*, et al.*, Molecular cloning of a chloride channel that is regulated by dehydration and expressed predominantly in kidney medulla. *J Biol Chem*, 1993. **268**: p. 3821-3824.

101. Kieferle S*, et al.*, Two highly homologous members of the ClC chloride channel family in both rat and human kidney. *Proc Natl Acad Sci U S A*, 1994. **91**: p. 6943-6947.

102. Adachi S*, et al.*, Two isoforms of a chloride channel predominantly expressed in thick ascending limb of Henle's loop and collecting ducts of rat kidney. *J Biol Chem*, 1994. **269**: p. 17677-17683.

103. Waldegger S & Jentsch TJ, Functional and structural analysis of ClC-K chloride channels involved in renal disease. *J Biol Chem*, 2000. **275**: p. 24527-24533.

104. Uchida S*, et al.*, Localization and functional characterization of rat kidney-specific chloride channel, ClC-K1. *J Clin Invest*, 1995. **95**: p. 104-113.

105. Estevez R*, et al.*, Barttin is a Cl^- channel beta-subunit crucial for renal Cl- reabsorption and inner ear K^+ secretion. *Nature*, 2001. **414**: p. 558-561.

106. Waldegger S*, et al.*, Barttin increases surface expression and changes current properties of ClC-K channels. *Pflugers Arch*, 2002. **444**: p. 411-418.

107. Scholl U*, et al.*, Barttin modulates trafficking and function of ClC-K channels. *Proc Natl Acad Sci U S A*, 2006. **103**: p. 11411-11416.

108. Jeck N, *et al.*, A common sequence variation of the CLCNKB gene strongly activates ClC-Kb chloride channel activity. *Kidney Int*, 2004. **65**: p. 190-197.

109. Sauve R, *et al.*, pH and external Ca(2+) regulation of a small conductance Cl(-) channel in kidney distal tubule. *Biochim Biophys Acta*, 2000. **1509**: p. 73-85.

110. Lourdel S, *et al.*, A chloride channel at the basolateral membrane of the distal-convoluted tubule: a candidate ClC-K channel. *J Gen Physiol*, 2003. **121**: p. 287-300.

111. Kobayashi K, *et al.*, Developmental expression of CLC-K1 in the postnatal rat kidney. *Histochem Cell Biol*, 2001. **116**: p. 49-56.

112. Yoshikawa M, *et al.*, Localization of rat CLC-K2 chloride channel mRNA in the kidney. *Am J Physiol*, 1999. **276**: p. F552-558.

113. Kobayashi K, *et al.*, Intrarenal and cellular localization of CLC-K2 protein in the mouse kidney. *J Am Soc Nephrol*, 2001. **12**: p. 1327-1334.

114. Qu C, *et al.*, Expression of CLC-K chloride channels in the rat cochlea. *Hear Res*, 2006. **213**: p. 79-87.

115. Mummery JL, Killey J, & Linsdell P, Expression of the chloride channel CLC-K in human airway epithelial cells. *Can J Physiol Pharmacol*, 2005. **83**: p. 1123-1128.

116. Hebert SC, Bartter syndrome. *Curr Opin Nephrol Hypertens*, 2003. **12**: p. 527-532.

117. Sile S, Vanoye CG, & George AL, Jr., Molecular physiology of renal ClC chloride channels/transporters. *Curr Opin Nephrol Hypertens*, 2006. **15**: p. 511-516.

118. Schlingmann KP, *et al.*, Salt wasting and deafness resulting from mutations in two chloride channels. *N Engl J Med*, 2004. **350**: p. 1314-1319.

119. Simon DB, *et al.*, Mutations in the chloride channel gene, CLCNKB, cause Bartter's syndrome type III. *Nat Genet*, 1997. **17**: p. 171-178.

120. Konrad M, *et al.*, Mutations in the chloride channel gene CLCNKB as a cause of classic Bartter syndrome. *J Am Soc Nephrol*, 2000. **11**: p. 1449-1459.

121. Birkenhager R, *et al.*, Mutation of BSND causes Bartter syndrome with sensorineural deafness and kidney failure. *Nat Genet*, 2001. **29**: p. 310-314.

122. Hayama A, Rai T, Sasaki S, & Uchida S, Molecular mechanisms of Bartter syndrome caused by mutations in the BSND gene. *Histochem Cell Biol*, 2003. **119**: p. 485-493.

123. Frey A*, et al.*, Influence of gain of function epithelial chloride channel ClC-Kb mutation on hearing thresholds. *Hear Res*, 2006. **214**: p. 68-75.

124. Matsumura Y*, et al.*, Overt nephrogenic diabetes insipidus in mice lacking the CLC-K1 chloride channel. *Nat Genet*, 1999. **21**: p. 95-98.

125. Maduke M, Pheasant DJ, & Miller C, High-level expression, functional reconstitution, and quaternary structure of a prokaryotic ClC-type chloride channel. *J Gen Physiol*, 1999. **114**: p. 713-722.

126. Accardi A & Miller C, Secondary active transport mediated by a prokaryotic homologue of ClC Cl^- channels. *Nature*, 2004. **427**: p. 803-807.

127. Accardi A, Kolmakova-Partensky L, Williams C, & Miller C, Ionic currents mediated by a prokaryotic homologue of CLC Cl- channels. *J Gen Physiol*, 2004. **123**: p. 109-119.

128. Nguitragool W & Miller C, Uncoupling of a CLC Cl^-/H^+ exchange transporter by polyatomic anions. *J Mol Biol*, 2006. **362**: p. 682-690.

129. Accardi A*, et al.*, Synergism between halide binding and proton transport in a CLC-type exchanger. *J Mol Biol*, 2006. **362**: p. 691-699.

130. Walden M*, et al.*, Uncoupling and turnover in a Cl^-/H^+ exchange transporter. *J Gen Physiol*, 2007. **129**: p. 317-329.

131. Kuang Z, Mahankali U, & Beck TL, Proton pathways and H^+/Cl^- stoichiometry in bacterial chloride transporters. *Proteins*, 2007. **68**: p. 26-33.

132. Accardi A*, et al.*, Separate ion pathways in a Cl^-/H^+ exchanger. *J Gen Physiol*, 2005. **126**: p. 563-570.

133. Nguitragool W & Miller C, CLC Cl^-/H^+ transporters constrained by covalent cross-linking. *Proc Natl Acad Sci U S A*, 2007. **104**: p. 20659-20665.

134. Iyer R, Iverson TM, Accardi A, & Miller C, A biological role for prokaryotic ClC chloride channels. *Nature*, 2002. **419**: p. 715-718.

135. Sasaki S*, et al.*, ClC family in the kidney. *Jpn J Physiol*, 1994. **44 Suppl 2**: p. S3-8.

136. Borsani G*, et al.*, Characterization of a human and murine gene (CLCN3) sharing similarities to voltage-gated chloride channels and to a yeast integral membrane protein. *Genomics*, 1995. **27**: p. 131-141.

137. Ogura T*, et al.*, ClC-3B, a novel ClC-3 splicing variant that interacts with EBP50 and facilitates expression of CFTR-regulated ORCC. *FASEB J*, 2002. **16**: p. 863-865.

138. Kawasaki M*, et al.*, Stable and functional expression of the CIC-3 chloride channel in somatic cell lines. *Neuron*, 1995. **14**: p. 1285-1291.

139. Duan D*, et al.*, Molecular identification of a volume-regulated chloride channel. *Nature*, 1997. **390**: p. 417-421.

140. Li X, Shimada K, Showalter LA, & Weinman SA, Biophysical properties of ClC-3 differentiate it from swelling-activated chloride channels in Chinese hamster ovary-K1 cells. *J Biol Chem*, 2000. **275**: p. 35994-35998.

141. Li X, Wang T, Zhao Z, & Weinman SA, The ClC-3 chloride channel promotes acidification of lysosomes in CHO-K1 and Huh-7 cells. *Am J Physiol Cell Physiol*, 2002. **282**: p. C1483-1491.

142. Huang P*, et al.*, Regulation of human CLC-3 channels by multifunctional Ca2+/calmodulin-dependent protein kinase. *J Biol Chem*, 2001. **276**: p. 20093-20100.

143. Robinson NC*, et al.*, Identification of an N-terminal amino acid of the CLC-3 chloride channel critical in phosphorylation-dependent activation of a CaMKII-activated chloride current. *J Physiol*, 2004. **556**: p. 353-368.

144. Matsuda JJ*, et al.*, Overexpression of CLC-3 in HEK293T cells yields novel currents that are pH dependent. *Am J Physiol Cell Physiol*, 2008. **294**: p. C251-262.

145. Hara-Chikuma M*, et al.*, ClC-3 chloride channels facilitate endosomal acidification and chloride accumulation. *J Biol Chem*, 2005. **280**: p. 1241-1247.

146. Wang XQ*, et al.*, CLC-3 channels modulate excitatory synaptic transmission in hippocampal neurons. *Neuron*, 2006. **52**: p. 321-333.

147. Stobrawa SM*, et al.*, Disruption of ClC-3, a chloride channel expressed on synaptic vesicles, leads to a loss of the hippocampus. *Neuron*, 2001. **29**: p. 185-196.

148. Arreola J*, et al.*, Secretion and cell volume regulation by salivary acinar cells from mice lacking expression of the Clcn3 Cl^- channel gene. *J Physiol*, 2002. **545**: p. 207-216.

149. Jentsch TJ, Chloride and the endosomal-lysosomal pathway: emerging roles of CLC chloride transporters. *J Physiol*, 2007. **578**: p. 633-640.

150. Zhao Z*, et al.*, The ClC-3 chloride transport protein traffics through the plasma membrane via interaction of an N-terminal dileucine cluster with clathrin. *J Biol Chem*, 2007. **282**: p. 29022-29031.

151. Salazar G*, et al.*, AP-3-dependent mechanisms control the targeting of a chloride channel (ClC-3) in neuronal and non-neuronal cells. *J Biol Chem*, 2004. **279**: p. 25430-25439.

152. Dickerson LW*, et al.*, Altered GABAergic function accompanies hippocampal degeneration in mice lacking ClC-3 voltage-gated chloride channels. *Brain Res*, 2002. **958**: p. 227-250.

153. Yoshikawa M*, et al.*, CLC-3 deficiency leads to phenotypes similar to human neuronal ceroid lipofuscinosis. *Genes Cells*, 2002. **7**: p. 597-605.

154. Wohlke A, Distl O, & Drogemuller C, Characterization of the canine CLCN3 gene and evaluation as candidate for late-onset NCL. *BMC Genet*, 2006. **7**: p. 13.

155. Wang GX*, et al.*, Functional effects of novel anti-ClC-3 antibodies on native volume-sensitive osmolyte and anion channels in cardiac and smooth muscle cells. *Am J Physiol Heart Circ Physiol*, 2003. **285**: p. H1453-1463.

156. Hume JR*, et al.*, Anion transport in heart. *Physiol Rev*, 2000. **80**: p. 31-81.

157. Duan DY*, et al.*, Functional role of anion channels in cardiac diseases. *Acta Pharmacol Sin*, 2005. **26**: p. 265-278.

158. Weylandt KH*, et al.*, ClC-3 expression enhances etoposide resistance by increasing acidification of the late endocytic compartment. *Mol Cancer Ther*, 2007. **6**: p. 979-986.

159. Moreland JG*, et al.*, Anion channels, including ClC-3, are required for normal neutrophil oxidative function, phagocytosis, and transendothelial migration. *J Biol Chem*, 2006. **281**: p. 12277-12288.

160. Miller FJ, Jr.*, et al.*, Cytokine activation of nuclear factor kappa B in vascular smooth muscle cells requires signaling endosomes containing Nox1 and ClC-3. *Circ Res*, 2007. **101**: p. 663-671.

161. van Slegtenhorst MA*, et al.*, A gene from the Xp22.3 region shares homology with voltage-gated chloride channels. *Hum Mol Genet*, 1994. **3**: p. 547-552.

162. Friedrich T, Breiderhoff T, & Jentsch TJ, Mutational analysis demonstrates that ClC-4 and ClC-5 directly mediate plasma membrane currents. *J Biol Chem*, 1999. **274**: p. 896-902.

163. Vanoye CG & George AL, Jr., Functional characterization of recombinant human ClC-4 chloride channels in cultured mammalian cells. *J Physiol*, 2002. **539**: p. 373-383.

164. Hebeisen S*, et al.*, Anion permeation in human ClC-4 channels. *Biophys J*, 2003. **84**: p. 2306-2318.

165. Picollo A & Pusch M, Chloride/proton antiporter activity of mammalian CLC proteins ClC-4 and ClC-5. *Nature*, 2005. **436**: p. 420-423.

166. Scheel O, Zdebik AA, Lourdel S, & Jentsch TJ, Voltage-dependent electrogenic chloride/proton exchange by endosomal CLC proteins. *Nature*, 2005. **436**: p. 424-427.

167. Zdebik AA*, et al.*, Determinants of anion-proton coupling in mammalian endosomal CLC proteins. *J Biol Chem*, 2008. **283**: p. 4219-4227.

168. Suzuki T*, et al.*, Intracellular localization of ClC chloride channels and their ability to form hetero-oligomers. *J Cell Physiol*, 2006. **206**: p. 792-798.

169. Mohammad-Panah R*, et al.*, The chloride channel ClC-4 contributes to endosomal acidification and trafficking. *J Biol Chem*, 2003. **278**: p. 29267-29277.

170. Mohammad-Panah R*, et al.*, The chloride channel ClC-4 co-localizes with cystic fibrosis transmembrane conductance regulator and may mediate chloride flux across the apical membrane of intestinal epithelia. *J Biol Chem*, 2002. **277**: p. 566-574.

171. Fisher SE*, et al.*, Isolation and partial characterization of a chloride channel gene which is expressed in kidney and is a candidate for Dent's disease (an X-linked hereditary nephrolithiasis). *Hum Mol Genet*, 1994. **3**: p. 2053-2059.

172. Fisher SE*, et al.*, Cloning and characterization of CLCN5, the human kidney chloride channel gene implicated in Dent disease (an X-linked hereditary nephrolithiasis). *Genomics*, 1995. **29**: p. 598-606.

173. Steinmeyer K*, et al.*, Cloning and functional expression of rat CLC-5, a chloride channel related to kidney disease. *J Biol Chem*, 1995. **270**: p. 31172-31177.

174. Sakamoto H*, et al.*, Identification of a new outwardly rectifying Cl^- channel that belongs to a subfamily of the ClC Cl- channels. *J Biol Chem*, 1996. **271**: p. 10210-10216.

175. Meyer S, Savaresi S, Forster IC, & Dutzler R, Nucleotide recognition by the cytoplasmic domain of the human chloride transporter ClC-5. *Nat Struct Mol Biol*, 2007. **14**: p. 60-67.

176. Wellhauser L*, et al.*, Nucleotides bind to the C-terminus of ClC-5. *Biochem J*, 2006. **398**: p. 289-294.

177. Devuyst O*, et al.*, Intra-renal and subcellular distribution of the human chloride channel, CLC-5, reveals a pathophysiological basis for Dent's disease. *Hum Mol Genet*, 1999. **8**: p. 247-257.

178. Thakker RV, Pathogenesis of Dent's disease and related syndromes of X-linked nephrolithiasis. *Kidney Int*, 2000. **57**: p. 787-793.

179. Jentsch TJ, Chloride transport in the kidney: lessons from human disease and knockout mice. *J Am Soc Nephrol*, 2005. **16**: p. 1549-1561.

180. Piwon N*, et al.*, ClC-5 Cl^- -channel disruption impairs endocytosis in a mouse model for Dent's disease. *Nature*, 2000. **408**: p. 369-373.

181. Gunther W, Piwon N, & Jentsch TJ, The ClC-5 chloride channel knock-out mouse - an animal model for Dent's disease. *Pflugers Arch*, 2003. **445**: p. 456-462.

182. Gunther W*, et al.*, ClC-5, the chloride channel mutated in Dent's disease, colocalizes with the proton pump in endocytotically active kidney cells. *Proc Natl Acad Sci U S A*, 1998. **95**: p. 8075-8080.

183. Vandewalle A*, et al.*, Tissue distribution and subcellular localization of the ClC-5 chloride channel in rat intestinal cells. *Am J Physiol Cell Physiol*, 2001. **280**: p. C373-381.

184. Christensen EI*, et al.*, Loss of chloride channel ClC-5 impairs endocytosis by defective trafficking of megalin and cubilin in kidney proximal tubules. *Proc Natl Acad Sci U S A*, 2003. **100**: p. 8472-8477.

185. Jentsch TJ, Poet M, Fuhrmann JC, & Zdebik AA, Physiological functions of CLC Cl- channels gleaned from human genetic disease and mouse models. *Annu Rev Physiol*, 2005. **67**: p. 779-807.

186. Wang Y*, et al.*, ClC-5: role in endocytosis in the proximal tubule. *Am J Physiol Renal Physiol*, 2005. **289**: p. F850-862.

187. Carr G, Simmons N, & Sayer J, A role for CBS domain 2 in trafficking of chloride channel CLC-5. *Biochem Biophys Res Commun*, 2003. **310**: p. 600-605.

188. Fuchs R*, et al.*, Rat liver endocytic coated vesicles do not exhibit ATP-dependent acidification in vitro. *Proc Natl Acad Sci U S A*, 1994. **91**: p. 4811-4815.

189. Hara-Chikuma M*, et al.*, Impaired acidification in early endosomes of ClC-5 deficient proximal tubule. *Biochem Biophys Res Commun*, 2005. **329**: p. 941-946.

190. Moulin P*, et al.*, Altered polarity and expression of H^+-ATPase without ultrastructural changes in kidneys of Dent's disease patients. *Kidney Int*, 2003. **63**: p. 1285-1295.

191. Schwake M, Friedrich T, & Jentsch TJ, An internalization signal in ClC-5, an endosomal Cl^-channel mutated in dent's disease. *J Biol Chem*, 2001. **276**: p. 12049-12054.

192. Hryciw DH*, et al.*, Cofilin interacts with ClC-5 and regulates albumin uptake in proximal tubule cell lines. *J Biol Chem*, 2003. **278**: p. 40169-40176.

193. Hryciw DH*, et al.*, Regulation of albumin endocytosis by PSD95/Dlg/ZO-1 (PDZ) scaffolds. Interaction of Na^+-H^+ exchange regulatory factor-2 with ClC-5. *J Biol Chem*, 2006. **281**: p. 16068-16077.

194. Lloyd SE*, et al.*, Characterisation of renal chloride channel, CLCN5, mutations in hypercalciuric nephrolithiasis (kidney stones) disorders. *Hum Mol Genet*, 1997. **6**: p. 1233-1239.

195. Silva IV, Blaisdell CJ, Guggino SE, & Guggino WB, PTH regulates expression of ClC-5 chloride channel in the kidney. *Am J Physiol Renal Physiol*, 2000. **278**: p. F238-245.

196. Wang SS*, et al.*, Mice lacking renal chloride channel, CLC-5, are a model for Dent's disease, a nephrolithiasis disorder associated with defective receptor-mediated endocytosis. *Hum Mol Genet*, 2000. **9**: p. 2937-2945.

197. Carr G, Simmons NL, & Sayer JA, Disruption of clc-5 leads to a redistribution of annexin A2 and promotes calcium crystal agglomeration in collecting duct epithelial cells. *Cell Mol Life Sci*, 2006. **63**: p. 367-377.

198. Weng TX*, et al.*, Oxidant and antioxidant modulation of chloride channels expressed in human retinal pigment epithelium. *Am J Physiol Cell Physiol*, 2002. **283**: p. C839-849.

199. Davies N*, et al.*, Chloride channel gene expression in the rabbit cornea. *Mol Vis*, 2004. **10**: p. 1028-1037.

200. Edmonds RD*, et al.*, ClC-5: ontogeny of an alternative chloride channel in respiratory epithelia. *Am J Physiol Lung Cell Mol Physiol*, 2002. **282**: p. L501-507.

201. Brandt S & Jentsch TJ, ClC-6 and ClC-7 are two novel broadly expressed members of the CLC chloride channel family. *FEBS Lett*, 1995. **377**: p. 15-20.

202. Kida Y*, et al.*, Localization of mouse CLC-6 and CLC-7 mRNA and their functional complementation of yeast CLC gene mutant. *Histochem Cell Biol*, 2001. **115**: p. 189-194.

203. Eggermont J*, et al.*, Alternative splicing of ClC-6 (a member of the CIC chloride-channel family) transcripts generates three truncated isoforms one of which, ClC-6c, is kidney-specific. *Biochem J*, 1997. **325 (Pt 1)**: p. 269-276.

204. Buyse G*, et al.*, Expression of human pICln and ClC-6 in Xenopus oocytes induces an identical endogenous chloride conductance. *J Biol Chem*, 1997. **272**: p. 3615-3621.

205. Buyse G*, et al.*, Evidence for the intracellular location of chloride channel (ClC)-type proteins: co-localization of ClC-6a and ClC-6c with the sarco/endoplasmic-reticulum Ca^{2+} pump SERCA2b. *Biochem J*, 1998. **330 (Pt 2)**: p. 1015-1021.

206. Ignoul S*, et al.*, Human ClC-6 is a late endosomal glycoprotein that associates with detergent-resistant lipid domains. *PLoS ONE*, 2007. **2**: p. e474.

207. Poet M*, et al.*, Lysosomal storage disease upon disruption of the neuronal chloride transport protein ClC-6. *Proc Natl Acad Sci U S A*, 2006. **103**: p. 13854-13859.

208. Ernest NJ, Weaver AK, Van Duyn LB, & Sontheimer HW, Relative contribution of chloride channels and transporters to regulatory volume decrease in human glioma cells. *Am J Physiol Cell Physiol*, 2005. **288**: p. C1451-1460.

209. Kornak U, Bosl MR, & Kubisch C, Complete genomic structure of the CLCN6 and CLCN7 putative chloride channel genes(1). *Biochim Biophys Acta*, 1999. **1447**: p. 100-106.

210. Diewald L*, et al.*, Activation by acidic pH of CLC-7 expressed in oocytes from Xenopus laevis. *Biochem Biophys Res Commun*, 2002. **291**: p. 421-424.

211. Graves AR, Curran PK, Smith CL, & Mindell JA, The Cl(-)/H(+) antiporter ClC-7 is the primary chloride permeation pathway in lysosomes. *Nature*, 2008.

212. Kornak U*, et al.*, Loss of the ClC-7 chloride channel leads to osteopetrosis in mice and man. *Cell*, 2001. **104**: p. 205-215.

213. Henriksen K*, et al.*, Characterization of osteoclasts from patients harboring a G215R mutation in ClC-7 causing autosomal dominant osteopetrosis type II. *Am J Pathol*, 2004. **164**: p. 1537-1545.

214. Kornak U*, et al.*, Polymorphisms in the CLCN7 gene modulate bone density in postmenopausal women and in patients with autosomal dominant osteopetrosis type II. *J Clin Endocrinol Metab*, 2006. **91**: p. 995-1000.

215. Henriksen K*, et al.*, Degradation of the organic phase of bone by osteoclasts: a secondary role for lysosomal acidification. *J Bone Miner Res*, 2006. **21**: p. 58-66.

216. Waguespack SG, Hui SL, Dimeglio LA, & Econs MJ, Autosomal dominant osteopetrosis: clinical severity and natural history of 94 subjects with a chloride channel 7 gene mutation. *J Clin Endocrinol Metab*, 2007. **92**: p. 771-778.

217. Cleiren E*, et al.*, Albers-Schonberg disease (autosomal dominant osteopetrosis, type II) results from mutations in the ClCN7 chloride channel gene. *Hum Mol Genet*, 2001. **10**: p. 2861-2867.

218. Kasper D*, et al.*, Loss of the chloride channel ClC-7 leads to lysosomal storage disease and neurodegeneration. *EMBO J*, 2005. **24**: p. 1079-1091.

219. Lange PF, Wartosch L, Jentsch TJ, & Fuhrmann JC, ClC-7 requires Ostm1 as a beta-subunit to support bone resorption and lysosomal function. *Nature*, 2006. **440**: p. 220-223.

220. Chalhoub N*, et al.*, Grey-lethal mutation induces severe malignant autosomal recessive osteopetrosis in mouse and human. *Nat Med*, 2003. **9**: p. 399-406.

221. Quarello P*, et al.*, Severe malignant osteopetrosis caused by a GL gene mutation. *J Bone Miner Res*, 2004. **19**: p. 1194-1199.

222. Pangrazio A*, et al.*, Mutations in OSTM1 (grey lethal) define a particularly severe form of autosomal recessive osteopetrosis with neural involvement. *J Bone Miner Res*, 2006. **21**: p. 1098-1105.

223. Yin X, Denton J, Yan X, & Strange K, Characterization of a novel voltage-dependent outwardly rectifying anion current in Caenorhabditis elegans oocytes. *Am J Physiol Cell Physiol*, 2007. **292**: p. C269-277.

224. He L, Denton J, Nehrke K, & Strange K, Carboxy terminus splice variation alters ClC channel gating and extracellular cysteine reactivity. *Biophys J*, 2006. **90**: p. 3570-3581.

225. Denton J*, et al.*, Altered gating and regulation of a carboxy-terminal ClC channel mutant expressed in the Caenorhabditis elegans oocyte. *Am J Physiol Cell Physiol*, 2006. **290**: p. C1109-1118.

226. Denton J*, et al.*, Alternative splicing of N- and C-termini of a C. elegans ClC channel alters gating and sensitivity to external Cl- and H+. *J Physiol*, 2004. **555**: p. 97-114.

227. Strange K, Of mice and worms: novel insights into ClC-2 anion channel physiology. *News Physiol Sci*, 2002. **17**: p. 11-16.

228. Rutledge E*, et al.*, CLH-3, a ClC-2 anion channel ortholog activated during meiotic maturation in C. elegans oocytes. *Curr Biol*, 2001. **11**: p. 161-170.

229. von der Fecht-Bartenbach J*, et al.*, Function of the anion transporter AtCLC-d in the trans-Golgi network. *Plant J*, 2007. **50**: p. 466-474.

230. Marmagne A*, et al.*, Two members of the Arabidopsis CLC (chloride channel) family, AtCLCe and AtCLCf, are associated with thylakoid and Golgi membranes, respectively. *J Exp Bot*, 2007. **58**: p. 3385-3393.

231. De Angeli A*, et al.*, The nitrate/proton antiporter AtCLCa mediates nitrate accumulation in plant vacuoles. *Nature*, 2006. **442**: p. 939-942.

232. Ludewig U, Pusch M, & Jentsch TJ, Two physically distinct pores in the dimeric ClC-0 chloride channel. *Nature*, 1996. **383**: p. 340-343.

233. Schmidt-Rose T & Jentsch TJ, Transmembrane topology of a CLC chloride channel. *Proc Natl Acad Sci U S A*, 1997. **94**: p. 7633-7638.

234. Mindell JA, Maduke M, Miller C, & Grigorieff N, Projection structure of a ClC-type chloride channel at 6.5 A resolution. *Nature*, 2001. **409**: p. 219-223.

235. Engh AM & Maduke M, Cysteine accessibility in ClC-0 supports conservation of the ClC intracellular vestibule. *J Gen Physiol*, 2005. **125**: p. 601-617.

236. Ramjeesingh M, Li C, She YM, & Bear CE, Evaluation of the membrane-spanning domain of ClC-2. *Biochem J*, 2006. **396**: p. 449-460.

237. Doyle DA*, et al.*, The structure of the potassium channel: molecular basis of K^+ conduction and selectivity. *Science*, 1998. **280**: p. 69-77.

238. Morais-Cabral JH, Zhou Y, & MacKinnon R, Energetic optimization of ion conduction rate by the K+ selectivity filter. *Nature*, 2001. **414**: p. 37-42.

239. Dutzler R, Campbell EB, & MacKinnon R, Gating the selectivity filter in ClC chloride channels. *Science*, 2003. **300**: p. 108-112.

240. Faraldo-Gomez JD & Roux B, Electrostatics of ion stabilization in a ClC chloride channel homologue from Escherichia coli. *J Mol Biol*, 2004. **339**: p. 981-1000.

241. Chen TY, Coupling gating with ion permeation in ClC channels. *Sci STKE*, 2003. **2003**: p. pe23.

242. Accardi A & Pusch M, Conformational changes in the pore of CLC-0. *J Gen Physiol*, 2003. **122**: p. 277-293.

243. Bykova EA, Zhang XD, Chen TY, & Zheng J, Large movement in the C terminus of CLC-0 chloride channel during slow gating. *Nat Struct Mol Biol*, 2006. **13**: p. 1115-1119.

244. Markovic S & Dutzler R, The structure of the cytoplasmic domain of the chloride channel ClC-Ka reveals a conserved interaction interface. *Structure*, 2007. **15**: p. 715-725.

245. Meyer S & Dutzler R, Crystal structure of the cytoplasmic domain of the chloride channel ClC-0. *Structure*, 2006. **14**: p. 299-307.

246. Alioth S, Meyer S, Dutzler R, & Pervushin K, The cytoplasmic domain of the chloride channel ClC-0: structural and dynamic characterization of flexible regions. *J Mol Biol*, 2007. **369**: p. 1163-1169.

247. Corry B, O'Mara M, & Chung SH, Conduction mechanisms of chloride ions in ClC-type channels. *Biophys J*, 2004. **86**: p. 846-860.

248. Cohen J & Schulten K, Mechanism of anionic conduction across ClC. *Biophys J*, 2004. **86**: p. 836-845.

249. McDonough S (2003) in *Calcium Channel Pharmacology*, ed. McDonough S (Kluwer-Academic-Plenum Publishing, New York).

250. Clark S, Jordt SE, Jentsch TJ, & Mathie A, Characterization of the hyperpolarization-activated chloride current in dissociated rat sympathetic neurons. *J Physiol*, 1998. **506 (Pt 3)**: p. 665-678.

251. Kurz LL*, et al.*, Identification of three cysteines as targets for the Zn^{2+} blockade of the human skeletal muscle chloride channel. *J Biol Chem*, 1999. **274**: p. 11687-11692.

252. Duffield MD, Rychkov GY, Bretag AH, & Roberts ML, Zinc inhibits human ClC-1 muscle chloride channel by interacting with its common gating mechanism. *J Physiol*, 2005. **568**: p. 5-12.

253. Osteen JD & Mindell J, Insights into the ClC-4 transport mechanism from studies of Zn2+ inhibition. *Biophys J*, 2008.

254. Pusch M*, et al.*, Mechanism of block of single protopores of the Torpedo chloride channel ClC-0 by 2-(p-chlorophenoxy)butyric acid (CPB). *J Gen Physiol*, 2001. **118**: p. 45-62.

255. Traverso S, Elia L, & Pusch M, Gating competence of constitutively open CLC-0 mutants revealed by the interaction with a small organic Inhibitor. *J Gen Physiol*, 2003. **122**: p. 295-306.

256. Liantonio A*, et al.*, Structural requisites of 2-(p-chlorophenoxy)propionic acid analogues for activity on native rat skeletal muscle chloride conductance and on heterologously expressed CLC-1. *Br J Pharmacol*, 2003. **139**: p. 1255-1264.

257. Pusch M*, et al.*, Pharmacological characterization of chloride channels belonging to the ClC family by the use of chiral clofibric acid derivatives. *Mol Pharmacol*, 2000. **58**: p. 498-507.

258. Aromataris EC*, et al.*, Modulation of the gating of CIC-1 by S-(-) 2-(4-chlorophenoxy) propionic acid. *Br J Pharmacol*, 1999. **126**: p. 1375-1382.

259. Aromataris EC*, et al.*, Fast and slow gating of CLC-1: differential effects of 2-(4-chlorophenoxy) propionic acid and dominant negative mutations. *Mol Pharmacol*, 2001. **60**: p. 200-208.

260. Estevez R*, et al.*, Conservation of chloride channel structure revealed by an inhibitor binding site in ClC-1. *Neuron*, 2003. **38**: p. 47-59.

261. Liantonio A*, et al.*, Investigations of pharmacologic properties of the renal CLC-K1 chloride channel co-expressed with barttin by the use of 2-(p-Chlorophenoxy)propionic acid derivatives and other structurally unrelated chloride channels blockers. *J Am Soc Nephrol*, 2004. **15**: p. 13-20.

262. Picollo A*, et al.*, Molecular determinants of differential pore blocking of kidney CLC-K chloride channels. *EMBO Rep*, 2004. **5**: p. 584-589.

263. Gentzsch M*, et al.*, The PDZ-binding chloride channel ClC-3B localizes to the Golgi and associates with cystic fibrosis transmembrane conductance regulator-interacting PDZ proteins. *J Biol Chem*, 2003. **278**: p. 6440-6449.

264. Matulef K*, et al.*, Discovery of potent CLC chloride channel inhibitors. *ACS Chem Biol*, 2008. **3**: p. 419-428.

265. Matulef K & Maduke M, Side-dependent inhibition of a prokaryotic ClC by DIDS. *Biophys J*, 2005. **89**: p. 1721-1730.

266. Linsdell P & Hanrahan JW, Disulphonic stilbene block of cystic fibrosis transmembrane conductance regulator Cl- channels expressed in a mammalian cell line and its regulation by a critical pore residue. *J Physiol*, 1996. **496 (Pt 3)**: p. 687-693.

267. Qu Z, Wei RW, & Hartzell HC, Characterization of Ca^{2+}-activated Cl^- currents in mouse kidney inner medullary collecting duct cells. *Am J Physiol Renal Physiol*, 2003. **285**: p. F326-335.

268. Liantonio A*, et al.*, Activation and inhibition of kidney CLC-K chloride channels by fenamates. *Mol Pharmacol*, 2006. **69**: p. 165-173.

269. Picollo A*, et al.*, Mechanism of interaction of niflumic acid with heterologously expressed kidney CLC-K chloride channels. *J Membr Biol*, 2007. **216**: p. 73-82.

270. Liantonio A*, et al.*, Molecular switch for CLC-K Cl- channel block/activation: optimal pharmacophoric requirements towards high-affinity ligands. *Proc Natl Acad Sci U S A*, 2008. **105**: p. 1369-1373.

271. Liantonio A*, et al.*, Niflumic acid inhibits chloride conductance of rat skeletal muscle by directly inhibiting the CLC-1 channel and by increasing intracellular calcium. *Br J Pharmacol*, 2007. **150**: p. 235-247.

272. Catterall WA*, et al.*, Voltage-gated ion channels and gating modifier toxins. *Toxicon*, 2007. **49**: p. 124-141.

273. McDonough SI, Gating modifier toxins of voltage-gated calcium channels. *Toxicon*, 2007. **49**: p. 202-212.

274. Swartz KJ, Tarantula toxins interacting with voltage sensors in potassium channels. *Toxicon*, 2007. **49**: p. 213-230.

275. Rodriguez de la Vega RC & Possani LD, Current views on scorpion toxins specific for K^+-channels. *Toxicon*, 2004. **43**: p. 865-875.

276. Tsetlin VI & Hucho F, Snake and snail toxins acting on nicotinic acetylcholine receptors: fundamental aspects and medical applications. *FEBS Lett*, 2004. **557**: p. 9-13.

277. Kristipati R*, et al.*, Characterization of the binding of omega-conopeptides to different classes of non-L-type neuronal calcium channels. *Mol Cell Neurosci*, 1994. **5**: p. 219-228.

278. Anderson CS, MacKinnon R, Smith C, & Miller C, Charybdotoxin block of single Ca^{2+}-activated K^+ channels. Effects of channel gating, voltage, and ionic strength. *J Gen Physiol*, 1988. **91**: p. 317-333.

279. Goldstein SA & Miller C, Mechanism of charybdotoxin block of a voltage-gated K+ channel. *Biophys J*, 1993. **65**: p. 1613-1619.

280. Gross A & MacKinnon R, Agitoxin footprinting the shaker potassium channel pore. *Neuron*, 1996. **16**: p. 399-406.

281. Naranjo D & Miller C, A strongly interacting pair of residues on the contact surface of charybdotoxin and a Shaker K^+ channel. *Neuron*, 1996. **16**: p. 123-130.

282. Hidalgo P & MacKinnon R, Revealing the architecture of a K+ channel pore through mutant cycles with a peptide inhibitor. *Science*, 1995. **268**: p. 307-310.

283. Ranganathan R, Lewis JH, & MacKinnon R, Spatial localization of the K^+ channel selectivity filter by mutant cycle-based structure analysis. *Neuron*, 1996. **16**: p. 131-139.

284. Jiang Y*, et al.*, X-ray structure of a voltage-dependent K^+ channel. *Nature*, 2003. **423**: p. 33-41.

285. Long SB, Campbell EB, & Mackinnon R, Crystal structure of a mammalian voltage-dependent Shaker family K^+ channel. *Science*, 2005. **309**: p. 897-903.

286. Swartz KJ & MacKinnon R, Hanatoxin modifies the gating of a voltage-dependent K^+ channel through multiple binding sites. *Neuron*, 1997. **18**: p. 665-673.

287. Chen H, Gordon D, & Heinemann SH, Modulation of cloned skeletal muscle sodium channels by the scorpion toxins Lqh II, Lqh III, and Lqh alphaIT. *Pflugers Arch*, 2000. **439**: p. 423-432.

288. Ruta V*, et al.*, Functional analysis of an archaebacterial voltage-dependent K^+ channel. *Nature*, 2003. **422**: p. 180-185.

289. Lee HC, Wang JM, & Swartz KJ, Interaction between extracellular Hanatoxin and the resting conformation of the voltage-sensor paddle in Kv channels. *Neuron*, 2003. **40**: p. 527-536.

290. Alabi AA*, et al.*, Portability of paddle motif function and pharmacology in voltage sensors. *Nature*, 2007. **450**: p. 370-375.

291. Lee SY & MacKinnon R, A membrane-access mechanism of ion channel inhibition by voltage sensor toxins from spider venom. *Nature*, 2004. **430**: p. 232-235.

292. Campos FV, Chanda B, Beirao PS, & Bezanilla F, beta-Scorpion toxin modifies gating transitions in all four voltage sensors of the sodium channel. *J Gen Physiol*, 2007. **130**: p. 257-268.

293. Siemens J*, et al.*, Spider toxins activate the capsaicin receptor to produce inflammatory pain. *Nature*, 2006. **444**: p. 208-212.

294. DeBin JA, Maggio JE, & Strichartz GR, Purification and characterization of chlorotoxin, a chloride channel ligand from the venom of the scorpion. *Am J Physiol*, 1993. **264**: p. C361-369.

295. Fuller MD*, et al.*, Inhibition of CFTR channels by a peptide toxin of scorpion venom. *Am J Physiol Cell Physiol*, 2004. **287**: p. C1328-1341.

296. Maertens C*, et al.*, Chlorotoxin does not inhibit volume-regulated, calcium-activated and cyclic AMP-activated chloride channels. *Br J Pharmacol*, 2000. **129**: p. 791-801.

297. Deshane J, Garner CC, & Sontheimer H, Chlorotoxin inhibits glioma cell invasion via matrix metalloproteinase-2. *J Biol Chem*, 2003. **278**: p. 4135-4144.

298. Fuller MD*, et al.*, State-dependent inhibition of cystic fibrosis transmembrane conductance regulator chloride channels by a novel peptide toxin. *J Biol Chem*, 2007. **282**: p. 37545-37555.

299. Fuller MD, Zhang ZR, Cui G, & McCarty NA, The block of CFTR by scorpion venom is state-dependent. *Biophys J*, 2005. **89**: p. 3960-3975.

300. Hechenberger M*, et al.*, A family of putative chloride channels from Arabidopsis and functional complementation of a yeast strain with a CLC gene disruption. *J Biol Chem*, 1996. **271**: p. 33632-33638.

301. Jentsch TJ, Neagoe I, & Scheel O, CLC chloride channels and transporters. *Curr Opin Neurobiol*, 2005. **15**: p. 319-325.

302. Devuyst O & Guggino WB, Chloride channels in the kidney: lessons learned from knockout animals. *Am J Physiol Renal Physiol*, 2002. **283**: p. F1176-1191.

303. Sherry AM*, et al.*, Localization of ClC-2 Cl- channels in rabbit gastric mucosa. *Am J Physiol Cell Physiol*, 2001. **280**: p. C1599-1606.

304. Murray CB, Chu S, & Zeitlin PL, Gestational and tissue-specific regulation of C1C-2 chloride channel expression. *Am J Physiol*, 1996. **271**: p. L829-837.

305. Li-Smerin Y & Swartz KJ, Gating modifier toxins reveal a conserved structural motif in voltage-gated Ca^{2+} and K^{+} channels. *Proc Natl Acad Sci U S A*, 1998. **95**: p. 8585-8589.

306. DeBin JA & Strichartz GR, Chloride channel inhibition by the venom of the scorpion Leiurus quinquestriatus. *Toxicon*, 1991. **29**: p. 1403-1408.

307. McCarty NA & Zhang ZR, Identification of a region of strong discrimination in the pore of CFTR. *Am J Physiol Lung Cell Mol Physiol*, 2001. **281**: p. L852-867.

308. Machaca K & Hartzell HC, Asymmetrical distribution of Ca-activated Cl channels in Xenopus oocytes. *Biophys J*, 1998. **74**: p. 1286-1295.

309. Qu Z & Hartzell HC, Anion permeation in Ca(2+)-activated Cl(-) channels. *J Gen Physiol*, 2000. **116**: p. 825-844.

310. Swartz KJ & MacKinnon R, Mapping the receptor site for hanatoxin, a gating modifier of voltage-dependent K+ channels. *Neuron*, 1997. **18**: p. 675-682.

311. Norton RS & Pallaghy PK, The cystine knot structure of ion channel toxins and related polypeptides. *Toxicon*, 1998. **36**: p. 1573-1583.

312. McDonough SI, Boland LM, Mintz IM, & Bean BP, Interactions among toxins that inhibit N-type and P-type calcium channels. *J Gen Physiol*, 2002. **119**: p. 313-328.

313. McDonough SI, Lampe RA, Keith RA, & Bean BP, Voltage-dependent inhibition of N- and P-type calcium channels by the peptide toxin omega-grammotoxin-SIA. *Mol Pharmacol*, 1997. **52**: p. 1095-1104.

314. Sidach SS & Mintz IM, Kurtoxin, a gating modifier of neuronal high- and low-threshold ca channels. *J Neurosci*, 2002. **22**: p. 2023-2034.

315. Fahlke C*, et al.*, Pore-forming segments in voltage-gated chloride channels. *Nature*, 1997. **390**: p. 529-532.

316. Adjadj E*, et al.*, Solution structure of Lqh-8/6, a toxin-like peptide from a scorpion venom--structural heterogeneity induced by proline cis/trans isomerization. *Eur J Biochem*, 1997. **246**: p. 218-227.

317. Maduke M, Miller C, & Mindell JA, A decade of CLC chloride channels: structure, mechanism, and many unsettled questions. *Annu Rev Biophys Biomol Struct*, 2000. **29**: p. 411-438.

318. Fahlke C, Ion permeation and selectivity in ClC-type chloride channels. *Am J Physiol Renal Physiol*, 2001. **280**: p. F748-757.

319. Jentsch TJ, Lorenz C, Pusch M, & Steinmeyer K, Myotonias due to CLC-1 chloride channel mutations. *Soc Gen Physiol Ser*, 1995. **50**: p. 149-159.

320. Possani LD*, et al.*, Peptides and genes coding for scorpion toxins that affect ion-channels. *Biochimie*, 2000. **82**: p. 861-868.

321. Blanc E*, et al.*, Solution structure of P01, a natural scorpion peptide structurally analogous to scorpion toxins specific for apamin-sensitive potassium channel. *Proteins*, 1996. **24**: p. 359-369.

322. Chang NS*, et al.*, Predominant interactions between mu-conotoxin Arg-13 and the skeletal muscle Na^+ channel localized by mutant cycle analysis. *Biochemistry*, 1998. **37**: p. 4407-4419.

323. Buisine E*, et al.*, Characterization of a new family of toxin-like peptides from the venom of the scorpion Leiurus quinquestriatus hebraeus. 1H-NMR structure of leiuropeptide II. *J Pept Res*, 1997. **49**: p. 545-555.

324. Mouhat S, De Waard M, & Sabatier JM, Contribution of the functional dyad of animal toxins acting on voltage-gated Kv1-type channels. *J Pept Sci*, 2005. **11**: p. 65-68.

325. Zerrouk H*, et al.*, Characterization of PO1, a new peptide ligand of the apamin-sensitive Ca2+ activated K^+ channel. *Int J Pept Protein Res*, 1996. **48**: p. 514-521.

326. Chicchi GG*, et al.*, Purification and characterization of a unique, potent inhibitor of apamin binding from Leiurus quinquestriatus hebraeus venom. *J Biol Chem*, 1988. **263**: p. 10192-10197.

327. Kharrat R*, et al.*, Chemical synthesis and characterization of maurotoxin, a short scorpion toxin with four disulfide bridges that acts on K+ channels. *Eur J Biochem*, 1996. **242**: p. 491-498.

328. Abdel-Mottaleb Y*, et al.*, The first potassium channel toxin from the venom of the Iranian scorpion Odonthobuthus doriae. *FEBS Lett*, 2006. **580**: p. 6254-6258.

329. Hui K, McIntyre D, & French RJ, Conotoxins as sensors of local pH and electrostatic potential in the outer vestibule of the sodium channel. *J Gen Physiol*, 2003. **122**: p. 63-79.

330. Yang XY*, et al.*, siRNA-mediated silencing of ClC-2 gene inhibits proliferation of human U-87 glioma cells. *Ai Zheng*, 2006. **25**: p. 805-810.

331. Lewis RJ & Garcia ML, Therapeutic potential of venom peptides. *Nat Rev Drug Discov*, 2003. **2**: p. 790-802.